Understanding the Complexity of Mucosal Immunity in Channel Catfish (*Ictalurus punctatus*)

by

Chao Li

A dissertation submitted to the Graduate Faculty of
Auburn University
in partial fulfillment of the
requirements for the Degree of
Doctor of Philosophy

Auburn, Alabama
August 3, 2013

Keywords: fish, catfish, mucosal immunity, bacteria, microarray, RNA-seq

Approved by

Eric Peatman, Co-chair, Assistant Professor, School of Fisheries
Zhanjiang Liu, Co-chair, Professor, School of Fisheries
Mark R. Liles, Associate Professor, Department of Biological Sciences
Jeffery Terhune, Associate Professor, School of Fisheries

Abstract

The mucosal surfaces of fish (gill, skin, intestine) serve as the first line of defense against a myriad of aquatic pathogens. Although interest in understanding components of the mucosal immune response in fish is growing, little is known about how host mucosal molecular and cellular constituents may impact rates of pathogen adhesion and tissue invasion. The freshwater bacterial pathogens *Edwardsiella ictaluri*, *Aeromonas hydrophila* and *Flavobacterium columnare* infect a variety of farmed fish species worldwide through various mucosal attachment points. The availability of transcriptomic tools including microarrays and RNA-Seq has recently opened a window through which we can observe the complexity of fish host-pathogen interactions during infection. In order to characterize the immune actors and events taking place at the mucosal surfaces and identify the routes of pathogen attachment and entry, RNA-seq and microarray approaches were utilized to broadly investaged the transcriptional effects during bacterial infection in channel catfish.

E.ictaluri is believed to gain entry through the intestinal epithelium. Following *E. ictaluri* challenge, the RNA-seq observed differentially expressed genes set indicated the centrality of actin cytoskeletal polymerization and junctional regulation in pathogen entry and subsequent inflammatory responses. A successful *A. hydrophila* infection always starts with the disturbed skin. At critical early timepoints following challenge in the skin, microarray analyses found that *A. hydrophila* infection rapidly altered a number of mucosal factors in a manner predicted to enhance its ability to adhere to and invade the catfish host. Adhesion of *F. columnare* to gill tissue is correlated to virulence and host

susceptibility. Here, the observed immune and mucin profiles between channel catfish differing in their susceptibility to *F. columnare* both before infection and at three early timepoints post-infection suggested a basal polarization in the gill mucosa. As the fasting impacts susceptibility to *F.columnare*, in gill and skin 7 day fasting significantly altered expression of critical innate immune factors.

Taken together, our results set a foundation for future studies comparing mechanisms of mucosal immunity across several important catfish pathogens. Understanding of molecular mechanisms of pathogen entry during infection will provide insight into strategies for selection of resistant catfish brood stocks against various diseases.

Acknowledgments

The author is very grateful to Dr. Eric Peatman for his constant guidance, support and patience in the past years. I have been very fortunate in having Dr. Eric Peatman as my supervisors. His scientific attitude and philosophy have had a profound influence on me. The author is also indebted to his co-chair Dr. Zhanjiang Liu for his invaluable advice and assistance in all stages of this work. He is grateful for time and expertise offered to him by his committee members: Dr. Mark Liles and Dr. Jeffery Terhune, and his dissertation outside reader, Dr. Joseph Newton. The author would like to express his gratitude to Dr. Benjamin H. Beck from Stuttgart National Aquaculture Research Center for his advice and support. Sincere thanks will also go to Huseyin Kucuktas and Ludmilla Kaltenboeck for technical help, and the colleagues in the laboratory for their help, collaboration, and friendship. I am grateful to my parents and my beloved wife for their endless love and support.

Table of Contents

List of Tables

List of Figures

List of Abbreviations

ESC	Enteric Septicemia Of Catfish
T3SS	Type III Secretion System
MALT	Mucosa-Associated Lymphoid Tissue
BHI	Brain Heart Infusion
CFU	Colony Forming Unit
PE	Paired-end
AJC	apical junction complex
RPKM	Reads Per Kilobase of exon model per Million mapped reads
FDR	False Discovery Rate
QPCR	Quantitative PCR
MID	Multiple Identifier
GO	Gene Ontology
PRR	Pathogen Recognition Receptor
Ig	Immunoglobulin
MAS	Motile Aeromonad Septicemia
TSA	Tryptic Soy Agar
TSB	Tryptic Soy Broth
BC	Base Composition
GEO	Gene Expression Omnibus
TAN	Total Ammonia Nitrogen

I. INTRODUCTION AND LITERATURE REVIEW

Mucosal Immunity

The immune system not only protects an organism against diseases by pathogenic organisms, but also plays an important role in maintaining homeostasis following inflammatory reactions [1, 2]. In vertebrates, the immune system includes both systemic and mucosal immune components, but it is the mucosal immune system which forms the front line of host defense against bacterial insults from the external environment, and acts as a dynamic interface between the external environment and the internal milieu. Mammalian mucosal surfaces including skin, intestine, and respiratory and reproductive tracts are in continuous contact with the external environment. Cellular and physical mechanisms at these sites play vital roles in host defense against bacteria, fungi, viruses and parasites searching to breach these surfaces [3, 4]. Similarly, the mucosal surfaces of fish (gill, skin, gastrointestinal tract) not only mediate physiological functions such as nutrient and oxygen absorption and waste secretion, the epithelial barrier and associated immune actors in the periphery are also responsible for sensing, sampling and screening pathogens while maintaining homeostasis in the presence of common and/or commensal microbes and foreign matter [5].

The mucosal barriers of fish are considered to be critical points of pathogen adhesion, entry and replication and host defense mechanisms [6]. In the aquatic environment where fish are confronted with a wide array of pathogens, the mucosal

surfaces are believed to possess more complex immune defense mechanisms than found in mammals. These surfaces serve as the first line of host defense against the myriad of aquatic pathogens present in the aquatic environment. It has long been hypothesized that observed differences in disease susceptibility between fish species or strains are due to the differing ability of the host to prevent pathogen attachment and entry at mucosal epithelial sites such as the gill, skin, and gastrointestinal tract. Although interest in understanding components of the mucosal immune response in fish is growing, little is known about how host mucosal molecular and cellular constituents may impact rates of pathogen adhesion, tissue invasion, and ultimately, mortality. Early studies on mucosal immune responses have been conducted in several fish species including rainbow trout [7], Atlantic salmon [8], Atlantic cod [9], and carp [10]. While most studies have been limited to examining *a priori* gene targets, a few have utilized microarray technology or next-generation sequencing to capture broader transcriptional profiles. In zebrafish intestine, microarray technology was utilized to examine the transcriptional consequences of the lack of adaptive immunity (rag1-/-) [11], while one 454-sequencing experiment was carried out in salmon skin to broadly characterize the skin transcriptome [12]. In rainbow trout, transcriptome profiling of gill tissue after temperature stress was conducted by screening a 4x44K oligonucleotide microarray [13]. Although recent progress has been made, and despite the obvious importance of mucosal surfaces, the precise molecular events that occur soon after encountering bacterial pathogens remain unclear.

Mucus

Fish are covered by a watery gel—mucus, on the surfaces of epithelium, providing the physical and biochemical barrier between the external environment and the interior milieu [6]. Although the function of mucus includes respiration, reproduction, excretion and osmotic regulation, it is clear that its primary role is to serve as a primary biological barrier to first prevent the attachment and entry of pathogens. Its composition can change rapidly follow infection [14], seasonal temperature changes [15], and dietary manipulations [16]. The mucus is continually secreted to physically trap and prevent pathogen attachment and invasion to the underlying epithelial surfaces, and also serves as a reservoir for many innate factors with antimicrobial activities which have a major role in fish survival. Key components of mucus have been well characterized including the high molecular mass mucin glycoproteins, immunoglobulins, lysozymes, proteases, lectins, complement factors and antimicrobial peptides than can benefit inhibition of pathogen trapping and sloughing [17-20].

Mucus continuously encounters, monitors and regulates a wide range of pathogens that are always present and continuously changing in the aquatic environment. The recognition of pathogens by pathogen recognition receptors triggers the production of the inflammatory factors and then induces the differentiation of mucus secretion related cells and alterations its composition as well as regulates the expression of the associated innate immune factors. But on the other hand, the mucus can also facilitate the disease processes. Many pathogens possess adhesins that can

specifically bind to the structures in mucus [21]. In addition, hyper or hypo-secretion of mucus also can lead to diseases. In human, hyper-secretion of mucus can be induced by pro-inflammatory cytokines, ATP, and bacterial infection [22, 23]. Furthermore, mucus expression and composition are altered in cancers of epithelial cells [24].

The dominant component of mucus are water and gel-forming proteins (mucins), which are high molecular weight glycoproteins (HMGs), secreted by the goblet cells in the epithelium. The goblet cells in fish have the similar structure to mammalian counterparts. Their products include glycoproteins, disulfides and lipids [25]. Defects in goblet cells can result in spontaneous inflammation and increased susceptibility to bacterial infection. The discharge of mucus in goblet cells can be rapidly altered due to pathogen infection. Increased number of goblet cells and output of mucus have been found in chronic airway insults in human [26]. In carp, the amount of skin mucus and their glycosylation increased after bacteria loading [27]. Moreover, mucus secretion from goblet cells is costly because they can not synthesize mucus a second time. During the lifespan of a fish, goblet cells continually turnover from the cells in the outer layer of the epidermis.

Mucin

Mucins are a family of heavily glycosylated filamentous proteins with high molecular weight [28, 29]. The concentration of mucins in the mucus layer is 2-5%. Mucins are characterized by domains rich in proline, threonine, and serine that are

heavily glycosylated (PTS or mucin domains), such as von willebrand D (VWD) and SEA domains. The mucin domains often contain tandemly repeated sequences and vary greatly in length of sequence [30]. Due to the large size of the central tandem repeats, the full-length sequences of mucins in fish are still poorly assembled [31]. To-date, 19 mucins have been identified in human, and their roles in the immune defense have been elucidated [32].

The mucins can be divided into two subfamilies: gel-forming mucins and membrane-bound mucins. Among the 19 mucins in human, there are five secreted gel-forming mucins (Muc2, Muc5B, Muc5AC, Muc6 and Muc19) [33]. Gel-forming mucins can be characterized by three VWD domains, followed by a PTS region, which are responsible for oligomerization, dimerization in the endoplasmic reticulum, and trimerization in the late secretary pathway [34]. In most cases, the VWD domain has neighboring VWE and TIL domains. The gel-forming mucins clearly play vital roles in the protection of the underlying epithelia and the trapping and elimination of pathogens. In mice a mucin2 deficiency can induce severe inflammation in the intestine, indicating that the importance of roles of gel-forming mucins in bacterial protection [35]. Many studies have showed that the gel-forming mucins can be up-regulated by the immune factors, such as interleukin, interferons and nitric oxide. Additionally, neutrophils can stimulate increased production of mucin during the inflammatory process [36-42]. The successful infection always starts with the penetration of the mucus barrier. Many bacteria can bind to their corresponding glycosylated receptors that are present on mucins. Mucins express many oligosaccharide structures on the mucosal surfaces which likely function as binding

sites for adhesions in pathogens. For example, *H. pylori* has four adhensins binding to mucin oligosaccharides [43, 44].

Skin

Skin is a structure that covers the body, and not only protects the host from the entry of pathogens, but also the leakage of water, solutes, or nutrients. Fish skin is a critical regulatory organ, serving not only as a physical barrier to pathogen entry, but also as a sophisticated integrator of environmental, social and nutritional cues through roles in immunity, osmoregulation, and endocrine signaling [1]. Although fish and human skin share many essential immune functions, they are structurally diverse. The structure and function of fish skin reflect the adaptation of fish to the physical, chemical, and biological properties of the aquatic environment. Fish skin is composed by two layers, epidermis and dermis. There is no keratinized layer of corneocytes in most fish epidermis, but the outermost layer of cells is alive and ready to divide. The major structural component in fish skin is the epithelial cell also known as keratocyte, suggested to play vital roles in the innate immune defense of skin in teleost fish by removing pathogens from the skin epidermis. Furthermore, the epithelial cells are also involved in wound repair and protection against infectious disease, with their migratory activity that can cover wounded skin within hours by forming a new protective layer of cells [45]. Many different immune cells, leukocytes, macrophages, granulocytes and the antibody-secreting cells (ASC) have been found in fish skin. The number of ASC cells rapidly increases after infection, the high level of ASC cells can be retained for weeks after exposure [46].

Fish live in pathogen rich environment. Disease susceptibility heavily depends on the ability of skin to prevent pathogen attachment and entry at the skin mucosal sites. Fish skin forms a thin physical barrier between the external environment and the internal milieu considered as the frontier of host defense against pathogen infection through skin epidermis [47]. Channel catfish showed high susceptibility to *A.hydrophila* with disturbed skin [48]. In order to trap and immobilize pathogens before they reach the epithelial layer, skin mucus is continuously secreted and replaced. The skin mucus is a complex fluid, and its composition varies among different locations. Skin mucus is mainly secreted by the goblet cells, but there are many other cells that can produce a more watery, serous fluid also present in the skin epidermis [49]. The antimicrobial property of skin mucus to inhibit the invasion and proliferation of different pathogens has been investigated in different fish species [17, 50-52]. Significantly differentially expressed mucus-related genes have been observed in fish skin following bacterial challenge [53].

Although skin is considered as the largest immunologically active organ, the molecular signatures of fish skin host-pathogen interaction are still limited. Transcriptomic approaches to examining fish skin samples have the benefit of capturing a more comprehensive picture of physiological responses to changes in stress or disease states compared to protein assays measuring known mucosal components. Recently, several studies in Atlantic salmon have utilized microarray technology and quantitative PCR (qPCR) to examine gene expression changes in skin after parasitic infection [54-56]. Also, microarray studies in zebrafish skin after bacterial infection showed more than 200 genes were differentially expressed

associated with wide range of immune functions [57]. While small scale study of the channel catfish skin transcriptome has been conducted [58], our knowledge of the broader skin transcriptome in the context of bacterial infection is lacking.

Lysozyme

Lysozyme is one of the most well-studied innate immune components in fish skin due to its bacteriolytic activity. It serves as an ubiquitous enzyme of all major taxa of living organisms. Lysozymes can catalyze the hydrolysis of 1, 4-beta-linkages between N-acetyl-D-glucosamine and N-acetylmuramic acid in peptidoglycan heteropolymers of bacteria cell walls leading to breakdown of bacteria [59, 60]. In addition, to help to kill bacterial pathogens through enzymatic and antimicrobial activity [61], it can promote phagocytosis by directly activating leucocytes and macrophages. Up to now, six types of lysozymes have been observed, including chicken-type lysozyme (c-type lysozyme), goose-type lysozyme (g-type lysozyme), invertebrate-type lysozyme (i-type lysozyme), phage lysozyme, bacterial lysozyme and plant lysozyme [62]. But different from the higher vertebrates, only g-type and c-type lysozymes have been reported in fish species. While the first fish c-type lysozyme was observed in rainbow trout [63], the g-type lysozyme was first isolated from *C. carpio*. Four lysozyme genes including three g-type lysozymes and one c-type lysozyme were isolated from channel catfish [64].

In the context of fish immunity [65], although the studies about plasma lysozyme levels started many years ago, the level and roles of lysozyme in mucosal surfaces are still overlooked [66, 67]. In mammals, lysozymes are among the most abundant secreted mucosal enzymes in mucosal surfaces. C-type lysozyme (lysozyme-like

protein 2) is considered as an important secreted mucus component (along with serine proteases) in fish species. In Ayu fish (*Plecoglossus altivelis*), lysozyme showed very high bacterialytic activity against *A.hydrophila* in skin. Increased lysozyme activities have been reported during skin regeneration in catfish [68].

Gill

The fish gill is a multipurpose organ, the dominant site of gas exchange, osmo-regulation, acid-base regulation, and excretion of nitrogenous waste. In order to facilitate the functions above, gill is composed of hundreds of filaments and thousands of lamellae [69]. Filamental epithelium is much thicker than the lamellar epithelium, with three or more layers [70]. Among the several distinct cell types in gill epithelium, pavement cells (PVCs) and mitochondrion-rich cells (MRCs) cover the vast majority of the gill filament surface area [71]. This thin epithelial barrier is relatively easy for the pathogen to breach and serves as the primary route of entry for many bacteria, such as *F.columnare*. Several pathogenesis studies have shown correlations between the capacity of *F. columnare* to adhere to gill epithelium and virulence [72]. Experimental infection protocols with *F. columnare* are more effective by contact exposure (i.e., immersion) than by injection. Accordingly, the ability to adhere to gill is thought to be a critical initial step in the infection of columnaris disease [72, 73]. Although gill plays vital roles in host defense, the studies of its immune role and mechanism during bacterial infection are still limited [74, 75]. In Atlantic cod, antibacterial genes were up-regulated early in gill after infection, together with some differentially expressed cytokines genes [9].

In earlier studies, researchers have identified lymphoid tissue in the gill lamellae, and also an interbranchial lymphoid tissue in salmonids [76]. A wide range of important immune cells, small and large lymphocytes, macrophages, neutrophils, eosinophilic granulocytes and antibody-secreting cells have been identified in fish gills [77]. In Atlantic salmon, MHC class II^+ cells can be found in the gill lesions during amoebic gill disease (AGD), indicating the antigen presentation capacity of the immune cells in fish gill [78]. Goblet cells spread along the filament epithelium in the gill and mucus production has been proven higher here than in the skin [6]. The IgM responses in gill mucus have already been investigated and are currently being targeted through immersion vaccination procedures in European eels [79].

Inducible nitric oxide synthase

Nitric oxide (NO), which is generated by the inducible nitric oxide synthase (iNOS), is often produced by macrophages. NO is a potent cytotoxic agent in immune defenses that can have beneficial antimicrobial activity but which can also have far-reaching tissue-damaging effects [80]. In both mammals and fish, iNOS and nitric oxide (NO) are well known innate immune factors against pathogens. In mammals, three different isoforms of NOS have been identified. Two of them are constitutively expressed, nNOS and eNOS which are mainly expressed in brain and endothelial cells, respectively. In contrast to nNOS and eNOS, the cytokine-induced iNOS is mainly present in macrophages and epithelial cells. Continuous high-level iNOS expression has been found in healthy human respiratory epithelium [81]. There, NO is believed to modulate mucociliary clearance and mediate cytotoxicity against a range of pathogens [80, 82]. High levels of NO can induce apoptosis in leukocytes responding to sites of

infection. NOS2b in zebrafish has been reported to be orthologous to mammalian iNOS, constitutively expressed in different tissues, and can be inducibled by LPS and Poly I:C [83]. Early study has reported the significantly regulated NO production during the host immune response to several pathogen infections in fish gill [84]. Constitutive expression of iNOS has been previously detected in gill in both control and *Neoparamoeba sp.* infected rainbow trout but low expression was found elsewhere. A similar finding of low expression of iNOS in kidney was reported by Campos-Perez in rainbow trout [85]. Taken together, the gill may be the dominant site of iNOS expression in fish.

Intestine

Intestine has important roles in food uptake, nutrition absorption, and the elimination of pathogens. Fish intestine is different from its mammalian counterparts in morphology and function. For example, there are no Peyer's patches, an organized lymphoid tissue, M cells, IgA and J-chain immunoglobulins [20]. However, a special mucosal IgM isotype, IgZ/IgT has recently described in teleost fish [86], as well as a smaller pIgR [20]. A wide array of immune cells including dendritic cells (DC), leucocytes, macrophages, eosinophilic and neutrophilic granulocytes are all present in fish intestine. Increased number of macrophages and neutrophils have been found under infection [20]. As with other mucosal tissues, the fish intestine is covered by a mucus layer which is secreted by goblet cells, forming a front line of innate host defense. Induction of goblet cells and mucus synthesis can be found in the early stages of intestinal infection, while decreased numbers of goblet cells and secreted mucus have been observed during chronic infection. $Muc2^{-/-}$ mice showed very high

susceptibility to IBD, and goblet cells lost their goblet-like shape, indicating the important innate immune roles of mucins in the intestinal mucosal immune barrier [35, 87].

The intestinal epithelium is a single cell layer targeted by many pathogens for disruption. The causative bacterium of enteric septicemia of catfish, *E.ictaluri*, is believed to gain entry through the intestinal epithelium. Previous research using a rat intestinal epithelial cell line (IEC-6) indicated actin polymerization and receptor-mediated endocytosis as potential mechanisms of uptake [88]. *E.ictaluri* can be found in channel catfish kidney by 0.25 h after intragastric intubation, indicating fast bacterial passage through the intestinal epithelium [89]. Very high levels of IgM have been detected in carp intestine at 5 weeks after feeding *A.hydrophila* [90]. In fish, many studies have examined the molecular process of teleost intestinal immunology during infection. The microarray studies about rag1-/- zebrafish intestine and gilthead sea bream intestinal responses to myxosporean parasite infection have revealed the crucial role of intestine during infection [11, 91]. But our knowledge about transcriptional changes of immune cellular factors in fish intestine following bacterial invasion and passage through the intestinal mucosa is still limited.

Host and bacteria interactions

Fish have established very powerful physical, biological and chemical mechanisms at mucosal barriers to prevent the pathogen attachment and entry. At the same time, pathogens have developed a wide range of strategies to subvert and avoid these barriers in order to establish successful infection [17]. In general, the invasion steps include attachment to the mucus, prevention of immune recognition or

phagocytosis, manipulation of the host cell to allow for invasion, induction of inflammatory responses, and, ultimately bacterial survival, replication and crossing of the mucosal barrier [92].

A common feature of the pathogens is motility on the mucosal surface by flagella. Pathogens with disturbed flagellar movement resulted in reduced pathogenicity. Among bacteria in fish, *A. hydrophila* motility depends on polar flagellum [93]. *F. columnare* has gliding motility on catfish mucus. Indeed, it has been shown that the gill and skin mucus of the catfish can promote chemotaxis of *F. columnare* [94]. After attachment, pathogens can penetrate and disrupt the mucus barrier, inducing host genes which can improve its pathogenicity. In humans, for example, *C. jejuni* has been shown to upregulate genes that encode the mucin-degrading enzymes after attachment [95].

After adhesion, pathogens also can secrete virulence factors to disrupt epithelial integrity, alter the production of mucins and antimicrobial proteins, and avoid and suppress the host immune defense [92]. Among the important catfish pathogens, *E. ictaluri* is believed to gain entry through the intestinal epithelium, but the pH in channel catfish intestine is very low. In order to survive and replicate in the low pH environment, *E. ictaluri* has the ability to alter the pH in intestine to protect itself during passage and subsequent replication in the epithelium [96]. *A. hydrophila* can secrete aerolysin, cytotoxic enterotoxin and extracellular serine protease to change the host structure of the cytoplasmic membrane to increase its infective ability [97].

Dissertation study overview

Catfish (*Ictalurus* spp.), the dominant aquaculture species in the U.S., suffers from widespread disease outbreaks due to a number of bacterial pathogens, including *A. hydrophila*, *F. columnare*, and *E. ictaluri*. While many previous disease studies have focused on disease responses in classical secondary lymphoid structures such as spleen and head kidney, not much is known about immune factors and responses in mucosal tissues (skin, gill and intestine) [98-100]. *E. ictaluri* is believed to gain entry through the intestine based on previous research using a rat intestinal epithelial cell line (IEC-6) [101]. While routes of *A. hydrophila* infection are still unclear, it is known that infection can be initated through disturbed skin [102]. The preferred mucosal targets of *F. columnare* are skin and gill [72]. The molecular processes during infection of these pathogens and the shared and tissue-specific innate immune actors in mucosal tissues are poorly understood. The research presented here seeks to fill this knowledge gap by using genomic tools to characterize the immune actors and events occurring during infection at the mucosal surfaces of fish–skin, gill, and intestine. We seek to better understand the key immune mediators at these surfaces as well as the routes of pathogen attachment and entry and, where possible, elucidate how these responses differ between resistant and susceptible fish. This understanding will be critical in evaluating the efficacy of nutritional and prophylactic approaches to reduce disease in aquaculture species.

The availability of transcriptomic tools including microarrays and RNA-Seq has recently opened a window through which we can observe the complexity of fish host-pathogen interactions during infection. In **Chapter 1**, high-throughput RNA-seq was utilized to characterize the role of the intestinal epithelial barriers following *E. ictaluri* challenge. We compared digital gene expression between challenged and control

samples at 3 h, 24 h, and 3 d following exposure. In **Chapter 2**, the transcriptional effects of virulent *A. hydrophila* infection in channel catfish skin was investigated by a new 8 x 60K Agilent microarray to examine gene expression profiles at critical early timepoints following challenge—2 h, 8 h, and 12 h. In **Chapter 3**, in order to identify how host gill mucosal molecular and cellular constituents may impact rates of adhesion, tissue invasion, and ultimately, mortality during the *F. columnare* infection, RNA-seq was employed to profile gill expression differences between channel catfish differing in their susceptibility to *F. columnare* both basally (before infection) and at three early timepoints post-infection (1 h, 2 h, and 8 h).

Short-term feed deprivation (or fasting) is a common occurrence in aquacultured fish species whether due to season, production targets, or disease. The manipulation of feeding regimens is one of the most common strategies in the US catfish industry for managing infectious disease. Studies have demonstrated that feeding concomitant with *E. ictaluri* exposure produced the highest rates of mortality [103]. Withholding feed after challenge reduced mortalities by close to 50%. Alternatively, feed deprivation of catfish for a 4 week period before and a 2 week period after *F. columare* challenge resulted in significantly higher mortality than was observed in fed groups [104]. In **Chapter 4**, in order to understand how short-term shifts in feed availability change the mucosal barrier profiles and modulate (and predict) pathogen susceptibility we utilized RNA-seq-based transcriptome profiling of skin and gill homogenates from fed and 7 d fasted channel catfish fingerlings.

References

[1] Ángeles Esteban M. An Overview of the Immunological Defenses in Fish Skin. ISRN Immunology 2012; 2012.

[2] Magnadóttir B. Innate immunity of fish (overview). Fish Shellfish Immunol 2006; 20:137-51.

[3] Turner JR. Intestinal mucosal barrier function in health and disease. Nat Rev Immunol 2009; 9:799-809.

[4] Gallo RL, Hooper LV. Epithelial antimicrobial defence of the skin and intestine. Nat Rev Immunol 2012; 12:503-16.

[5] Cerutti A, Chen K, Chorny A. Immunoglobulin Responses at the Mucosal Interface. Annual Review of Immunology, Vol 29 2011; 29:273-93.

[6] Shephard KL. Functions for Fish Mucus. Reviews in Fish Biology and Fisheries 1994; 4:401-29.

[7] Perez-Sanchez T, Balcazar JL, Merrifield DL, Carnevali O, Gioacchini G, de Blas I, et al. Expression of immune-related genes in rainbow trout (*Oncorhynchus mykiss*) induced by probiotic bacteria during *Lactococcus garvieae* infection. Fish Shellfish Immunol 2011; 31:196-201.

[8] Niklasson L, Sundh H, Fridell F, Taranger GL, Sundell K. Disturbance of the intestinal mucosal immune system of farmed Atlantic salmon (*Salmo salar*), in response to long-term hypoxic conditions. Fish Shellfish Immunol 2011; 31:1072-80.

[9] Caipang CM, Lazado CC, Brinchmann MF, Kiron V. Infection-induced changes in expression of antibacterial and cytokine genes in the gill epithelial cells of Atlantic cod, *Gadus morhua* during incubation with bacterial pathogens. Comp Biochem Physiol B Biochem Mol Biol 2010; 156:319-25.

[10] Ryo S, Wijdeven RH, Tyagi A, Hermsen T, Kono T, Karunasagar I, et al. Common carp have two subclasses of bonyfish specific antibody IgZ showing differential expression in response to infection. Dev Comp Immunol 2010; 34:1183-90.

[11] Jima DD, Shah RN, Orcutt TM, Joshi D, Law JM, Litman GW, et al. Enhanced transcription of complement and coagulation genes in the absence of adaptive immunity. Mol Immunol 2009; 46:1505-16.

[12] Micallef G, Bickerdike R, Reiff C, Fernandes JM, Bowman AS, Martin SA. Exploring the transcriptome of Atlantic salmon (*Salmo salar*) skin, a major defense organ. Mar Biotechnol (NY) 2012; 14:559-69.

[13] Rebl A, Verleih M, Kobis JM, Kuhn C, Wimmers K, Kollner B, et al. Transcriptome Profiling of Gill Tissue in Regionally Bred and Globally Farmed Rainbow Trout Strains Reveals Different Strategies for Coping with Thermal Stress. Mar Biotechnol (NY) 2013; 15:445-460.

[14] Easy RH, Ross NW. Changes in Atlantic salmon (*Salmo salar*) epidermal mucus protein composition profiles following infection with sea lice (*Lepeophtheirus salmonis*). Comp Biochem Physiol Part D Genomics Proteomics 2009; 4:159-67.

[15] Jung TS, Del Castillo CS, Javaregowda PK, Dalvi RS, Nho SW, Park SB, et al. Seasonal variation and comparative analysis of non-specific humoral immune substances in the skin mucus of olive flounder (*Paralichthys olivaceus*). Dev Comp Immunol 2012; 38:295-301.

[16] Sheikhzadeh N, Panchah IK, Asadpour R, Tayefi-Nasrabadi H, Mahmoudi H. Effects of Haematococcus pluvialis in maternal diet on reproductive performance and egg quality in rainbow trout (*Oncorhynchus mykiss*). Anim Reprod Sci 2012; 130:119-23.

[17] Ellis AE. Innate host defense mechanisms of fish against viruses and bacteria. Dev Comp Immunol 2001; 25:827-39.

[18] Rajan B, Fernandes JM, Caipang CM, Kiron V, Rombout JH, Brinchmann MF. Proteome reference map of the skin mucus of Atlantic cod (*Gadus morhua*) revealing immune competent molecules. Fish Shellfish Immunol 2011; 31:224-31.

[19] Palaksha KJ, Shin GW, Kim YR, Jung TS. Evaluation of non-specific immune components from the skin mucus of olive flounder (*Paralichthys olivaceus*). Fish Shellfish Immunol 2008; 24:479-88.

[20] Rombout JH, Abelli L, Picchietti S, Scapigliati G, Kiron V. Teleost intestinal immunology. Fish Shellfish Immunol 2011; 31:616-26.

[21] Scharfrnan A, Lamblin G, Roussel P. Interactions between human respiratory mucins and pathogens. 1995.

[22] Levine SJ, Larivee P, Logun C, Angus CW, Ognibene FP, Shelhamer JH. Tumor necrosis factor-alpha induces mucin hypersecretion and MUC-2 gene expression by human airway epithelial cells. Am J Respir Cell Mol Biol 1995; 12:196-204.

[23] Zhu Z, Homer RJ, Wang Z, Chen Q, Geba GP, Wang J, et al. Pulmonary expression of interleukin-13 causes inflammation, mucus hypersecretion, subepithelial fibrosis, physiologic abnormalities, and eotaxin production. J Clin Invest 1999; 103:779-88.

[24] Hollingsworth MA, Swanson BJ. Mucins in cancer: protection and control of the cell surface. Nat Rev Cancer 2004; 4:45-60.

[25] Harris J, Hunt S. The fine structure of the epidermis of two species of salmonid fish, the atlantic salmon (*Salmo solar L.*) and the brown trout (*Salmo trutta L.*). Cell Tissue Res 1975; 157:553-65.

[26] Rogers DF. Airway goblet cells: responsive and adaptable front-line defenders. Eur Respir J 1994; 7:1690-706.

[27] van der Marel M, Caspari N, Neuhaus H, Meyer W, Enss ML, Steinhagen D. Changes in skin mucus of common carp, *Cyprinus carpio L.*, after exposure to water with a high bacterial load. J Fish Dis 2010; 33:431-9.

[28] Bansil R, Turner BS. Mucin structure, aggregation, physiological functions and biomedical applications. Curr Opin Colloid In 2006; 11:164-70.

[29] Roussel P, Delmotte P. The diversity of epithelial secreted mucins. Current Organic Chemistry 2004; 8:413-37.

[30] Hollingsworth MA, Swanson BJ. Mucins in cancer: protection and control of the cell surface. Nat Rev Cancer 2004; 4:45-60.

[31] Marel M, Adamek M, Gonzalez SF, Frost P, Rombout JH, Wiegertjes GF, et al. Molecular cloning and expression of two beta-defensin and two mucin genes in common carp (*Cyprinus carpio L.*) and their up-regulation after beta-glucan feeding. Fish Shellfish Immunol 2012; 32:494-501.

[32] Linden S, Sutton P, Karlsson N, Korolik V, McGuckin M. Mucins in the mucosal barrier to infection. Mucosal Immunol 2008; 1:183-97.

[33] Lang T, Hansson GC, Samuelsson T. Gel-forming mucins appeared early in metazoan evolution. Proc Natl Acad Sci U S A 2007; 104:16209-14.

[34] Godl K, Johansson ME, Lidell ME, Mörgelin M, Karlsson H, Olson FJ, et al. The N terminus of the MUC2 mucin forms trimers that are held together within a trypsin-resistant core fragment. J Biol Chem 2002; 277:47248-56.

[35] Van der Sluis M, De Koning BA, De Bruijn AC, Velcich A, Meijerink JP, Van Goudoever JB, et al. Muc2-deficient mice spontaneously develop colitis, indicating that MUC2 is critical for colonic protection. Gastroenterology 2006; 131:117-29.

[36] Temann UA, Prasad B, Gallup MW, Basbaum C, Ho SB, Flavell RA, et al. A novel role for murine IL-4 in vivo: induction of MUC5AC gene expression and mucin hypersecretion. Am J Respir Cell Mol Biol 1997; 16:471-8.

[37] Dabbagh K, Takeyama K, Lee HM, Ueki IF, Lausier JA, Nadel JA. IL-4 induces mucin gene expression and goblet cell metaplasia in vitro and in vivo. J Immunol 1999; 162:6233-7.

[38] Smirnova MG, Birchall JP, Pearson JP. TNF-alpha in the regulation of MUC5AC secretion: some aspects of cytokine-induced mucin hypersecretion on the in vitro model. Cytokine 2000; 12:1732-36.

[39] Kim YD, Kwon EJ, Kwon TK, Baek SH, Song SY, Suh JS. Regulation of IL-1beta-mediated MUC2 gene in NCI-H292 human airway epithelial cells. Biochem Biophys Res Commun 2000; 274:112-6.

[40] Louahed J, Toda M, Jen J, Hamid Q, Renauld JC, Levitt RC, et al. Interleukin-9 upregulates mucus expression in the airways. Am J Respir Cell Mol Biol 2000; 22:649-56.

[41] Smirnova MG, Guo L, Birchall JP, Pearson JP. LPS up-regulates mucin and cytokine mRNA expression and stimulates mucin and cytokine secretion in goblet cells. Cell Immunol 2003; 221:42-9.

[42] Song JS, Kang CM, Yoo MB, Kim SJ, Yoon HK, Kim YK, et al. Nitric oxide induces MUC5AC mucin in respiratory epithelial cells through PKC and ERK dependent pathways. Respir Res 2007; 8:28.

[43] Lindén SK, Wickström C, Lindell G, Gilshenan K, Carlstedt I. Four modes of adhesion are used during Helicobacter pylori binding to human mucins in the oral and gastric niches. Helicobacter 2008; 13:81-93.

[44] Mahdavi J, Sonden B, Hurtig M, Olfat FO, Forsberg L, Roche N, et al. Helicobacter pylori SabA adhesin in persistent infection and chronic inflammation. Science 2002; 297:573-8.

[45] Böckelmann P, Ochandio B, Bechara I. Histological study of the dynamics in epidermis regeneration of the carp tail fin (*Cyprinus carpio, Linnaeus*, 1758). Braz J Biol 2010; 70:217-23.

[46] Zhao X, Findly RC, Dickerson HW. Cutaneous antibody-secreting cells and B cells in a teleost fish. Dev Comp Immunol 2008; 32:500-8.

[47] Woof JM, Mestecky J. Mucosal immunoglobulins. Immunol Rev 2005; 206:64-82.

[48] Ventura M, Grizzle JM. Evaluation of portals of entry of *Aeromonas hydrophila* in channel catfish. Aquaculture 1987; 65:205-14.

[49] Schempp C, Emde M, Wölfle U. Dermatology in the Darwin anniversary. Part 1: evolution of the integument. JDDG: Journal der Deutschen Dermatologischen Gesellschaft 2009; 7:750-57.

[50] Nagashima Y, Kikuchi N, Shimakura K, Shiomi K. Purification and characterization of an antibacterial protein in the skin secretion of rockfish Sebastes schlegeli. Comp Biochem Physiol C Toxicol Pharmacol 2003; 136:63-71.

[51] Kuppulakshmi C, Prakash M, Gunasekaran G, Manimegalai G, Sarojini S. Antibacterial properties of fish mucus from Channa punctatus and Cirrhinus mrigala. Eur Rev Med Pharmacol Sci 2008; 12:149-53.

[52] Su Y. Isolation and identification of pelteobagrin, a novel antimicrobial peptide from the skin mucus of yellow catfish (*Pelteobagrus fulvidraco*). Comp Biochem Physiol B Biochem Mol Biol 2011; 158:149-54.

[53] Aranishi F, Mano N. Response of skin cathepsins to infection of *Edwardsiella tarda* in Japanese flounder. Fisheries Science 2000; 66:169-70.

[54] Tadiso TM, Krasnov A, Skugor S, Afanasyev S, Hordvik I, Nilsen F. Gene expression analyses of immune responses in Atlantic salmon during early stages of infection by salmon louse (*Lepeophtheirus salmonis*) revealed bi-phasic responses coinciding with the copepod-chalimus transition. BMC Genomics 2011; 12:141.

[55] Krasnov A, Skugor S, Todorcevic M, Glover KA, Nilsen F. Gene expression in Atlantic salmon skin in response to infection with the parasitic copepod *Lepeophtheirus salmonis*, cortisol implant, and their combination. BMC Genomics 2012; 13:130.

[56] Braden LM, Barker DE, Koop BF, Jones SR. Comparative defense-associated responses in salmon skin elicited by the ectoparasite *Lepeophtheirus salmonis*. Comp Biochem Physiol Part D Genomics Proteomics 2012; 7:100-9.

[57] Lü A, Hu X, Xue J, Zhu J, Wang Y, Zhou G. Gene expression profiling in the skin of zebrafish infected with *Citrobacter freundii*. Fish Shellfish Immunol 2012; 32:273-83.

[58] Karsi A, Cao D, Li P, Patterson A, Kocabas A, Feng J, et al. Transcriptome analysis of channel catfish (*Ictalurus punctatus*): initial analysis of gene expression and microsatellite-containing cDNAs in the skin. Gene 2002; 285:157-68.

[59] Chipman DM, Sharon N. Mechanism of lysozyme action. Science (New York, N.Y.) 1969; 165:454-65.

[60] Jollès P, Jollès J. What's new in lysozyme research? Molecular and Cellular Biochemistry 1984; 63:165-89.

[61] Davis KM, Weiser JN. Modifications to the peptidoglycan backbone help bacteria to establish infection. Infect Immun 2011; 79:562-70.

[62] Jiménez-Cantizano RM, Infante C, Martin-Antonio B, Ponce M, Hachero I, Navas JI, et al. Molecular characterization, phylogeny, and expression of c-type and g-type lysozymes in brill (*Scophthalmus rhombus*). Fish Shellfish Immunol 2008; 25:57-65.

[63] Dautigny A, Prager E, Pham-Dinh D, Jollès J, Pakdel F, Grinde B, et al. cDNA and amino acid sequences of rainbow trout (*Oncorhynchus mykiss*) lysozymes and their implications for the evolution of lysozyme and lactalbumin. J Mol Evol 1991; 32:187-98.

[64] Wang R, Feng J, Li C, Liu S, Zhang Y, Liu Z. Four lysozymes (one c-type and three g-type) in catfish are drastically but differentially induced after bacterial infection. Fish Shellfish Immunol 2013; 35:136-45.

[65] Ellis A. Innate host defense mechanisms of fish against viruses and bacteria. Dev Comp Immunol 2001; 25:827-39.

[66] Bergsson G, Agerberth B, Jörnvall H, Gudmundsson GH. Isolation and identification of antimicrobial components from the epidermal mucus of Atlantic cod (*Gadus morhua*). Febs Journal 2005; 272:4960-69.

[67] Nigam AK, Kumari U, Mittal S, Mittal AK. Comparative analysis of innate immune parameters of the skin mucous secretions from certain freshwater teleosts, inhabiting different ecological niches. Fish Physiol Biochem 2012; 38:1245-56.

[68] Rai A, Mittal A. Histochemical response of alkaline phosphatase activity during the healing of cutaneous wounds in a cat-fish. Experientia 1983; 39:520-22.

[69] Wilson JM, Laurent P. Fish gill morphology: inside out. J Exp Zool 2002; 293:192-213.

[70] Laurent P, Dunel S. Morphology of gill epithelia in fish. Am J Physiol 1980; 238:R147-59.

[71] Evans DH, Piermarini PM, Choe KP. The multifunctional fish gill: dominant site of gas exchange, osmoregulation, acid-base regulation, and excretion of nitrogenous waste. Physiol Rev 2005; 85:97-177.

[72] Decostere A, Haesebrouck F, Turnbull J, Charlier G. Influence of water quality and temperature on adhesion of high and low virulence *Flavobacterium columnare* strains to isolated gill arches. J Fish Dis 1999; 22:1-11.

[73] Beck BH, Farmer BD, Straus DL, Li C, Peatman E. Putative roles for a rhamnose binding lectin in *Flavobacterium columnare* pathogenesis in channel catfish *Ictalurus punctatus*. Fish Shellfish Immunol 2012; 33:1008-15.

[74] Morrison RN, Cooper GA, Koop BF, Rise ML, Bridle AR, Adams MB, et al. Transcriptome profiling the gills of amoebic gill disease (AGD)-affected Atlantic salmon (*Salmo salar L*.): a role for tumor suppressor p53 in AGD pathogenesis? Physiol Genomics 2006; 26:15-34.

[75] Wynne JW, O'Sullivan MG, Cook MT, Stone G, Nowak BF, Lovell DR, et al. Transcriptome analyses of amoebic gill disease-affected Atlantic salmon (*Salmo salar*) tissues reveal localized host gene suppression. Mar Biotechnol (NY) 2008; 10:388-403.

[76] Haugarvoll E, Bjerkas I, Nowak BF, Hordvik I, Koppang EO. Identification and characterization of a novel intraepithelial lymphoid tissue in the gills of Atlantic salmon. J Anat 2008; 213:202-9.

[77] Salinas I, Zhang Y-A, Sunyer JO. Mucosal immunoglobulins and B cells of teleost fish. Dev Comp Immunol 2011; 35:1346-65.

[78] Morrison RN, Koppang EO, Hordvik I, Nowak BF. MHC class II+ cells in the gills of Atlantic salmon (*Salmo salar L*.) affected by amoebic gill disease. Vet Immunol Immunopathol 2006; 109:297-303.

[79] Esteve-Gassent MD, Nielsen ME, Amaro C. The kinetics of antibody production in mucus and serum of European eel (*Anguilla anguilla L*.) after vaccination against Vibrio vulnificus: development of a new method for antibody quantification in skin mucus. Fish Shellfish Immunol 2003; 15:51-61.

[80] Bogdan C. Nitric oxide and the immune response. Nat Immunol 2001; 2:907-16.

[81] Guo FH, De Raeve HR, Rice TW, Stuehr DJ, Thunnissen F, Erzurum SC. Continuous nitric oxide synthesis by inducible nitric oxide synthase in normal human airway epithelium in vivo. Proc Natl Acad Sci U S A 1995; 92:7809-13.

[82] Jain B, Rubinstein I, Robbins RA, Leise KL, Sisson JH. Modulation of airway epithelial cell ciliary beat frequency by nitric oxide. Biochem Biophys Res Commun 1993; 191:83-8.

[83] Lepiller S, Franche N, Solary E, Chluba J, Laurens V. Comparative analysis of zebrafish nos2a and nos2b genes. Gene 2009; 445:58-65.

[84] Campos-Perez JJ, Ellis AE, Secombes CJ. Toxicity of nitric oxide and peroxynitrite to bacterial pathogens of fish. Dis Aquat Organ 2000; 43:109-15.

[85] Campos‐perez J, Ward M, Grabowski P, Ellis A, Secombes C. The gills are an important site of iNOS expression in rainbow trout Oncorhynchus mykiss after challenge with the Gram‐positive pathogen *Renibacterium salmoninarum*. Immunology 2000; 99:153-61.

[86] Hansen JD, Landis ED, Phillips RB. Discovery of a unique Ig heavy-chain isotype (IgT) in rainbow trout: Implications for a distinctive B cell developmental pathway in teleost fish. Proc Natl Acad Sci U S A 2005; 102:6919-24.

[87] Velcich A, Yang W, Heyer J, Fragale A, Nicholas C, Viani S, et al. Colorectal cancer in mice genetically deficient in the mucin Muc2. Science 2002; 295:1726-29.

[88] Skirpstunas RT, Baldwin TJ. Edwardsiella ictaluri invasion of IEC-6, Henle 407, fathead minnow and channel catfish enteric epithelial cells. Dis Aquat Organ 2002; 51:161-7.

[89] Baldwin TJ, Newton JC. Pathogenesis of enteric septicemia of channel catfish, caused by *Edwardsiella ictaluri*: bacteriologic and light and electron microscopic findings. J. Aquat 1993; 5:189-98.

[90] Tu FP, Chu WH, Zhuang XY, Lu CP. Effect of oral immunization with Aeromonas hydrophila ghosts on protection against experimental fish infection. Lett Appl Microbiol 2010; 50:13-7.

[91] Davey GC, Calduch-Giner JA, Houeix B, Talbot A, Sitja-Bobadilla A, Prunet P, et al. Molecular profiling of the gilthead sea bream (*Sparus aurata L.*) response to chronic exposure to the myxosporean parasite Enteromyxum leei. Mol Immunol 2011; 48:2102-12.

[92] McGuckin MA, Linden SK, Sutton P, Florin TH. Mucin dynamics and enteric pathogens. Nat Rev Microbiol 2011; 9:265-78.

[93] Canals R, Vilches S, Wilhelms M, Shaw JG, Merino S, Tomás JM. Non-structural flagella genes affecting both polar and lateral flagella-mediated motility in *Aeromonas hydrophila*. Microbiology 2007; 153:1165-75.

[94] Klesius PH, Pridgeon JW, Aksoy M. Chemotactic factors of *Flavobacterium columnare* to skin mucus of healthy channel catfish (*Ictalurus punctatus*). FEMS Microbiol Lett 2010; 310:145-51.

[95] Tu QV, McGuckin MA, Mendz GL. Campylobacter jejuni response to human mucin MUC2: modulation of colonization and pathogenicity determinants. J Med Microbiol 2008; 57:795-802.

[96] Booth NJ, Beekman JB, Thune RL. Edwardsiella ictaluri encodes an acid-activated urease that is required for intracellular replication in channel catfish (*Ictalurus punctatus*) macrophages. Appl Environ Microbiol 2009; 75:6712-20.

[97] Yu HB, Zhang YL, Lau YL, Yao F, Vilches S, Merino S, et al. Identification and characterization of putative virulence genes and gene clusters in Aeromonas hydrophila PPD134/91. Appl Environ Microbiol 2005; 71:4469-77.

[98] Zhang H, Peatman E, Liu H, Feng T, Chen L, Liu Z. Molecular characterization of three L-type lectin genes from channel catfish, Ictalurus punctatus and their responses to *Edwardsiella ictaluri* challenge. Fish Shellfish Immunol 2012; 32:598-608.

[99] Zhou Z, Liu H, Liu S, Sun F, Peatman E, Kucuktas H, et al. Alternative complement pathway of channel catfish (*Ictalurus punctatus*): molecular characterization, mapping and expression analysis of factors Bf/C2 and Df. Fish Shellfish Immunol 2012; 32:186-95.

[100] Peatman E, Baoprasertkul P, Terhune J, Xu P, Nandi S, Kucuktas H, et al. Expression analysis of the acute phase response in channel catfish (*Ictalurus punctatus*) after infection with a Gram-negative bacterium. Dev Comp Immunol 2007; 31:1183-96.

[101] Skirpstunas RT, Baldwin TJ. Edwardsiella ictaluri invasion of IEC-6, Henle 407, fathead minnow and channel catfish enteric epithelial cells. Dis Aquat Organ 2002; 51:161-67.

[102] Ventura MT, Grizzle JM. Evaluation of Portals of Entry of Aeromonas-Hydrophila in Channel Catfish. Aquaculture 1987; 65:205-14.

[103] Wise DJ, Greenway T, Li MH, Camus AC, Robinson EH. Effects of variable periods of food deprivation on the development of enteric septicemia in channel catfish. J Aquat Anim Health 2008; 20:39-44.

[104] Shoemaker C, Klesius P, Lim C, Yildirim M. Feed deprivation of channel catfish, *Ictalurus punctatus* (*Rafinesque*), influences organosomatic indices, chemical composition and susceptibility to Flavobacterium columnare. J Fish Dis 2003; 26:553-61.

II. RNA-SEQ ANALYSIS OF MUCOSAL IMMUNE RESPONSES REVEALS SIGNATURES OF INTESTINAL BARRIER DISRUPTION AND PATHOGEN ENTRY FOLLOWING *EDWARDSIELLA ICTALURI* INFECTION IN CHANNEL CATFISH, *ICTALURUS PUNCTATUS*

1. Introduction

Mucosal surfaces form a thin physical barrier between the external environment and the internal milieu. This epithelial monolayer not only serves to mediate interactions between pathogen sensors and mucosa-associated lymphoid tissue (MALT) but also carries out other physiological roles such as nutrient absorption and waste secretion [1]. In mammalian systems, the intestinal mucosal epithelium is well characterized as both a selectively permeable barrier regulated by junctional proteins and as a primary site of infection for a number of enteric pathogens including viruses, bacteria, and parasites [2]. Intestinal diseases often lead to disruption or exploitation of barrier components either through co-opting them as receptors for attachment and internalization, through pathogen release of targeted effector molecules, or through stimulation of host inflammatory responses which ultimately compromise junctional integrity. Disruption of the apical junction complex (AJC), consisting of the tight junction, adherens junction, and desmosome, structurally impacts epithelial cell integrity via junctionally-linked actin filaments and disrupts large cytoplasmic scaffolding proteins leading to dysregulated cell signaling and regulation [3].

The mucosal surfaces of fish (gills, skin, gastrointestinal tract) are also known as sites of pathogen exposure and are the focus of specific host defense mechanisms.

Several studies have begun to examine the cellular and molecular composition of mucosal surfaces in salmonids [4-10], carp [11], cod [12] and flounder [13]. Farmed fish, like other vertebrates, are susceptible to a large number of pathogens with primary or secondary routes of entry through the gastrointestinal (GI) tract and which are capable of causing widespread mortality. Among these are *Aeromonas hydrophila*, *Aeromonas salmonicida*, *Mycobacterium marinum*, *Edwardsiella ictaluri*, *Edwardsiella tarda*, *Vibrio anguillarum*, and *Streptococcus iniae*. While our knowledge of cellular actors in teleost intestinal immunology has grown considerably [14], few studies have examined the molecular processes and pathways triggered following bacterial invasion and passage through the intestinal mucosa. Jima et al. [15] examined the transcriptional consequences of the lack of adaptive immunity (rag1-/-) in the zebrafish intestine, while Davey et al. [16] recently profiled gilthead sea bream intestinal responses to myxosporean parasite infection. Both studies utilized microarrays to examine expression levels of known transcripts.

Catfish (*Ictalurus* spp.), the dominant aquaculture species in the U.S., suffers from widespread disease outbreaks due to a number of enteric pathogens, including *A. hydrophila*, *E. tarda*, and *E. ictaluri*. The last of these, the gram-negative, rod-shaped bacterium *E. ictaluri*, and its associated disease enteric septicemia of catfish (ESC), is commonly associated with widespread mortality through both acute and chronic infections in ponds. It has long been hypothesized that observed differences in disease susceptibility between catfish species and strains are due to the differing ability of the host to prevent pathogen attachment and entry at mucosal epithelial sites on the gill, skin, and gastrointestinal tract [17-19]. However, no studies have systematically studied the intestinal mucosal barrier and associated immune responses in this context. Hebert et al. [20] evaluated the composition of intestinal tract immune cells in channel

catfish. Most relevant to this study, Skirpstunas and Baldwin [21] conducted invasion trials using *E. ictaluri* and mammalian, fish and harvested channel catfish enteric epithelial cells. They reported that pre-incubation of intestinal cell lines with cytochalasin D (microfilament depolymerizer) and monodansylcadaverine (blocks receptor-mediated endocytosis) reduced *E. ictaluri* invasion, indicating potential routes of entry. To begin to understand the elements of catfish mucosal immune responses, here we examined transcriptional profiles of the catfish intestine at three timepoints following experimental infection with *E. ictaluri*. Utilizing RNA-seq technology we captured 1,633 differentially expressed genes with critical functional roles in cytoskeletal/muscle fiber dynamics, junctional modification, lysosome/phagosome regulation, immune activation and inflammation, attachment and pathogen recognition, and endocrine/growth disruption. Identification of the molecular actors in catfish mucosal immunity will advance our knowledge of teleost immunology and speed the development of targeted detection assays and therapeutants.

2. Materials and methods

2.1. Experimental animals and tissue collection

All procedures involving the handling and treatment of fish used during this study were approved by the Auburn University Institutional Animal Care and Use Committee (AU-IACUC) prior to initiation. Channel catfish were reared at the Auburn University Fish Genetics Research Unit prior to challenge. Challenges followed established detailed protocols for ESC [22] and [23]. Fish were challenged

in 30 L aquaria with 3 control and 3 treatment groups. Aquaria were randomly divided into sampling timepoints-3 h treatment, 24 h treatment, 3 d treatment, 3 h control, 24 h control, and 3 d control with forty fish in each aquarium. *E. ictaluri* bacteria were cultured from a single isolate, and were re-isolated from a single symptomatic fish and biochemically confirmed to be *E. ictaluri*, before being inoculated into brain heart infusion (BHI) medium and incubated in a shaker incubator at 25℃ overnight. The concentration of the bacteria was determined using colony forming unit (CFU) per mL by plating 10 µl of 10-fold serial dilutions onto BHI agar plates. During challenge, the bacterial culture with a concentration of 4×10^8 CFU/ml was added into the aquaria. Water was turned off in the aquaria for 2 h of immersion exposure, and then continuous water flow-through resumed for the duration of the challenge experiment.

At 3 h, 24 h and 3 d after challenge, 30 fish were collected from each of the appropriate control and treatment aquaria at each timepoint and euthanized with MS-222 (300 mg/L). The entire intestinal tracts from 10 fish were dissected, bisected and gently washed and pooled together in RNAlater. Samples were flash frozen in liquid nitrogen during collection and stored at -80 ℃ until RNA extraction. During the challenge, symptomatic treatment fish and control fish of each species were collected and confirmed to be infected with *E. ictaluri* and pathogen-free, respectively, at the Fish Disease Diagnostic Laboratory, Auburn University.

2.2. RNA extraction, library construction and sequencing

Total RNA was extracted from tissues using the RNeasy Plus Kit (Qiagen) following manufacturer's instructions and treated with RNase free DNase I (Qiagen) to remove genomic DNA. RNA concentration and integrity of each sample was

measured on an Agilent 2100 Bioanalyzer using a RNA Nano Bioanalysis chip. For each timepoint, equal amounts of RNA from the three replicates were pooled for RNA-seq library construction.

RNA-seq library preparation and sequencing was carried out by HudsonAlpha Genomic Services Lab (Huntsville, AL, USA). cDNA libraries were prepared with 2.14-3.25 ug of starting total RNA and using the Illumina TruSeq RNA Sample Preparation Kit (Illumina), as dictated by the TruSeq protocol. The libraries were amplified with 15 cycles of PCR and contained TruSeq indexes within the adaptors, specifically indexes 1-4. Finally, amplified library yields were 30 ul of 19.8-21.4 ng/ul with an average length of ~270 bp, indicating a concentration of 110-140 nM. After KAPA quantitation and dilution, the libraries were clustered 4 per lane and sequenced on an Illumina HiSeq 2000 instrument with 100 bp PE reads.

2.3. De novo assembly of sequencing reads

Before assembly, raw reads were trimmed by removing adaptor sequences and ambiguous nucleotides. Reads with quality scores less than 20 and length below 30 bp were all trimmed. The resulting high-quality sequences were used in subsequent assembly.

The *de novo* assembly was performed by various de Brujin graph assemblers to obtain the best assembly results [24]. Briefly, the clean reads were first hashed according to a predefined k-mer length, the ‘k-mers’. After capturing overlaps of length k-1 between these k-mers, the short reads were assembled into contigs. We used publicly available programs ABySS version 1.2.5 [25] and Trans-ABySS version 1.2.0, Velvet version 1.1.04 [26] and AssemblyAssembler version 1.3, and

commercially available CLC Genomics Workbench version 4.7.2.

The clean reads from all timepoints were used as input in all the assemblers. ABySS and Velvet assemblies were performed at various k-mer lengths. In ABySS, the k-mer size was set from 50 to 96, assemblies from all k-mers were merged into one assembly by Trans-ABySS. In Velvet, the k-mer was equal to 50, 55, 61, 67, 75, 85 and 97 with insert length 268, and AssemblyAssembler version 1.3 was used to merge different assemblies. In CLC Genomics Workbench, the assembly was performed using default settings. In order to reduce redundancy, the assembly results from different assemblers were passed to CD-Hit [27] version 4.5.4 and CAP3 [28] for multiple alignment and consensus building after trimming contigs less than 200 bp. The threshold was set as identity equal to 1 in CD-Hit, the minimal overlap length and identity equal to 100 bp and 99% in CAP3.

2.4. Gene Annotation and Ontology

Following selection of the Trans-ABySS assembly based on contig number and contig length, assembly contigs were used as queries against the NCBI zebrafish protein database, the UniProtKB/SwissProt database and the non-redundant (nr) protein database using the BLASTX program. The cutoff E-value was set at 1e-5 and only the top gene id and name were initially assigned to each contig. Gene ontology (GO) annotation analysis was performed using the zebrafish BLAST results in Blast2GO version 2.5.0 [29], which is an automated tool for the assignment of gene ontology terms. The zebrafish BLAST result or the nr BLAST result (when a "hypothetical" result was returned in the zebrafish database), was imported to BLAST2GO. The final annotation file was produced after gene-ID mapping, GO term

assignment, annotation augmentation and generic GO-Slim process. The annotation result was categorized with respect to Biological Process, Molecular Function, and Cellular Component at level 2.

2.5. Identification of differentially expressed contigs

The high quality reads from each sample were mapped onto the TransABySS reference assembly using CLC Genomics Workbench software. During mapping, at least 95% of the bases were required to align to the reference and a maximum of two mismatches were allowed. The total mapped reads number for each transcript was determined, and then normalized to detect RPKM (Reads Per Kilobase of exon model per Million mapped reads). The proportions-based test was used to identify the differently expressed genes between control and 3 h, 24 h and 3 d with p-value < 0.05. After quantile normalization of the RPKM values, fold changes were calculated. Analysis was performed using the RNA-seq module and the expression analysis module in CLC Genomics Workbench. Transcripts with absolute fold change values of larger than 1.5 and total read number larger than 5 were included in analysis as differently expressed genes.

Contigs with previously identified gene matches were carried forward for further analysis. Functional groups and pathways encompassing the differently expressed genes were identified based on GO analysis, pathway analysis based on the Kyoto Encyclopedia of Genes and Genomes (KEGG) database, and manual literature review.

2.6. Gene Ontology and Enrichment Analysis

In order to identify overrepresented GO annotations in the differentially expressed gene set compared to the broader reference assembly, GO analysis and enrichment analysis of significantly expressed GO terms was performed using Ontologizer 2.0 [30] using the Parent-Child-Intersection method with a Benjammini-Hochberg multiple testing correction [31]. GO terms for each gene were obtained by utilizing zebrafish annotations for the unigene set. The difference of the frequency of assignment of gene ontology terms in the differentially expressed genes sets were compared to the overall catfish reference assembly. The threshold was set as FDR value < 0.1.

2.7. Experimental validation—QPCR

Fifteen significantly expressed genes were selected for validation using real time QPCR with gene specific primers designed using Primer3 software. Total RNA was extracted using the RNeasy Plus kit (Qiagen) following manufacturer's instructions. First strand cDNA was synthesized by iScript™ cDNA Synthesis Kit (Bio-Rad) according to manufacturer's protocol. All the cDNA products were diluted to 250 ng/μl and utilized for the quantitative real-time PCR reaction using the SsoFast™ EvaGreen® Supermix on a CFX96 real-time PCR Detection System (Bio-Rad Laboratories, Hercules, CA). The thermal cycling profile consisted of an initial denaturation at 95 ℃ (for 30 s), followed by 40 cycles of denaturation at 94 ℃ (5 s), an appropriate annealing/extension temperature (58 ℃, 5 s). An additional temperature ramping step was utilized to produce melting curves of the reaction from 65 ℃ to 95 ℃. The housekeeping gene 18S was set as the reference gene, relative fold changes were calculated in the Relative Expression Software Tool version 2009 [32] based on

the cycle threshold (Ct) values generated by q-RT-PCR.

3. Results

3.1. ESC Challenge

The artificial challenge with virulent *E. ictaluri* resulted in widespread mortality of infected fish at day 7 after exposure. No control fish manifested symptoms of ESC, and randomly selected control fish were confirmed to be negative for *E. ictaluri* by standard diagnosis procedures. Dying fish manifested behavior and external signs associated with ESC infection including hanging in the water column with head up and tail down and petechial hemorrhages along their ventral surface. *E. ictaluri* bacteria were successfully isolated from randomly selected treatment fish.

3.2 Sequencing of short expressed reads from catfish intestine

Illumina-based RNA-sequencing (RNA-seq) was carried out on intestine samples from control catfish as well as from those experimentally-challenged with *E. ictaluri* (3 h, 24 h and 3 d groups). Reads from timepoint-specific samples were distinguished through the use of multiple identifier (MID) tags. A total of 197.6 million 100 bp PE reads were generated on an Illumina HiSeq 2000 instrument in a single lane. Greater than 44 million reads were sequenced for each of the four libraries. After removing ambiguous nucleotides, low-quality sequences (quality scores <20) and sequences less than 30 bp, 99.19% (196 million) of the short reads were preserved. Raw read data are archived at the NCBI Sequence Read Archive (SRA) under Accession **SRP009069**.

3.2. De novo assembly of catfish intestinal transcriptome

Several differing sequence contig assembly algorithms and software programs recently have been developed to address assembly of RNA-seq reads [33]. Given the importance of assembly of long, accurate contigs to capture catfish genes and to correctly identify differential expression, we compared three prominent options for de novo transcriptome assembly as follows: Trans-ABySS, Velvet, and CLC Genomics Workbench (CLC). Among the three, CLC Genomics Workbench differs as commercial software with the ability to operate through a graphic-user interface (GUI) versus a Linux-based command-line interface for Velvet and Trans-ABySS.

3.2.1. Trans-ABySS

Forty-seven mutiple k-mer (k-mer sizes 50-96) assemblies were performed in ABySS, and totally 15 million contigs were generated. Assemblies ranged from 44,663 contigs to 321,992 contigs with N50 sizes from 531 bp to 1453 bp. The combined assembly utilizing Trans-ABySS generated 630,209 contigs with average length of 725 bp and N50 size of 1,676 bp (Table 1). The Trans-ABySS assembly contained 59.7% contigs longer than 200 bp, and 22.3% of contigs were longer than 1000 bp. Contigs less than 200 bp were removed from further analysis. Multiple-k algorithms produce redundant assemblies which may cause errors in subsequent analyses. Despite Trans-ABySS having its own built-in redundancy elimination solutions, we found that additional steps were required to identify a unique reference. Approximately 0.5 million contigs were removed during the length and redundancy filtration steps (CD-Hit and CAP-3), resulting in a final average contig size and contig

number of 893.7 bp and 176,481, respectively (Table 1).

3.2.2. Velvet

Seven assemblies (seven k-mers between 50 and 99 bp) were generated in Velvet totaling 1.2 million contigs. Velvet's AssemblyAssembler was utilized to obtain the combined assembly, resulting in 186,451 contigs with average length of 500.8 bp and N50 of 1,508 bp. Contig length distributions were distinct from the assembly from Trans-ABySS—69.2% of contigs were longer than 200 bp but only 11.2% of contigs were longer than 1000 bp. The average contig size and contig numbers were increased to 743 bp and reduced to 67,081, respectively, after stand-alone redundancy filtration (CD-Hit and CAP3) using conservative cut-off parameters (Table 1).

3.2.3. CLC Genomics Workbench

A fast single k-mer length (k=24; automatically selected) assembly was performed by CLC Genomics Workbench resulting in 332,383 contigs with average length 691.2 bp and N50 size 611 bp (Table 1). Only 36.3% of contigs were longer than 200 bp and 6.15% of contigs were longer than 1000 bp. Due to the non-redundant single-k approach, no changes resulted following CD-Hit/CAP-3 filtering.

3.2.4. Best assembly selection

In a comparison of the assemblies among the three different approaches (Table 1), Trans-ABySS consistently generated a larger percentage of large contigs, the longest

final contig size, and the largest number of contigs after filtering. Additionally, a total of 88.42% of the initial reads mapped to the final Trans-ABySS reference assembly, compared to 54.26% in Velvet and 38.88% in CLC, illustrating the more comprehensive nature of the Trans-ABySS assembly. Therefore, the Trans-ABySS assembly was selected for subsequent gene discovery and differential expression analysis. Assembled contig sequences are available upon request.

3.3. Gene identification and annotation

BLAST-based gene identification was performed to annotate the channel catfish transcriptome and inform downstream differential expression analysis. After gene annotation, 73,330 (41.55%) of the Trans-ABySS contigs had a significant BLAST hit against 15,640 unique zebrafish genes (unigenes; Table 2). In order to further evaluate the quality of the assembled genes, 14,457 unigenes were identified based on hits to the zebrafish database with the more stringent criteria of a BLAST score ≥100 and E-value ≤ 1e-20 (quality matches). Among these quality unigene matches, 2,719 represented genes which had not been

Table 1 Summary of *de novo* assembly results of Illumina sequence data from catfish intestine using various assemblers.

	Trans-ABySS	Velvet	CLC
Contigs(≥100bp)	630,209	186,451	332,383
Large contigs (≥1000bp)	140,357	20,881	20,431
Maximum length (bp)	17,585	16,860	17,653
Average length (bp)	725.1	500.8	339.0
N50 (bp)	1,676	1,508	611
Contigs after length filtering(≥200bp)	376,005	129,025	120,534
Percentage contigs kept after length filtering	59.66%	69.20%	36.26%
Average contig length after length filtering (bp)	1,120	653.7	691.2
Contigs (After CD-HIT-EST+ CAP3)	176,481	67,081	120,534
Average length (bp) (After CD-HIT + CAP3)	893.7	743.0	691.2
Reads mapped to final reference (%)	88.42%	54.26%	38.88%

previously captured by previous EST and general RNA-seq transcriptome work in catfish [34,35]. The same BLAST criteria were used in comparison of the Trans-ABySS reference contigs with the UniProt and nr databases. The largest number of matches was to the nr database with 77,577 contigs with putative gene matches to nr and 19,960 quality unigene matches (Table 2).

Table 2 Summary of gene identification and annotation of assembled catfish contigs based on BLAST homology searches against various protein databases (Zebrafish, UniProt, nr). Putative gene matches were at E-value ≤ 1e-5. Hypothetical gene matches denote those BLAST hits with uninformative annotation. Quality unigene hits denote more stringent parameters, including score≥100, E-value ≤ 1e-20.

	Contigs with putative gene matches	Annotated contigs ≥500bp	Annotated contigs ≥1000bp	Unigene matches	Hypothetical gene matches	Quality Unigene matches
Zebrafish	73,330	37,500	14,868	15,640	1,154	14,457
UniProt	55,551	42,524	31,136	17,476	0	15,786
NR	77,577	51,215	34,742	23,205	2,130	19,960

Unique gene-coding contigs from the channel catfish reference assembly were then used as inputs to perform gene ontology (GO) annotation by Blast2GO [29]. A total of 21,877 GO terms including 5,448 (29.9%) cellular process terms, 6,596 (30.15%) molecular functions terms and 9,833 (44.95%) biological process terms were assigned to 14,457 unique gene matches. Analysis of level 2 GO term distribution showed that metabolic process (GO:0008152), cellular process (GO:0009987), binding (GO:0005488) and cell (GO:0005623) were the most common annotation terms in the three GO categories.

3.4. Identification and analysis of differentially expressed genes

A total of 4,414 of the 176,481 (2.50%) final reference contigs showed significant differential expression for at least one timepoint following infection. Differentially expressed contigs had an average consensus length of 1,088.5 bp. The identified contigs represented 1,633 unigenes, including 1,474 unique genes with more stringent criteria of a BLAST score ≥100 and E-value ≤ 1e-20, and 159 unique genes with BLAST E-value from 1e-20 to 1e-5. In detail, there were 693 genes differentially expressed at 3 h after challenge relative to control, 918 genes differently expressed at 24 h after challenge relative to control, and 1,035 genes differently expressed at 3 d after challenge relative to control (Table 3). Similar numbers of genes were up-regulated and down-regulated at 3 h and 24 h, with the largest number of genes (607) down-regulated at 3 d. Read coverage (average contig size) within the differentially expressed contigs ranged from 256 reads/contig at 3 d to 365 reads/contig at 3 h.

Table 3 Statistics of differently expressed genes at different timepoints following ESC challenge. Values indicate contigs/genes passing cutoff values of fold change ≥1.5 ($p<0.05$) and read number per contig ≥5. Average contig size refers to reads/contig.

	3h	24h	3d
Up-regulated	319	469	428
Down-regulated	374	449	607
Total	693	918	1,035
Average contig size	365	285	256
Total unigenes		1,633	

3.5. Enrichment and Pathway Analysis

The differently expressed unique genes were then used as inputs to perform gene ontology (GO) annotation by Blast2GO. Parent-child GO term enrichment analysis was performed for the 1,633 unigenes to detect significantly overrepresented GO terms. A total of 49 terms with p-value (FDR-corrected) < 0.1 were considered

significantly overrepresented. Ten higher level GO terms were retained as informative for further pathway analysis (Table 4). The GO terms include functions and processes including response to chemical stimulus, MHC protein complex, antigen processing and presentation, intermediate filament cytoskeleton, and antioxidant activity.

Table 4 Summary of GO term enrichment result of significantly expressed genes in channel catfish following ESC challenge. The 1,633 differentially expressed genes were analyzed as the study set in comparison to a total of 14,457 catfish unigenes. p-value≤0.1 was considered significant. Population count is the number of genes associated with the term in the population set. Study count is the number of genes associated with the term in the study set.

GO ID	GO Name	p-Value(FDR)	Population count	Study count
GO:0042221	Response to chemical stimulus	5.311E-05	397	70
GO:0046906	Tetrapyrrole binding	9.551E-05	70	24
GO:0016209	Antioxidant activity	1.515E-03	26	12
GO:0042611	MHC protein complex	7.504E-03	16	8
GO:0006508	Proteolysis	7.936E-03	335	73
GO:0017171	Serine hydrolase activity	9.385E-03	61	21
GO:0030219	Megakaryocyte differentiation	3.328E-02	6	5
GO:0045111	Intermediate filament cytoskeleton	6.465E-02	36	13
GO:0019882	Antigen processing and presentation	9.680E-02	18	8
GO:0008092	Cytoskeletal protein binding	9.880E-02	156	28

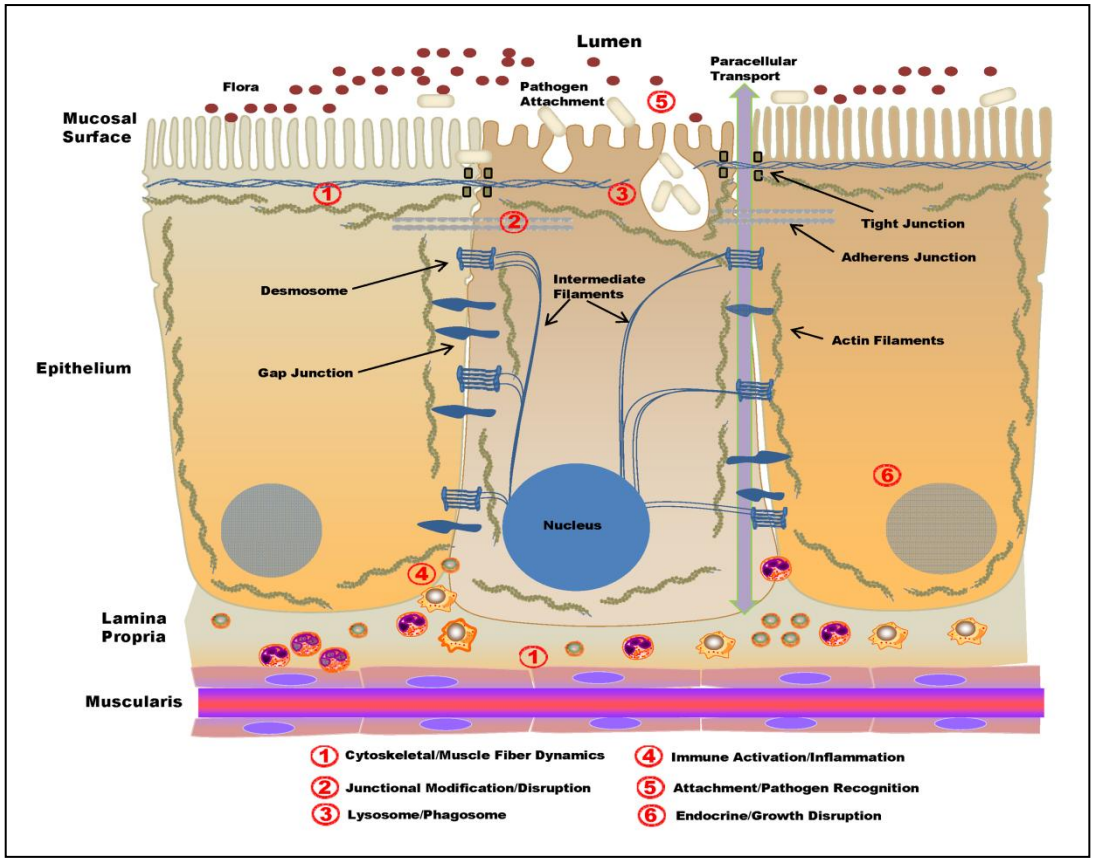

Fig. 1. Diagram of intestinal mucosal barrier structures and components. Putative functional categories of catfish responses to *E. ictaluri* infection are noted with circled numbers (1-6) referring to the accompanying legend.

GO term analysis and downstream pathway analysis were complicated by the incomplete annotation and unique nomenclature characteristic of zebrafish proteins. Automated pathway analysis software often could not resolve zebrafish annotations into large functional categories or pathways. We used a combination of KEGG pathway analysis, manual re-annotation based on the nr database, and manual literature searches to identify six broad functional categories of genes observed to be differentially expressed in the catfish intestine following infection with an enteric pathogen, *E. ictaluri*. These categories are illustrated in the context of a representative diagram of the intestinal mucosal barrier (Fig. 1) and include: 1) cytoskeletal and muscle fiber dynamics; 2) junctional modification and disruption; 3) lysosome/phagosome-associated responses; 4) immune activation and inflammation; 5)

attachment and pathogen recognition; and 6) endocrine/growth disruption. Table 5 lists key, non-redundant gene components of these categories. Putative functional roles and interactions of the genes in the context of *E. ictaluri* invasion and replication are discussed in detail below (Discussion).

Table 5 Key channel catfish genes differentially expressed following ESC challenge. Bold values indicate timepoints where the gene was significantly changed relative to the control.

Functional classification	Gene Name	Contig ID	3h fold change	24h fold change	3d fold change
Cytoskeletal/ Muscle Fiber Dynamics	14-3-3 protein epsilon	Contig19138	**6.92**	2.13	2.33
	Actin, cytoplasmic 1	Contig5287	**-6.03**	-1.49	**2.09**
	AHNAK nucleoprotein	Contig22801	**7.27**	**9.02**	**8.73**
	Alpha actin-1	Contig5133	**-21.4**	**-18.67**	**-20.74**
	Annexin A2	k66_684752	**-5.99**	-1.03	-2.34
	Annexin A2-like	Contig24251	-1.74	**-2.19**	**-3.86**
	Arp2/3	Contig17702	-1.62	**-1.98**	**-2.17**
	Calmodulin 1a	Contig10653	**3.12**	**2.55**	**2.3**
	CDC42SE2	Contig11032	**-5.54**	-1.37	-1.22
	Cofilin 2, like	Contig25509	-1.17	-1.5	**-1.81**
	Collagen alpha-1(V) chain	k_90380157	3.36	**4.81**	4.09
	EMILIN-1	Contig16606	**2.78**	**4.91**	**4.92**
	Epiplakin-like	Contig13325	3.04	**5.85**	**4.46**
	Ezrin like	Contig20491	1.21	**-4.2**	**-2.76**
	Filamin A, alpha	Contig476	**1.98**	**2.18**	**2.31**
	Gelsolin-like (CAPG)	k70_862348	**6.93**	**5.78**	**7.3**
	Keratin, type I cytoskeletal 13	Contig10499	**-11.31**	**-4.43**	**-7.34**
	LIMA1	Contig38617	**3.86**	**4.76**	**3.44**
	Myosin heavy chain	Contig14966	**-72.4**	**-21.66**	**-43.6**
	Myosin light chain kinase b	Contig24474	**1.51**	**1.46**	**1.47**
	Myosin regulatory light polypeptide 9	Contig42338	**3.01**	**6.47**	**7.45**
	Myosin, light polypeptide 3	Contig10157	**-6.2**	**-8.78**	**-4.31**
	Myosin-VII	Contig6265	**2.02**	**2.55**	**2.11**
	Paxillin	Contig11500	1.61	**2.23**	**2.19**
	Profilin-2	Contig16251	-1.06	**-2.37**	1.12
	Protocadherin 1-like	Contig20123	2.01	**2.65**	2.07
	Ras-related protein R-Ras	Contig15983	**4.2**	2.86	**3.85**
	Small GTPase RhoA	Contig4251	-1.43	**-1.73**	**-3.23**
	Supervillin-like, partial	Contig12472	**4.82**	2.9	**4.18**
	Synaptopodin-2	Contig17899	1.95	**2.37**	**2.96**
	Tropomyosin alpha-3 chain 2	k76_731419	**-4.65**	**-3.37**	-1.15
	Type I cytokeratin, enveloping layer	Contig38426	2.49	1.2	**5.96**
Junctional Modification/ Disruption	Aquaporin 8	Contig14861	1.35	**3.02**	**6.42**
	Cadherin 1, type 1 preproprotein	Contig34588	2.01	**3.12**	**4.57**
	Claudin 15a	k65_774609	**-3.28**	**-3.09**	-1.26
	Claudin-9	Contig16617	**-2.31**	-1.24	-1.11

	Desmocollin 2	Contig26678	**3.39**	**3.47**	**3.67**
	Desmoglein-2	Contig6653	2.18	**2.83**	1.95
	Desmoplakin	Contig14264	1.62	**2.16**	**2.36**
	Epithelial cadherin precursor	Contig38947	**-2.75**	-1.22	**-6.04**
	MAGI3	Contig3167	2.76	**5.13**	2.75
	Occludin-like	Contig1340	1.48	**1.86**	1.32
	Plakophilin 3	Contig27202	**1.45**	**1.6**	1.38
	Zonadhesin-like	Contig19706	**2.39**	**1.3**	**1.59**
Lysosome/ Phagosome	ADP-ribosylation factor 1	Contig6638	**2.7**	1.75	1.56
	Beta-galactosidase	k51_958092	**2.06**	**-2.87**	-1.46
	Cathepsin Z	Contig3027	**9.78**	**6.36**	**15.49**
	CD209 antigen (DC-SIGN)	Contig3473	-1.64	**-2.84**	**-2.43**
	CD63 antigen	Contig39977	**3.34**	**2.22**	1.51
	Cytoplasmic dynein 1 heavy chain 1	Contig5492	2.28	2.54	**4.73**
	ER aminopeptidase 2	Contig23351	-1.01	1.42	**3.94**
	Glucocerebrosidase-like	k_87479012	1.41	**2.87**	1.83
	Hexosaminidase B	k_92109136u	-1.04	**-3.29**	**-5.5**
	Immunoglobulin heavy mu-like	Contig31220	-1.38	**-3.68**	**-2.89**
	Legumain	Contig15202	**1.71**	**-1.27**	**1.58**
	Lysosomal alpha-mannosidase	Contig19918	**1.69**	**-1.43**	1.23
	Lysosomal membrane glycoprotein 2	Contig18023	**2.95**	2.21	1.01
	Lysosomal protective protein	Contig3023	**2.21**	**1.58**	**1.53**
	Lysosomal transmembrane protein 4A	Contig996	-1.33	**2.31**	1.59
	Lysosome glycoprotein 1 isoform 2	Contig16856	-1.24	**-1.57**	-1.03
	Lysozyme G-like 1	Contig26961	-1.33	-1.39	**2.44**
	Lysozyme-like protein 2	Contig39554	**-2.75**	-2.41	**7.36**
	MHC class I UXA2	Contig29433	**-12.4**	**-2.52**	-1.14
	MHC class I ZE like	Contig33016	**3.79**	**10.1**	**5.59**
	MHC class II alpha chain 1	Contig35822	**-8.39**	**-20.92**	**-9.48**
	MHC class II beta	Contig23428	**-4.56**	**-6.92**	**-3.88**
	MMP9	Contig9368	-2.14	**-3.98**	-2.15
	MMP13	k54_922997	**-3.02**	**-5.91**	**-8.39**
	NADPH oxidase 1	Contig38009	**-2.98**	**-4.55**	**-3.21**
	NOXO1	Contig4675	**-2.68**	**-7.35**	**-6.47**
	Pip5k1b	k51_308390	2.22	2.86	**6.87**
	Prosaposin	Contig10452	1.49	1.08	**1.63**
	Sialidase-1	k50_918038	**4.58**	2.76	**4.33**
	Sphingosine--phosphate phosphotase 2	k58_866656	-3.39	-1.48	**-5.01**
	Thrombospondin 1	k52_945196	2.83	**3.82**	**3.97**
	Transport protein Sec61 alpha-like 1	k56_745918u	**-2.98**	-1.45	-1.59
Immune Activation/ Inflammation	Apolipoprotein B	Contig5210	**3.16**	**3.36**	**2.05**
	C1Q subcomponent-binding protein	k66_875137	**-9.95**	-1.81	-1.45
	C1q-like 3	k66_929422	**-4.34**	-1.97	-2.79
	CC chemokine 25-like	Contig43069	**-2.43**	-1.47	**1.65**
	CC chemokine SCYA102	Contig10839	1.37	**-3.27**	-1.28
	CC chemokine SCYA104-like	Contig37889	1.02	**-4.19**	**-3.8**
	CC chemokine SCYA113	Contig1891	**-1.87**	**-2.63**	**1.39**
	CC chemokine SCYA117-like	Contig29792	1.52	**4.83**	2.05
	CC chemokine SCYA124	k64_453703u	-1.6	**2.79**	2.39
	Chemokine CXCL12	Contig160	**2.55**	**2.51**	**2.41**
	Chemokine CXCL2	Contig22481	1.23	1.45	**3.53**

	Chemokine receptor-like 1-like	Contig4932	1.98	2.55	**3.21**
	Complement C4-1-like	Contig1264	**3.46**	1.68	-1.18
	Complement C6	Contig11023	1.23	1.23	**5.03**
	Complement C7	Contig17426	-2.62	-1.31	**2.99**
	Glutathione peroxidase 3	Contig16143	**-3.8**	**-3.74**	**-6.59**
	Hypermethylated in cancer 1 protein	k66_275227	**4.79**	**5.76**	3.83
	IgGFc-binding protein	k61_673619	**4**	**2.41**	**2.13**
	Interleukin 11 receptor, alpha	Contig853	**2.42**	**2.81**	**2.3**
	Interleukin 7 receptor	Contig26716	1.87	**3.79**	2.29
	Jun D proto-oncogene-like	k70_513305	**6.6**	**4.59**	2.3
	LEAP-2	Contig14731	**-2.1**	**-2.3**	-1.44
	Macrophage MIF	Contig40086	**3.96**	**9.6**	**4.4**
	Metallothionein-2	Contig38077	**-1.81**	**-1.54**	**-3.04**
	Microfibrillar-associated protein 4-like	Contig40286	1.59	1.04	**2.79**
	Nattectin precursor	Contig16280	**-30.08**	**-12.82**	**-7.71**
	Neurotoxin/C59/Ly-6-like protein	k71_580318	**-1.58**	**-3.86**	**-5.96**
	NF-kappa-B p100 subunit	Contig2282	2.61	2.2	**3.71**
	Novel immune-type receptor 6a	Contig39942	**-2.07**	-1.71	**-2.18**
	Novel immune-type receptor 7	Contig39943	**4.17**	**3.83**	**4.56**
	Prostaglandin E synthase 3	k50_966012u	**5.18**	**5.39**	**4**
	Serum amyloid P component-like 2	Contig32897	**-3.07**	**-2.42**	**-3.42**
	Sialoadhesin	Contig10481	3.57	2.03	**8.5**
	Suppressor of cytokine signaling 1	Contig38899	**3.08**	**-1.95**	**-1.85**
	T-cell receptor beta C beta region	k66_937487	1.17	**4.33**	1.22
	TNF receptor superfamily, member 1a	k78_684621	**7.09**	4.71	**7.89**
	Tnf receptor-associated factor 2b 1	Contig5463	**2.43**	1.05	1.15
	Tumor protein p53-inducible protein 1	Contig15021	1.7	**-10.06**	**-5.06**
Attachment/ Pathogen Recognition	Basigin	Contig3778	**3.22**	**4.98**	**2.9**
	Fibronectin 1b-like 1	Contig8744	4.22	5.08	**8.75**
	Integrin, alpha 3a	Contig4954	2.19	**3.25**	**2.68**
	Integrin, beta 1b	k50_930983	**2.19**	**2.17**	**2.32**
	Integrin, beta 4	Contig1086	1.75	**2.19**	**2.43**
	Mucin 2-like	Contig16584	**4.42**	**5.67**	**5.17**
	Mucin 5, subtype B	Contig43499	1.12	**-2.02**	**-2.19**
	NLRC like-1	Contig37947	**3.85**	**3.74**	1.13
	NLRC like-10	Contig39985	1.93	2.49	**3.88**
	NLRC like-2	Contig42687	**3.34**	2.28	2.02
	NLRC like-3	Contig31182	1.98	**4.42**	2.24
	NLRC like-4	Contig36542	-1.47	1.83	**2.55**
	NLRC like-5	Contig31317	1.48	**2.71**	2.18
	NLRC like-6	Contig35090	1.46	**3.31**	1.29
	NLRC like-7	Contig14252	4.24	**7.2**	**9.36**
	NLRC like-8	Contig17611	1.75	1.64	**2.68**
	NLRC like-9	Contig29963	2.13	2.31	**2.75**
	NOD-3 like	k_93466446	**2.5**	**2.28**	**2.32**
	Podocan-like (ECMP2-like)	Contig8588	**13.42**	6.6	3.53
	Toll-like receptor 5	Contig14983	1.06	1.51	**2.06**
Endocrine/ Growth Disruption	Ghrelin/obestatin preprohormone	Contig41751	**-3.19**	-1.42	1.06
	Igfbp7	Contig7012	**2.24**	-1.02	1.45
	Insulin receptor a	Contig11984	**6.15**	**7.47**	**6.42**
	Insulin-induced gene 1 protein	Contig25801	1.84	-1.77	**-3.08**

	Peptide Y-like	k_83558074	**-5.11**	**-1.52**	**-2.5**
	Relaxin-3	Contig20841	-1.26	-1.52	**-2.92**
	Somatostatin 2-like	k53_727376	**-3.92**	1.2	-2.33

3.7. Validation of RNA-seq profiles by QPCR

In order to validate the differentially expressed genes identified by RNA-Seq, we selected 15 genes for QPCR confirmation, selecting from those with differing expression patterns and from genes of interest based on functional enrichment and pathway results. Samples from control, and 3 h, 24 h and 3 d following challenge (with three replicate samples per timepoint) were used for QPCR. Primers were designed based on contig sequences. Melting-curve analysis revealed a single product for all tested genes. Fold changes from QPCR were compared with the RNA-seq expression analysis results. As shown in Fig. 2, QPCR results were significantly correlated with the RNA-seq results at each timepoint (correlation coefficients 0.86-0.95, p-value <0.001). In general, the RNA-seq results were confirmed by the QPCR results, indicating the reliability and accuracy of the Trans-ABySS reference assembly and RNA-seq expression analysis.

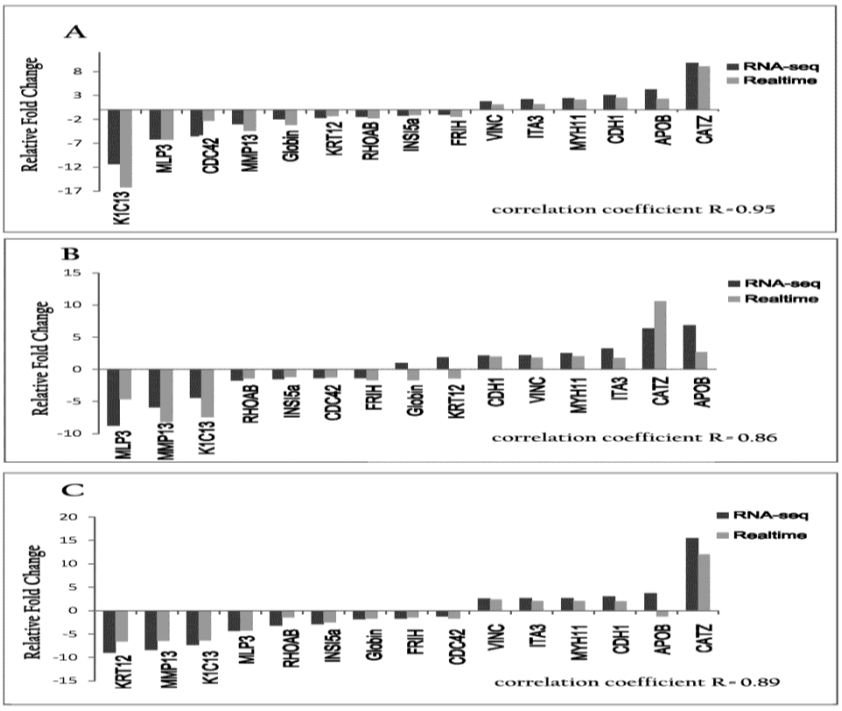

Fig. 2. Comparison of relative fold changes between RNA-seq and QPCR results in catfish intestine
Gene abbreviations are: Insl5a, Insulin-like 5a; KRT12, Keratin 12; FRIH, Ferritin heavy chain; Globin, Alpha globin-like; MLP3, Myosin light polypeptide 3; APOB, Apolipoprotein B; CDH1, Cadherin 1; VINC, Vinculin; RHOAB, Small GTPase RhoA; Integrin, Integrin, ITA3; CATZ, Cathepsin Z; K1C13, Keratin, type I cytoskeletal 13; MMP13, Matrix metalloproteinase 13 preproprotein-like; CDC42, CDC42 small effector protein 2; MYH11, Myosin heavy chain 11.

4. Discussion

Invasive pathogenic bacteria use a multitude of different strategies to penetrate host cells and evade killing. While these mechanisms have been the intense focus of microbiologists for decades, only recently have tools been developed to allow the capture of molecular signatures related to host responses and host-pathogen interactions during infection. Here we have utilized RNA-seq-based expression profiling to examine the transcriptional responses of channel catfish intestinal cells following experimental challenge with *E. ictaluri*, a Gram-negative bacterium.

The present work represents, to our best knowledge, the first RNA-seq-based expression study in catfish and one of a small, but growing, handful in fish species [e.g. 36,37]. It is, therefore, of interest to evaluate the suitability of sequence-based transcript quantification versus established standards such as real-time PCR and microarrays. In catfish, we previously used both a 19K [38] and a 28K microarray [22,39] to analyse changes in gene expression after perturbations of the immune system either from LPS injection or ESC challenge. These studies captured relatively small gene sets (e.g. 76 significant genes in blue catfish liver, [22]) in comparison with the 1,633 unique differentially expressed genes reported here. This could reflect, in part, the ability of RNA-seq to quantify expression levels of novel transcripts. Trans-ABySS-based assembly of our Illumina sequence reads resulted in 176,481 contigs with average length of 893.7 bp. These contigs represented as many as 23,205 unique genes based on BLAST identity (Table 2), including 2,719 genes previously missed in EST sequencing. These results match up well in comparison with previous extensive EST sequencing in multiple tissues from channel catfish and blue catfish which resulted in 14,776 unique genes from 111,578 contigs of average length of 771.3 bp [34].

Additional validation of RNA-seq methods for gene expression analysis was gained through QPCR analysis of expression of selected genes in each of the three timepoints. Transcripts with a variety of expression patterns in the RNA-seq results were tested. Overall, there was significant correlation between the two methods with coefficients

ranging from 0.86-0.95, p-value <0.001 (Fig. 2). There was no consistent bias in expression level observed for either method (i.e. degree of fold-change was not correlated with method). Additionally, a single product was amplified with all tested primer pairs, providing evidence that the contig assembly was accurate and did not result in chimeric transcripts. The QPCR validation also was an important indication that the master pooled samples (3 pools of 10 fish each) used for RNA-seq analysis reflected expression levels in the individual pools. While pooling samples obviously could have masked individual variation, our goal in the present study was to gain a broad understanding of catfish intestinal gene responses to infection and to provide early insights into important pathways and processes. Follow-up studies in our lab (either planned or underway) will use our results here as a foundation for more targeted studies comparing mucosal immune responses between susceptible and resistant lines of catfish, comparing mucosal immune responses to several enteric pathogens, and comparing immune responses to pathogens with that to associated vaccines.

Our study also represents the first characterization of the catfish intestinal transcriptome following infection and is, arguably, among the most comprehensive analyses of intestinal gene expression in teleost fish. The heterogeneous nature of the intestine, with mucosal epithelium, lamina propria, migrating leukocytes, and muscularis (Fig. 1), is additionally complicated by the expectation of differing cellular contributions and expression patterns over its length [14]. Clearly, by utilizing pools

of the entire length of the intestine, the potential exists for masking or confusing gene expression patterns between differing cellular components or intestinal segments. However, we accepted this compromise in this initial study to more broadly characterize intestinal gene expression. The large number of sequenced contigs and differentially expressed genes captured provided ample numbers of candidates which are likely confined to a single cell type (e.g. mucins, aquaporins), while others such as MHC members and chemokines may be derived from multiple intestinal components. Depending on goals of future research, it may be more appropriate to examine gene expression of these candidates solely in the epithelium (or lamina propria) via laser-capture microdissection or enzymatic purification techniques. The time-consuming and expensive nature of these techniques, however, makes it likely that targeted gene assays on large numbers of samples will continue to use whole tissue samples.

Of primary interest in this study was the detection of expression signatures indicative of novel defense strategies and of pathogen-driven manipulation of the cellular machinery of the intestinal epithelium to facilitate entry and replication. We attempted to categorize differentially expressed genes based on six broad functional categories reflective of likely cellular and physiological responses (Table 4). When the identified genes had additional roles outside of or bridging the assigned categories, we attempted to assign functions most appropriate to the context (intestine during infection).

4.1. Cytoskeletal/Muscle Fiber Dynamics

Skirpstunas and Baldwin [21] previously highlighted the potential use of actin polymerization and receptor-mediated endocytosis as modes of infection for *E. ictaluri* in the intestine. Our expression results support their findings with the enrichment of many genes known to play key roles in cytoskeletal rearrangements following infection. The ability of *Salmonella* and *Yersinia*-type bacteria to gain entry through the gut also depends on targeting the actin cytoskeleton [40] and [41] and these bacteria may be excellent models to help inform our understanding of observed molecular changes following *E. ictaluri* infection. Indeed, recent research by Thune et al. [42] indicates that a type III secretion system (T3SS), with functional similarity to that of *Salmonella,* is required for the virulence and replication of *E. ictaluri*. Actin can polymerise into fine and dynamic fibrils or filaments which provide shape and mobility to epithelial cells. Adhesion of bacteria to the host cell surface triggers the accumulation of actin cytoskeletal components forming aggregates and promoting the development of membrane extensions, termed ruffles in the context of *Salmonella* invasion [43]. This bundling of actin filaments facilitates entry via a membrane-containing vacuole that protects the bacteria from lysosomal degradation [3]. Genes associated with bacterially-induced creation of actin-rich structures and observed to be differentially expressed in catfish intestine included Arp2/3, ezrin, filamin, Rho-GTPase, Cdc42SE2, integrins, gelsolin-like (CAPG), supervillin, AHNAK, and

basigin (CD147) among others (Table 4). Gelsolin-like (up-regulated greater than 5-fold at each timepoint) has been observed to be up-regulated in microarray-based studies of *Salmonella* infections in mouse intestine [44] and appears to control membrane ruffling [45]. Some components of actin-rich structures may also serve as receptors or attachment points for pathogens, as in the case of AHNAK, a binding partner for *Chlamydia trachomatis* [46] and up-regulated greater than 7-fold at all timepoints. AHNAK has also been reported to interact with annexin A2 (also differentially expressed in catfish intestine) to regulate cell membrane cytoarchitecture [47]. Another example is basigin, responsible for cell aggregation through cytoskeletal rearrangements, and recently identified as a receptor for *Plasmodium falciparum* [48].

Actomyosin-driven contraction and dynamics can be important in the context of invasion as a central switch controlling both actin polymerization [41] and regulating permeability of apical junctions [49] and [50]. Different myosin components have been reported to be manipulated during pathogen invasion to facilitate entry via endocytosis [41,51]. In *Salmonella* infections, actin and myosin dynamics are manipulated by secreted virulence factors to initially foster entry and then reversed (actin depolymerisation) to lead to host cell apoptosis and further spread of the intracellular infection through macrophage uptake [52]. Inflammation, driven by the TNF pathway, may also function to perturb fiber dynamics [53]. Interestingly, actin and myosin genes featured prominently in our differentially expressed gene set (Table

4), with some patterns likely indicative of up-regulation due to invasion (e.g. Myosin VII), while others may be indicative of pathogen-induced depolymerisation, apoptosis and inflammation (e.g. myosin heavy chain—down-regulated as much as 72-fold; and alpha-actin—down-regulated as much as 21-fold).

4.2. Junctional Modification/Disruption

Enteric pathogens also often seek to disrupt cellular junctions to gain additional routes of access into the host [3,54]. We observed dysregulation of components of the apical junction complex (AJC), consisting of the tight junction, adherens junction, and desmosome. While permeability-regulating claudins were down-regulated, most other junctional proteins were up-regulated (albeit modestly), including cadherins, desmoplakin, and MAGI3 among others, potentially as a part of pathogen-induced cytoskeletal rearrangements and binding [55].

4.3. Lysosome/Phagosome Patterns

A gene signature suggestive of exploitation of the endosomal machinery of catfish for intracellular infection was also detected (Table 4). This included up-regulation of a number of lysosomal surface proteins, and differential expression of a number of MHC subunits [40] and several lysosomal acid hydrolases. This latter

group, which would be expected to contribute to bacterial killing, was mixed in its expression pattern, with a stronger trend towards down-regulation. NADPH oxidase, and the related NOXO1, responsible for production of reactive oxygen species as part of the intracellular host defense, were both notably down-regulated in the catfish intestine, consistent with reported *Salmonella* evasion strategies [56]. This pattern is particularly notable in the light of the ability of virulent *E. ictaluri* (like *Salmonella*) to survive and replicate within macrophages [57,58]. NADPH oxidase and related genes may serve as potential expression markers for assessing ESC-resistant catfish strains.

4.4. Immune Activation/Inflammation

The set of differentially expressed genes encoding innate immune mediators, while large, differed from our initial expectation of a robust up-regulation of defensive strategies and pathways. Indeed, the captured pattern is far more characteristic of immune evasion driven by *E. ictaluri* secreted effectors. We observed dramatic down-regulation (>30-fold at 3 h post infection) of nattectin, a fish C-type lectin, which has been demonstrated to induce the recruitment of specific subsets of monocytes which possess dendritic cell (DC) functions [59]. Interestingly, in one of the few previous studies of intestinal responses to infection in fish, nattectin levels were observed to be higher in disease resistant gilthead seabream [16]. CD209 (DC-

SIGN), another C-type lectin was also down-regulated, as were MMP13 and MMP9, critical in facilitating migration of DC and monocytes to sites of infection [60]. Indicative of shared mucosal immune responses to fish pathogens, we observed sharp down-regulation of tumor suppressor protein p53 at 24 h and 3 d following infection similar to results reported in gills of amoebic gill disease-affected Atlantic salmon [10]. Some innate immune factors known to be up-regulated in response to fish pathogens, were also observed to be down-regulated here, including C1q-like genes [61]; neurotoxin/CD59-like [10,62]; liver-expressed antimicrobial peptide 2 (LEAP-2) [63]; and serum amyloid P [64].

A number of chemokines were differentially expressed following *E. ictaluri* infection. The CC chemokines, highly divergent in fish and extensively characterized by our group previously [23,65,66] were well-represented and showed the largest fold changes at 24 h following infection. CXCL2 and CXCL12, with closer conservation with mammalian counterparts [67], were both up-regulated. Recent research [68,69] indicates that CXCL12 is critical in healing in damaged intestinal epithelium. The pattern of immune evasion continued even among up-regulated genes with macrophage migration inhibitory factor (MIF) and suppressor of cytokine signalling-1 (SOCS1) both induced following bacterial exposure. TNF pathway members, often indicative of harmful inflammation and sepsis, were also up-regulated (Table 4).

4.5. Attachment/Pathogen Recognition

We separated into a discrete category a number of differentially expressed genes with putative roles in pathogen attachment or host recognition. Among these was an abundance of nucleotide-oligomerization domain (NOD)-like receptor subfamily C (NLRC) genes [70,71] with putative roles in intracellular pathogen recognition. These genes, also referred to as NLRP genes, have dramatically expanded in teleost species [71], often assuming non-canonical domain structures. A subset of the differentially expressed NLRC genes are included in Table 4, and were observed to be largely up-regulated in contrast to many other immune mediators. Further work is clearly needed to understand the functions and cellular distributions of this diverse group of receptors in fish. Also in this category was TLR5, known to recognize bacterial flagellin, and well-studied in the context of ESC (e.g. [39,72]). Interestingly, in contrast to previous reports of strong up-regulation, we observed only modest up-regulation at 3 d following infection. The lack of a robust TLR5 response may be due to differing sampled tissues (intestine vs. head kidney, spleen, or liver), or may be consistent with a pathogen-suppressed immune response. Russo et al. [73] reported significantly higher TLR5 expression following infection with attenuated *E. ictaluri* relative to expression of TLR5 in fish infected with virulent *E. ictaluri*.

4.6. Endocrine/Growth Disruption

A final category of interest was composed of differentially expressed genes with putative roles in appetite and growth. Infections in farmed fish are often accompanied by diminished appetite or altered feeding patterns. We observed significant down-regulation of ghrelin, peptide Y-like (PYY), and somatostatin 2-like at 3 h following infection, suggesting that pathogen attachment and entry may rapidly impact important endocrine mediators. In mammals, infection with Gram-negative *Helicobacter pylori* leads to reduced ghrelin concentrations and may be associated with faltering growth [74]. Similarly, decreased concentrations of PYY have been reported in rabbit intestine in response to *Shigella* infections [75]. Future studies should build from these initial observations to study the impact of catfish enteric pathogens and potential therapeutants on neuroendocrine regulation of appetite and growth.

5. Conclusions

Using Illumina RNA-seq technology, we surveyed here for the first time channel catfish transcriptomic responses in the intestine following challenge with the Gram-negative bacterium *E. ictaluri*. The approach was successful in capturing a broad representation of catfish genes (including previously un-sequenced transcripts) and accurately quantifying transcript levels of 1,633 differentially expressed genes. The study revealed novel patterns of teleost mucosal gene expression and highlighted unexpected roles for candidate genes and pathways often missed in *a priori* approaches. Utilization of these findings will improve strategies for selection of disease-resistant catfish broodstock and evaluation of prevention and treatment

options.

References

[1] Turner JR. Intestinal mucosal barrier function in health and disease. *Nat Rev Immunol* 2009;9:799-809.

[2] O'Hara JR, Buret AG. Mechanisms of intestinal tight junctional disruption during infection. *Front Biosci* 2008;13:7008-21.

[3] Guttman JA, Finlay BB. Tight junctions as targets of infectious agents. *Biochim Biophys Acta* 2009;1788:832-41.

[4] Niklasson L, Sundh H, Fridell F, Taranger GL, Sundell K. Disturbance of the intestinal mucosal immune system of farmed Atlantic salmon (*Salmo salar*), in response to long-term hypoxic conditions. *Fish Shellfish Immunol* 2011;31:1072-80.

[5] Perez-Sanchez T, Balcazar JL, Merrifield DL, Carnevali O, Gioacchini G, de Blas I. Ruiz-Zarzuela I. Expression of immune-related genes in rainbow trout (*Oncorhynchus mykiss*) induced by probiotic bacteria during *Lactococcus garvieae* infection. *Fish Shellfish Immunol* 2011;31:196-201.

[6] Russell S, Hayes MA, Lumsden JS. Immunohistochemical localization of rainbow trout ladderlectin and intelectin in healthy and infected rainbow trout (*Oncorhynchus mykiss*). *Fish Shellfish Immunol* 2009;26:154-63.

[7] Komatsu K, Tsutsui S, Hino K, Araki K, Yoshiura Y, Yamamoto A, Nakamura O, Watanabe T. Expression profiles of cytokines released in intestinal epithelial cells of the rainbow trout, *Oncorhynchus mykiss*, in response to bacterial infection. *Dev Comp Immunol* 2009; 33:499-506.

[8] Bernard D, Six A, Rigottier-Gois L, Messiaen S, Chilmonczyk S, Quillet E, Boudinot P, Benmansour A. Phenotypic and functional similarity of gut intraepithelial and systemic T cells in a teleost fish. *J Immunol* 2006;176:3942-9.

[9] Bridle AR, Morrison RN, Nowak BF. The expression of immune-regulatory genes in rainbow trout, *Oncorhynchus mykiss*, during amoebic gill disease (AGD). *Fish Shellfish Immunol* 2006;20:346-64.

[10] Morrison RN, Cooper GA, Koop BF, Rise ML, Bridle AR, Adams MB, Nowak BF. Transcriptome profiling the gills of amoebic gill disease (AGD)-affected Atlantic salmon (*Salmo salar L.*): a role for tumor suppressor p53 in AGD pathogenesis? *Physiol Genomics* 2006;26:15-34.

[11] Rombout JH, van der Tuin SJ, Yang G, Schopman N, Mroczek A, Hermsen T, Taverne-Thiele JJ. Expression of the polymeric Immunoglobulin Receptor (pIgR) in mucosal tissues of common carp (*Cyprinus carpio L.*). *Fish Shellfish Immunol* 2008;24:620-8.

[12] Rajan B, Fernandes JM, Caipang CM, Kiron V, Rombout JH, Brinchmann MF. Proteome reference map of the skin mucus of Atlantic cod (*Gadus morhua*) revealing immune competent molecules. *Fish Shellfish Immunol* 2011;31:224-31.

[13] Palaksha KJ, Shin GW, Kim YR, Jung TS. Evaluation of non-specific immune components from the skin mucus of olive flounder (*Paralichthys olivaceus*). *Fish Shellfish Immunol* 2008;24:479-88.

[14] Rombout JH, Abelli L, Picchietti S, Scapigliati G, Kiron V. Teleost intestinal immunology. *Fish Shellfish Immunol* 2011;31:616-26.

[15] Jima DD, Shah RN, Orcutt TM, Joshi D, Law JM, Litman GW, et al. Enhanced transcription of complement and coagulation genes in the absence of adaptive immunity. *Mol Immunol* 2009;46:1505-16.

[16] Davey GC, Calduch-Giner JA, Houeix B, Talbot A, Sitja-Bobadilla A, Prunet P, et al. Molecular profiling of the gilthead sea bream (*Sparus aurata L.*) response to chronic exposure to the myxosporean parasite *Enteromyxum leei*. *Mol Immunol* 2011;48:2102-12.

[17] Plumb JA, Chappell J. Susceptibility of blue catfish to channel catfish virus. *Proc. Annu. Conf. Southeast. Assoc. Fish Wildl. Agen* 1978;32: 680-5.

[18] Ourth DD, Chung KT: Purification of antimicrobial factor from granules of channel catfish peripheral blood leucocytes. *Biochem Biophys Res Commun* 2004;313:28-36.

[19] Griffin BR, Mitchell AJ. Susceptibility of channel catfish, *Ictalurus punctatus* (Rafinesque), to *Edwardsiella ictaluri* challenge following copper sulphate exposure. *J Fish Dis* 2007;30:581-5.

[20] Hebert P, Ainsworth AJ, Boyd B. Histological enzyme and flow cytometric analysis of channel catfish intestinal tract immune cells. *Dev Comp Immunol* 2002;26:53-62.

[21] Skirpstunas RT, Baldwin TJ. *Edwardsiella ictaluri* invasion of IEC-6, Henle 407, fathead minnow and channel catfish enteric epithelial cells. *Dis Aquat Organ* 2002;51:161-7.

[22] Peatman E, Terhune J, Baoprasertkul P, Xu P, Nandi S, Wang S, et al. Microarray analysis of gene expression in the blue catfish liver reveals early activation of the MHC class I pathway after infection with *Edwardsiella ictaluri*. *Mol Immunol* 2008;45:553-66.

[23] Peatman E, Bao B, Peng X, Baoprasertkul P, Brady Y, Liu Z. Catfish CC chemokines: genomic clustering, duplications, and expression after bacterial infection with *Edwardsiella ictaluri*. *Mol Genet Genomics* 2006;275:297-309.

[24] Miller JR, Koren S, Sutton G. Assembly algorithms for next-generation sequencing data. *Genomics* 2010;95:315-27.

[25] Simpson JT, Wong K, Jackman SD, Schein JE, Jones SJM, Birol I. ABySS: A parallel assembler for short read sequence data. *Genome Res* 2009;19:1117-23.

[26] Zerbino DR, Birney E. Velvet: Algorithms for de novo short read assembly using de Bruijn graphs. *Genome Res* 2008;18:821-9.

[27] Li W, Godzik A. Cd-hit: a fast program for clustering and comparing large sets of protein or nucleotide sequences. *Bioinformatics* 2006;22:1658-9.

[28] Huang X, Madan A. CAP3: A DNA sequence assembly program. *Genome Res* 1999;9:868-77.

[29] Gotz S, Garcia-Gomez JM, Terol J, Williams TD, Nagaraj SH, Nueda MJ, et al. High-throughput functional annotation and data mining with the Blast2GO suite. *Nucleic Acids Res* 2008;36:3420-35.

[30] Bauer S, Grossmann S, Vingron M, Robinson PN. Ontologizer 2.0-a multifunctional tool for GO term enrichment analysis and data exploration. *Bioinformatics* 2008;24:1650-1.

[31] Grossmann S, Bauer S, Robinson PN, Vingron M. Improved detection of overrepresentation of Gene-Ontology annotations with parent child analysis. *Bioinformatics* 2007;23:3024-31.

[32] Pfaffl MW, Horgan GW, Dempfle L. Relative expression software tool (REST) for group-wise comparison and statistical analysis of relative expression results in real-time PCR. *Nucleic Acids Res* 2002;30:e36.

[33] Martin JA, Wang Z. Next-generation transcriptome assembly. *Nat Rev Genet 2011*;12:671-82.

[34] Wang S, Peatman E, Abernathy J, Waldbieser G, Lindquist E, Richardson P, et al.

Assembly of 500,000 inter-specific catfish expressed sequence tags and large scale gene-associated marker development for whole genome association studies. *Genome Biol* 2010;11:R8.

[35] Liu S, Zhou Z, Lu J, Sun F, Wang S, Liu H, et al. Generation of genome-scale gene-associated SNPs in catfish for the construction of a high-density SNP array. *BMC Genomics* 2011;12:53.

[36] Xiang LX, He D, Dong WR, Zhang YW, Shao JZ. Deep sequencing-based transcriptome profiling analysis of bacteria-challenged *Lateolabrax japonicas* reveals insight into the immune-relevant genes in marine fish. *BMC Genomics* 2010;11:472.

[37] Mu Y, Ding F, Cui P, Ao J, Hu S, Chen X. Transcriptome and expression profiling analysis revealed changes of multiple signaling pathways involved in immunity in the large yellow croaker during *Aeromonas hydrophila* infection. *BMC Genomics* 2010;11:506.

[38] Li RW, Waldbieser GC. Production and utilization of a high-density oligonucleotide microarray in channel catfish, *Ictalurus punctatus*. *BMC Genomics* 2006;7:134.

[39] Peatman E, Baoprasertkul P, Terhune J, Xu P, Nandi S, Kucuktas H, et al. Expression analysis of the acute phase response in channel catfish (*Ictalurus punctatus*) after infection with a Gram-negative bacterium. *Dev Comp Immunol* 2007;31:1183-96.

[40] Garcia-del Portillo F, Pucciarelli MG, Jefferies WA, Finlay BB. *Salmonella typhimurium* induces selective aggregation and internalization of host cell surface proteins during invasion of epithelial cells. *J Cell Sci* 1994; 107:2005-20.

[41] Hanisch J, Kolm R, Wozniczka M, Bumann D, Rottner K, Stradal TE. Activation

of a RhoA/myosin II-dependent but Arp2/3 complex-independent pathway facilitates *Salmonella* invasion. *Cell Host Microbe* 2011;9:273-85.

[42] Thune RL, Fernandez DH, Benoit JL, Kelly-Smith M, Rogge ML, Booth NJ, Landry CA, Bologna RA: Signature-tagged mutagenesis of *Edwardsiella ictaluri* identifies virulence-related genes, including a salmonella pathogenicity island 2 class of type III secretion systems. *Appl Environ Microbiol* 2007;73:7934-46.

[43] Hallstrom K, McCormick BA. *Salmonella* Interaction with and Passage through the Intestinal Mucosa: Through the Lens of the Organism. *Front Microbiol* 2011;2:88.

[44] Liu X, Lu R, Xia Y, Sun J. Global analysis of the eukaryotic pathways and networks regulated by *Salmonella typhimurium* in mouse intestinal infection in vivo. *BMC Genomics* 2010;11:722.

[45] Parikh SS, Litherland SA, Clare-Salzler MJ, Li W, Gulig PA, Southwick FS. CapG(-/-) mice have specific host defense defects that render them more susceptible than CapG(+/+) mice to *Listeria monocytogenes* infection but not to *Salmonella enterica serovar Typhimurium* infection. *Infect Immun* 2003;71:6582-90.

[46] Hower S, Wolf K, Fields KA. Evidence that CT694 is a novel *Chlamydia trachomatis* T3S substrate capable of functioning during invasion or early cycle development. *Mol Microbiol* 2009;72:1423-37.

[47] Benaud C, Gentil BJ, Assard N, Court M, Garin J, Delphin C, Baudier J. AHNAK interaction with the annexin 2/S100A10 complex regulates cell membrane cytoarchitecture. *J Cell Biol* 2004;164:133-44.

[48] Crosnier C, Bustamante LY, Bartholdson SJ, Bei AK, Theron M, Uchikawa M, et al. Basigin is a receptor essential for erythrocyte invasion by *Plasmodium*

falciparum. *Nature* 2011;480:534-7.

[49] Turner JR. 'Putting the squeeze' on the tight junction: understanding cytoskeletal regulation. *Semin Cell Dev Biol* 2000;11:301-8.

[50] Ivanov AI, Bachar M, Babbin BA, Adelstein RS, Nusrat A, Parkos CA. A unique role for nonmuscle myosin heavy chain IIA in regulation of epithelial apical junctions. PLoS ONE 2007;2:e658.

[51] Sousa S, Cabanes D, El-Amraoui A, Petit C, Lecuit M, Cossart P. Unconventional myosin VIIa and vezatin, two proteins crucial for *Listeria* entry into epithelial cells. *J Cell Sci* 2004;117:2121-30.

[52] Guiney DG, Lesnick M. Targeting of the actin cytoskeleton during infection by *Salmonella* strains. *Clin Immunol* 2005; 114:248-55.

[53] Dekelbab BH, Witchel SF, DeFranco DB. TNF-alpha and glucocorticoid receptor interaction in L6 muscle cells: a cooperative downregulation of myosin heavy chain. *Steroids* 2007;72:705-12.

[54] Fasano A, Nataro JP. Intestinal epithelial tight junctions as targets for enteric bacteria-derived toxins. *Adv Drug Deliv Rev* 2004;56:795-807.

[55] Eckmann L, Kagnoff MF. Intestinal mucosal responses to microbial infection. *Springer Semin Immunopathol* 2005;27:181-96.

[56] Vazquez-Torres A, Xu Y, Jones-Carson J, Holden DW, Lucia SM, Dinauer MC, et al. *Salmonella* pathogenicity island 2-dependent evasion of the phagocyte NADPH oxidase. *Science* 2000;287:1655-8.

[57] Booth NJ, Beekman JB, Thune RL. *Edwardsiella ictaluri* encodes an acid-activated urease that is required for intracellular replication in channel catfish (*Ictalurus punctatus*) macrophages. *Appl Environ Microbiol* 2009;75:6712-20.

[58] Russo R, Shoemaker CA, Panangala VS, Klesius PH. In vitro and in vivo

interaction of macrophages from vaccinated and non-vaccinated channel catfish (*Ictalurus punctatus*) to *Edwardsiella ictaluri*. *Fish Shellfish Immunol* 2009;26:543-52.

[59] Saraiva TC, Grund LZ, Komegae EN, Ramos AD, Conceicao K, Orii NM, et al. Nattectin a fish C-type lectin drives Th1 responses in vivo: licenses macrophages to differentiate into cells exhibiting typical DC function. *Int Immunopharmacol* 2011;11:1546-56.

[60] Nagase H, Woessner JF, Jr.. Matrix metalloproteinases. *J Biol Chem* 1999; 274: 21491-4.

[61] Carland TM, Locke JB, Nizet V, Gerwick L. Differential expression and intrachromosomal evolution of the sghC1q genes in zebrafish (*Danio rerio*). *Dev Comp Immunol* 2012;36:31-8.

[62] Martin SA, Blaney SC, Houlihan DF, Secombes CJ. Transcriptome response following administration of a live bacterial vaccine in Atlantic salmon (*Salmo salar*). *Mol Immunol* 2006;43:1900-11.

[63] Bao B, Peatman E, Xu P, Li P, Zeng H, He C, Liu Z. The catfish liver-expressed antimicrobial peptide 2 (LEAP-2) gene is expressed in a wide range of tissues and developmentally regulated. *Mol Immunol* 2006;43:367-77.

[64] Huong Giang DT, Van Driessche E, Vandenberghe I, Devreese B, Beeckmans S. Isolation and characterization of SAP and CRP, two pentraxins from Pangasianodon (*Pangasius*) *hypophthalmus*. *Fish Shellfish Immunol* 2010;28:743-53.

[65] Bao B, Peatman E, Peng X, Baoprasertkul P, Wang G, Liu Z. Characterization of 23 CC chemokine genes and analysis of their expression in channel catfish (*Ictalurus punctatus*). *Dev Comp Immunol* 2006;30:783-96.

[66] Peatman E, Liu Z. CC chemokines in zebrafish: evidence for extensive intrachromosomal gene duplications. *Genomics* 2006;88:381-5.

[67] Baoprasertkul P, He C, Peatman E, Zhang S, Li P, Liu Z. Constitutive expression of three novel catfish CXC chemokines: homeostatic chemokines in teleost fish. *Mol Immunol* 2005;42:1355-66.

[68] Agle KA, Vongsa RA, Dwinell MB. Calcium mobilization triggered by the chemokine CXCL12 regulates migration in wounded intestinal epithelial monolayers. *J Biol Chem* 2010;285:16066-75.

[69] Agle KA, Vongsa RA, Dwinell MB. Chemokine stimulation promotes enterocyte migration through laminin-specific integrins. *Am J Physiol Gastrointest Liver Physiol* 2011;301:G968-80.

[70] Sha Z, Abernathy JW, Wang S, Li P, Kucuktas H, Liu H, Peatman E, Liu Z: NOD-like subfamily of the nucleotide-binding domain and leucine-rich repeat containing family receptors and their expression in channel catfish. *Dev Comp Immunol* 2009;33:1-999.

[71] Hansen JD, Vojtech LN, Laing KJ. Sensing disease and danger: a survey of vertebrate PRRs and their origins. *Dev Comp Immunol* 2011;35:886-97.

[72] Bilodeau AL, Waldbieser GC: Activation of TLR3 and TLR5 in channel catfish exposed to virulent *Edwardsiella ictaluri*. *Dev Comp Immunol* 2005;29:713-21.

[73] Russo R. An Attenuated Strain of *Edwardsiella ictaluri* is killed by channel catfish (*Ictalurus punctatus*) macrophages and confers protection in few days. *Dyn. Biochem. Process Biotech. Mol. Biol* 2011;76-82.

[74] Osawa H, Nakazato M, Date Y, Kita H, Ohnishi H, Ueno H, Shiiya T, Satoh K, Ishino Y, Sugano K. Impaired production of gastric ghrelin in chronic gastritis associated *with Helicobacter pylori*. *J Clin Endocrinol Metab*.2005;90:10-6.

[75] Svensson L, Bergquist J, Wennerås C. Neuromodulation of experimental *Shigella* infection reduces damage to the gut mucosa. *Microbes Infect* 2004;6:256-64.

III. EVASION OF MUCOSAL DEFENSES DURING *AEROMONAS HYDROPHILA* INFECTION OF CHANNEL CATFISH (*ICTALURUS PUNCTATUS*) SKIN

1. Introduction

The mucosal surfaces of mammals have long been recognized as the first defensive barrier against infection by pathogenic microorganisms [1]. While classical immunoregulatory tissues and organs such as spleen, liver, and lymphoid follicles often control the nature and scope of the secondary, systemic response, the local immune actors in the gastrointestinal, respiratory, and genitourinary tracts determine the success of critical early steps in pathogenesis including adhesion, entry, and replication. Similarly, interest in understanding components of the mucosal immune response in fish (gills, skin, gastrointestinal tract) is growing [2, 3]. Our current knowledge of mucosal immune factors in fish, while still limited, now includes a startling diversity of antimicrobial peptides, lectins, assorted pathogen recognition receptor (PRR) family members, lysozymes, and novel teleost immune respondents [4, 5]. Differential expression and regulation of these genes likely play critical roles in determining patterns of host resistance to the myriad of aquatic pathogens present in culture environments. Furthermore, because of the role of mucosal tissues as sensors and integrators of environmental and nutritional status cues, mucosal immune actors are sensitive, critical targets for manipulation using improved diets and topical therapeutants [6].

Catfish (*Ictalurus sp.*) are an important aquaculture organism and a long-standing research model for teleost immunology. Catfish researchers have developed a large base of biochemical information on the structure and function of catfish immunoglobulins (Igs) and antibodies [7],

while genomic approaches have helped to characterize a growing cross-section of the catfish innate immune system [8-12]. While catfish remains the dominant aquaculture species in the United States, the industry has faced a series of setbacks in recent years. Among these have been severe outbreaks of a motile aeromonad septicemia (MAS), whose etiological agent is *Aeromonas hydrophila*. *A. hydrophila*, a Gram-negative bacterium, is usually considered as a secondary pathogen in disease outbreaks among cultured fish species. However, in these cases, *A. hydrophila* appears to have emerged as a primary pathogen, causing the loss of more than 3 million pounds of channel catfish (*Ictalurus punctatus*) in 2009 alone [13].

Recently, we have successfully employed transcriptomic tools including microarrays [14, 15] and RNA-Seq [5, 16] to identify non-classical immune candidates following bacterial infection in catfish. Follow-up studies have served to further characterize roles of these candidates and examine their utility as potential biomarkers in genetic selection programs [6, 17]. In this same vein, here we utilized an 8 x 60K Agilent microarray to examine global mucosal immune responses in the channel catfish skin following experimental challenge with virulent *A. hydrophila*.

2. Materials and methods

2.1. Experimental animals and tissue collection

All procedures involving the handling and treatment of fish used during this study were approved by the Auburn University Institutional Animal Care and Use Committee (AU-IACUC) prior to initiation. Marion channel catfish (30 ± 1.6 g) were reared at the Auburn University Fish Genetics Research Unit prior to challenge.

Prior to experiments, fish were maintained in 30 L tanks (20 L water) and acclimatized for 5 days before immersion bath. Experimental fish were confirmed to be culture negative for bacterial infection by culturing posterior kidney tissues from representative groups of fish on tryptic soy agar (TSA) plates. A 12:12 hour light:dark period was maintained and supplemental aeration was supplied by an air stone. The water temperature was controlled at 28℃.

Fish were challenged in 3 control and 3 treatment groups per timepoint in each group. Aquaria were randomly divided into sampling timepoints-2 h treatment, 8 h treatment, 12 h treatment, 2 h control, 8 h control, and 12 h control with thirty fish in each aquarium. *A. hydrophila* bacteria were cultured from a single isolate (AL09-71), used in a trial challenge, re-isolated from a single symptomatic fish and biochemically confirmed to be *A. hydrophila*, before being inoculated into tryptic soy broth (TSB) and incubated in a shaker incubator at 28℃ overnight. The concentration of the bacteria was determined using colony forming unit (CFU) per mL by plating 10 µl of 10-fold serial dilutions onto TSA agar plates.

To aid in infection, skin mucus was removed by gentle scraping with a dull spatula from an approximately 4 cm^2 area below the dorsal fin immediately prior to immersion challenge. Immersion experiments were performed in a 25 L bucket with aeration. Briefly, 50 ml of overnight bacterial cells 1.5×10^9 were added to water to give a final volume of 5 L (1.5×10^7 final exposure concentration). Thirty channel catfish were immersed in each bucket for 2 h. After the 2 h immersion, the catfish were distributed to 30 L glass aquaria. Control fish were treated in the same manner as the infected fish with mucus scraped and were held in buckets with the addition of sterilized TSB prior to transfer to aquaria.

At 2 h, 8 h and 12 h after challenge, 30 fish were collected from each of the appropriate control and treatment aquaria at each timepoint and euthanized with MS-222 (300 mg/L). The

skin from 8 fish/replicate pool were pooled together in equal amounts and flash frozen in liquid nitrogen during collection and stored at -80 ℃ until RNA extraction. During the challenge, symptomatic treatment fish and control fish were collected and confirmed to be infected with *A. hydrophila* and pathogen-free, respectively, at the Fish Disease Diagnostic Laboratory, Auburn University.

2.2. RNA extraction and probe labeling

Samples were homogenized with mortar and pestle in the presence of liquid nitrogen. Total RNA was extracted from tissues using the RNeasy Plus Universal Mini Kit (Qiagen) following manufacturer's instructions. RNA concentration and integrity of each sample was measured using NanoDrop ND-1000 UV-VIS Spectrophotometer version 3.2.1. Fluorescently labeled complementary RNA (cRNA) probes were generated using the Two Color Microarray Quick Labeling kit (Agilent Technologies, Palo Alto, CA, USA) and following the manufacturer's instructions. Briefly, cDNA was generated from 500 ng of each isolated RNA sample; cRNA was then made using Cy3-CTP or Cy5-CTP incorporation for labeling purposes. The fluorescently labeled cRNA probes were purified using the Qiagen RNeasy Mini Kit (Qiagen Inc., Valencia, CA, USA), and the concentration, fluorescent intensities, and quality of labeled cRNA probes were determined using a Nano-drop spectrophotometer. At each timepoint, 3 Cy3 labeled cRNA and 3 Cy5 labeled cRNA were generated with randomized dye assignments between treatment and control samples.

2.3. Microarray design and probe hybridization

Microarray interrogations were performed using a custom-designed, Agilent-based microarray platform with 8 x 60K probes per slide layout. Catfish cDNA contigs were collected from previous catfish EST and RNA-seq studies [14, 18, 19]. Annotation was conducted based on the NCBI zebrafish database using the BLASTX program, a cutoff E-value of e^{-5}, and selection of the top informative hit. In total, 29,732 contigs from channel catfish and 21,208 contigs from blue catfish were selected, and 38 genes were selected as controls and repeated 10 times across the array (Table 1). The rest of the array was populated with Agilent positive and negative controls. Specific probes were designed using Agilent's eArray online probe design tool with X-hyb potential less than 2 and a Base Composition (BC) content score below BC3.

Table 1 Summary of the probe design for a catfish Agilent 8 x 60K two-color gene expression microarray containing features from both channel catfish and blue catfish. Known probes were designed from unique transcripts which had a significant BLAST hit (E value e-10, score >100).

	Channel_known	Channel_unknown	Blue_known	Blue_unknown
Probes	17,038	12,694	13,377	7,831
Total		50,940		

Hybridization, washing and scanning were performed according to the Agilent two-color microarray-based gene expression analysis protocol (version 5.5, February 2007) by the University of Florida.

2.4. Microarray data analysis

Following hybridization, the slides were scanned using a GenePix personal 4100A Scanner (Axon Instruments) and initial analysis were performed with Feature Extraction software v9.5.3

(Agilent). Background correction of feature intensities was performed within this software. After lowess normalization of background-corrected data, normalized data was imported to ArrayStar software 5 (DNASTAR Inc., Madison, WI), and then the Moderated t-test was performed to detect the differently expressed genes [20]. At each timepoint, the expression values of the three replicates of *A. hydrophila* infected fish were compared to that of the three replicates of the control fish and used to calculate fold changes and p-values. The genes with fold change greater than 2.0 and $p \leq 0.05$ were considered as differently expressed. Only channel catfish features (known and unknown) were used for expression analysis in this experiment. Functional groups of the differently expressed genes were identified based on GO analysis and manual literature review and were subjected to further BLAST analysis to verify their identities.

2.5. Gene ontology analysis

Gene ontology (GO) annotation analysis was performed using the zebrafish BLAST results in Blast2GO version 2.5.0 (http://www.blast2go.org/), which is an automated tool for the assignment of gene ontology terms. The final annotation file was produced after gene-ID mapping, GO term assignment, annotation augmentation and generic GO-Slim process. The annotation result was categorized with respect to Biological Process, Molecular Function, and Cellular Component at level 2.

In order to identify overrepresented GO annotations in the differentially expressed gene set compared to the whole channel microarray gene set, GO analysis and enrichment analysis of significantly expressed GO terms was performed using Ontologizer 2.0 [21] using the Parent-Child-Intersection method with a Benjammini-Hochberg multiple testing correction [22]. GO terms for each gene were obtained by utilizing zebrafish annotations for the unigene set. The

frequency of assignment of gene ontology terms in the differentially expressed genes sets were compared to frequency within the overall channel catfish reference transcriptome. The threshold was set as FDR value < 0.1.

2.6. Experimental validation—QPCR

Ten significantly expressed genes were selected for validation using real time QPCR with gene specific primers designed using Primer3 software. Total RNA was extracted using the RNeasy Plus Universal Mini Kit (Qiagen) following manufacturer's instructions. First strand cDNA was synthesized by iScript™ cDNA Synthesis Kit (Bio-Rad) according to manufacturer's protocol. All the cDNA products were diluted to 250 ng/µl and utilized for the quantitative real-time PCR reaction using the SsoFast™ EvaGreen® Supermix on a CFX96 real-time PCR Detection System (Bio-Rad Laboratories, Hercules, CA). Real-time PCR was performed in a total volume of 20 µl with cycling conditions: 94°C for 5 s, followed by 40 cycles of 94°C for 5 s, 60 ℃ for 5 s (fluorescence measured), and a disassociation curve profile of 65 ℃ to 95 ℃ for 5 s/0.5 ℃ increment. Results were expressed relative to the expression levels of 18S rRNA in each sample using the Relative Expression Software Tool (REST) version 2009 [23]). The biological replicate fluorescence intensities of the control and treatment products for each gene, as measured by crossing-point (*C*t) values, were compared and converted to fold differences by the relative quantification method. Expression differences between groups were assessed for statistical significance using a randomization test in the REST software. The mRNA expression levels of all samples were normalized to the levels of 18S ribosomal RNA gene in the same samples. A no-template control was run on all plates. QPCR analysis was repeated in triplicate

runs (technical replicates) to confirm expression patterns.

3. Results

3.1. A. hydrophila challenge

Extensive pre-challenge experiments examined the ability of virulent *A. hydrophila* to infect channel catfish fingerlings following bath challenge to allow natural routes of infection vs. i.p. injection [24]. Bath challenges alone, regardless of exposure concentration or conditions, were unsuccessful in initiating *A. hydrophila* infection. However, disrupting the mucus covering of the skin by gentle scraping (see Methods), followed by immediate challenge produced an effective, reproducible challenge model. We, therefore, adopted this model here to study infection-based changes in skin following infection.

The artificial challenge with virulent *A. hydrophila* showed initial mortality of infected fish beginning at 18 h after exposure and resulting in a final cumulative mortality of 42.5% at 48 h. No control fish manifested symptoms of *A. hydrophila*, and randomly selected control fish were confirmed to be negative for *A. hydrophila* by standard diagnosis procedures. Dying fish manifested external signs associated with *A. hydrophila* infection including redness in the eyes, petechial hemorrhaging and exophthalmia. *A. hydrophila* bacteria were successfully isolated from randomly selected treatment fish.

3.2. Identification and analysis of differentially expressed genes

A total of 2,168 unique genes (based on assigned identifies from the zebrafish unigene

database) showed significant differential expression in skin during at least one timepoint following infection. In detail, there were 82 differentially expressed genes at 2 h after challenge relative to control, 567 genes differently expressed at 8 h after challenge relative to control, and 1,744 genes differently expressed at 12 h after challenge relative to control. At 8 h and 12 h, there were much greater numbers of upregulated genes than down-regulated genes. For example, at 12 h post infection, 1,559 genes were upregulated, compared to only 185 downregulated genes (Table 2). Feature values and metadata of the experiment are archived at the NCBI Gene Expression Omnibus (GEO) under Accession **GSE40733**.

Table 2 Statistics of differently expressed genes at different timepoints following *A. hydrophila* challenge. Values indicate cutoff values of fold change ≥2 ($p<0.05$) at a least one timepoint following challenge.

	2h	8h	12h
Upregulated	20	529	1,559
Downregulated	62	38	185
Total	82	567	1,744
Total unigenes		2,168	

3.3. Gene ontology and Eenrichment Analysis

Differently expressed genes were then used as inputs to perform gene ontology (GO) annotation by Blast2GO. A total of 4,155 GO terms including 1,080 (25.99%) cellular component terms, 1,026 (24.69%) molecular functions terms and 2,049 (49.31%) biological process terms were assigned to 3,354 unique gene matches. Analysis of level 2 GO term distribution showed that metabolic process (GO:0008152), cellular process (GO:0009987), binding (GO:0005488) and cell (GO:0005623) were the most common annotation terms in the three GO categories.

The differently expressed unique genes were then used as inputs to perform enrichment analysis using Ontologizer. Parent-child GO term enrichment analysis was performed for the 2,168 unigenes to detect significantly overrepresented GO terms. A total of 29 terms with p-value (FDR-corrected) < 0.1 were considered significantly overrepresented. Ten higher level GO terms were retained as informative for further pathway analysis (Table 3). The GO terms include functions and processes including cellular response to stress, receptor signaling protein activity, G-protein coupled peptide receptor activity and protein kinase C-activating G-protein coupled receptor signaling pathway.

Table 3 Summary of GO term enrichment result of significantly expressed genes in channel catfish following *A. hydrophila* challenge. The 2,168 differentially expressed genes were analyzed as the study set in comparison to all the catfish unigenes. P-value ≤ 0.1 was considered significant. Population count is the number of genes associated with the term in the population set. Study count is the number of genes associated with the term in the study set. GO names were retained only from GO terms of levels >2.

GO ID	GO Name	p-Value(FDR)	Population count	Study count
GO:0007167	Enzyme linked receptor protein signaling pathway	1.02E-05	190	40
GO:0035556	Intracellular signal transduction	0.000153	702	123
GO:0071841	Cellular component organization or biogenesis at cellular level	0.00438	924	180
GO:0006950	Response to stress	0.00635	497	97
GO:0033554	Cellular response to stress	0.0175	204	47
GO:0031974	Membrane-enclosed lumen	0.0425	379	73
GO:0005057	Receptor signaling protein activity	0.0425	43	11
GO:0060249	Anatomical structure homeostasis	0.0499	19	9
GO:0008528	G-protein coupled peptide receptor activity	0.0847	84	11
GO:0007205	Protein kinase C-activating G-protein coupled receptor signaling pathway	0.0961	9	4

Based on enrichment analysis and manual annotation and literature searches, representative key genes were arranged into 5 categories, including antioxidant/cellular stress response,

cytoskeletal rearrangement, immune response, junctional/adhesion, and neural/nervous system regulation (Table 4). Imputed putative functional roles of these genes are covered in the Discussion.

Table 4 Representative key functional categories and gene members differentially expressed in skin following *A. hydrophila* challenge. Bold values indicate significant fold change ($p \leq 0.05$).

Gene Name	Probe_ID	2h	8h	12h
Antioxidant/Cellular Stress Response				
15 kDa selenoprotein precursor	Contig39146	2.15	**2.21**	1.65
60 kDa heat shock protein, mitochondrial	Contig3790	**-12.80**	-3.28	**-52.40**
Cysteine and histidine-rich DCP1	Contig361	**-20.71**	-3.94	**-71.02**
FK506 binding protein 4	Contig13508	**-16.86**	-3.69	**-71.21**
Heat shock protein HSP 90-alpha 1	UN13454	2.48	-1.02	**5.78**
Heat shock protein HSP 90-beta	UN17753	1.68	1.23	**3.66**
Hsp90 co-chaperone Cdc37-like 1	Contig9447	4.61	-1.17	**2.50**
Selenoprotein O	Contig8	-1.13	1.21	**3.15**
Selenoprotein T2 precursor	UN14891	1.46	1.13	**2.95**
Selenoprotein X, 1b	UN06529	1.32	-1.52	**5.48**
Superoxide dismutase	Contig24529	2.13	1.02	**9.81**
Cytoskeletal Rearrangement				
Capping protein (actin filament), gelsolin	k66_388284	2.86	1.28	**3.37**
Cell division cycle 42	k50_454763	**-9.94**	-1.36	**-12.24**
Dynein, light chain, LC8-type 2a	UN18480	**-25.54**	-1.62	**-94.55**
Ephrin type-A receptor 2	Contig17991	-1.23	1.36	**7.63**
F-actin capping protein alpha-1 subunit	Contig20689	4.32	1.17	**3.85**
Gelsolin b	UN26079	**-24.96**	1.71	**2.18**
Integrin, beta 4	Contig12705	**6.90**	1.80	**5.02**
Myosin heavy chain, fast skeletal muscle	UN07214	**-7.12**	**-2.90**	-2.06
Myosin, light polypeptide 7, regulatory	UN33792	**-13.98**	**-10.88**	**-625.18**
Neurabin-1-like	Contig18327	2.64	1.78	**6.79**
PAK-interacting exchange factor beta	Contig18296	**8.91**	2.02	2.63
Plakophilin 1	UN47575	3.83	**2.84**	**12.67**
Villin 1-like	UN82082	3.04	1.41	**3.78**
Villin-1	Contig12533	2.37	-1.12	**2.43**
Vimentin	Contig348	**-15.58**	-1.00	**2.12**
Junctional/Adhesion				
Claudin 32b-like	Contig8592	4.48	1.44	**3.31**
Claudin 8	k55_469604	2.33	1.65	**2.58**
Claudin-12	Contig3397	1.30	1.30	**4.86**
Claudin-like protein ZF-A89	UN06974	**-96.11**	**4.67**	2.40
Desmocollin 1 isoform Dsc1a preproprotein	UN27141	**8.55**	1.07	1.34
Desmocollin 2 like isoform 2	Contig8394	2.49	1.76	**7.11**
Desmoglein 2	Contig36771	1.70	-1.07	**-4.23**

Junction plakoglobin	Contig21521	2.53	1.31	**4.22**
Junctional adhesion molecule 2a	Contig2744	-1.82	-1.02	**3.61**
Tight junction protein ZO-2 isoform 1	Contig37989	2.05	1.25	**4.82**
Neural/Nervous System Regulation				
Ataxin-1	Contig4206	-2.11	1.33	**-11.82**
Contactin-1	UN82293	**-26.99**	-2.76	**-93.55**
Heterogeneous nuclear ribonucleoprotein Q	Contig3267	**-19.80**	-2.55	**-81.75**
Kelch-like protein 24	Contig15304	-3.91	-2.98	**-23.03**
Kv channel interacting protein 1 b	UN09508	**-8.01**	-2.34	**-30.13**
Liprin-alpha-2	k51_531132	**-24.37**	-3.13	**-80.27**
Mitochondrial glutamate carrier 1(SLC25A22**)**	Contig11144	**-26.91**	-1.43	**-84.81**
Rabphilin 3A homolog (mouse), b	k58_452731	**-25.56**	-3.65	**-93.54**
Ral GTPase-activating protein subunit alpha-1	Contig6603	**-22.56**	-2.85	**-100.99**
Uromodulin-like	UN07746	**-35.74**	**6.59**	1.89
Zwilling	UN55526	**-10.05**	-1.46	**-26.11**
Immune Response				
B-cell receptor C22-like	Contig4299	**-18.41**	-3.17	**-72.48**
Beta-2-glycoprotein 1	k50_611578	**10.25**	2.52	3.50
C-C chemokine receptor type 2	UN33208	**7.78**	**3.27**	3.99
C-C motif chemokine 21	UN25591	**8.78**	**4.81**	3.73
CD8 beta chain	Contig13919	2.71	**2.97**	2.24
Chemokine (C-X-C motif) ligand 12b	Contig15070	1.64	**4.13**	2.29
Chemokine CCL-C11b	k50_637838	1.86	**3.17**	2.19
Galectin-3	Contig6999	**13.45**	2.34	**9.39**
C1qb	UN16436	1.72	-2.51	**5.34**
Complement component 6-like	UN17892	1.04	**-14.88**	-1.16
Complement factor D	UN16329	5.47	**6.30**	6.26
FinTRIM family, member 6 isoform 1	Contig43055	**-14.99**	-3.45	**-70.51**
Fish virus induced TRIM protein-like	Contig12784	1.03	1.42	**6.12**
Granzyme B-like	k50_2540	2.13	**2.17**	-1.09
H2A histone family, member X-like	UN19029	**-27.45**	1.97	**2.03**
Interferon gamma inducible protein 30	UN13983	1.92	1.45	**3.66**
Interferon, gamma	k51_690246	2.30	**2.36**	1.65
Interferon-inducible protein Gig1-like	UN34145	**12.85**	4.33	**14.36**
Interferon-inducible protein IFI58-like	k54_927290	2.00	2.26	**4.31**
Interleukin 1, beta	UN20464	-7.22	**-12.34**	-2.67
Interleukin 17a/f2	k50_480774	-1.20	1.01	**2.61**
Interleukin 2 receptor, beta	k50_951131	**-16.57**	-19.02	**-758.49**
Interleukin-1 receptor type II	k50_622521	-5.75	-8.90	**-5.99**
Lectin, mannose-binding, 1	Contig32944	1.70	2.06	**2.50**
Lysozyme-like protein 2	UN30680	1.34	-2.23	**2.66**
MHC class II integral membrane protein alpha 3	UN12194	1.67	1.30	**8.76**
Microfibrillar-associated protein 4	UN09372	-1.28	**-6.40**	**2.20**
Mucin-5AC	Contig13257	1.83	-1.04	**2.83**
Mucin 5 B	UN20160	1.56	**2.15**	1.60
MyD88	Contig20402	-1.14	-1.20	**6.83**
Myxovirus (influenza virus) resistance E	Contig_32861	4.32	**5.47**	**-10.32**

NLR family, pyrin domain containing 1-like	Contig20868	1.69	1.05	**6.42**
Perforin-1-like	Contig23107	2.82	1.60	**3.17**
Polymeric immunoglobulin receptor	UN06743	4.10	1.35	**5.88**
Prostaglandin E synthase	UN81767	-1.30	1.18	**13.43**
Toll-interacting protein	Contig2969	1.65	1.16	**7.87**
Toll-like receptor 5a	k78_362431	**-15.97**	**-15.07**	**-10.72**
Transforming growth factor beta 1-like isoform 2	Contig6652	1.38	-1.72	**3.46**
IgGFc-binding protein (FCGBP)	k50_877718	**18.11**	**5.51**	3.11
YWHAQBY	UN06631	**3.78**	**1.86**	**18.88**
Xanthine dehydrogenase	Contig8033	**8.45**	2.64	1.03
Zona pellucida protein 4-like	UN14757	**-137.72**	**2.64**	**1.96**

3.4. Validation of microarray profiles by QPCR

In order to validate the differentially expressed genes identified by microarray, 10 genes were selected for QPCR confirmation, selecting from those with differing expression patterns and from genes of interest based on functional enrichment and pathway results. Samples from 2 h control, 8 h control, 12 h control, and 2 h, 8 h and 12 h following challenge (with three replicate sample pools per timepoint) were used for QPCR. Primers were designed based on channel catfish contig sequences. Melting-curve analysis revealed a single product for all tested genes. Fold changes from QPCR were compared with the microarray expression analysis results. As shown in Table 5, QPCR results were significantly correlated with the microarray results at each timepoint (correlation coefficient $R=0.73$, p-value <0.001). With the exception of GTPase 1 at the 12 h timepoint, all examined genes had the same direction of differential expression by both methods. No consistent bias toward higher expression levels was observed by either method. We observed that concordance between QPCR values and microarray expression levels decreased at higher fold changes. For example, in the cases of myosin light polypeptide 7 and syncollin-like, expression changes of several hundred fold were registered by the microarray and QPCR,

respectively, but more modest changes were observed by the alternative method. These differences likely represented differential hybridization kinetics and/or the presence of paralogues contributing to expression levels which we were unable to predict without a fully annotated genome. In spite of these discordant results in regards to fold change levels, the microarray platform consistently indicated differentially expressed genes for further analysis.

Table 5 QPCR validation details. Fold changes of selected genes are given either according to microarray or QPCR results.

Gene	2h fold change after infection		8h fold change after infection		12h fold change after infection	
	QPCR	Microarray	QPCR	Microarray	QPCR	Microarray
Syncollin-like	-2.49	-1.38	-307.97	-12.21	1.22	1.65
Superoxide dismutase	6.53	2.13	7.82	1.02	1.84	9.81
B-cell receptor C22-like	-2.09	-1.41	48.84	18.41	-6.96	-72.48
Very large inducible GTPase 1	-14.75	-9.97	8.28	9.97	1.65	-5.69
S100 calcium binding protein A1	-9.71	-70.44	9.38	3.92	2.23	2.53
Suppressor of cytokine signaling 6	32.36	1.13	3.94	1.29	1.90	2.44
NIMA-related kinase 1	-2.11	-1.28	1.44	1.98	2.45	2.26
Myosin, light polypeptide 7	-5.03	-13.98	-3.52	-10.88	-21.06	-625.18
YWHAQBY	1.90	3.78	3.78	1.86	3.53	18.88
Interferon-inducible protein IFI58-like	1.54	2.00	2.80	2.26	1.84	4.31

4. Discussion

A. hydrophila is an important pathogen of a range of vertebrate species, including humans, amphibians, reptiles and both freshwater and marine fishes [25]. The existence of an ever-changing array of phenotypically, genotypically, and antigenically-diverse members of the species has long complicated the study of the disease and has made it difficult to pursue development of broad prophylactic and treatment solutions [26, 27]. Beginning in 2009 and continuing to the present, acute *A. hydrophila* outbreaks have devastated a significant portion of

the U.S. catfish industry. Recent studies on the recovered isolates (including one used in this work) have shown that they are at least 200-fold more virulent than stock *A. hydrophila* isolates, and that they have significant molecular differences when compared with low virulence isolates [13, 28]. The virulent isolates are capable of producing mass mortality less than 24 h after exposure, mimicking the epidemiology of natural outbreaks on catfish farms. Recently, Mu et al. [24] examined the transcriptional levels of several key genes in the head kidney of channel catfish exposed to attenuated and virulent *A. hydrophila* by i.p. injection. We sought here to expand our understanding of the host response by utilizing microarrays for global gene expression analysis and by focusing on early responses at the mucosal surface.

A clear consensus is lacking as to the primary route of entry of *A. hydrophila* into a fish host. Early reports implicated both skin lesions [29] and the gastrointestinal tract. Several studies have reported the resistance of host fish to infection through an undisturbed skin/mucus layer, but high infectivity of *A. hydrophila* in abraded or otherwise disturbed skin. Ventura and Grizzle [26] found that abrading catfish skin prior to exposure was necessary for initiating infection in normal culture conditions. Similarly, Chu and Lu [30] found that gills and damaged skin (wounded or mucus removed) were routes of invasion in crucian carp using GFP-labeled *A. hydrophila*. They concluded that while intact skin was not a primary portal, even minor disturbances of the mucosal layer allowed invasion. Studies in zebrafish with a virulent *A. hydrophila* isolate also revealed that introducing a slight tail cut was necessary to initiate infection using a bath challenge [27]. Our preliminary experiments mirrored these findings. Bath challenge of 30 g fingerlings did not result in *A. hydrophila* infection, regardless of dose, feeding status, or presence of i.p. injected (*A. hydrophila* positive) cohabitants (data not shown). Infection was readily initiated through disturbance of skin mucosa, however, leading us to conclude that one

route of natural infection of channel catfish may be through a disturbed skin barrier, potentially obtained through fighting, seine wounds, lesions introduced by other infections, etc. It is additionally possible that stressful pond conditions, poor nutrition and/or chronic low dissolved oxygen, for example, may change the molecular and chemical nature of mucosal surfaces and allow entry in the absence of physical disruption.

A total of 17,038 unique, annotated channel catfish features were present in the utilized 8 x 60K Agilent microarray. Of these, expression of 2,168 was significantly perturbed during at least one early timepoint following infection. While only 20 transcripts showed significant induction at 2 h, this number rose steeply to 529 by 8 h and to 1,559 by 12 h (Table 2). While these timepoints were chosen to capture early, critical immune responses, they likely led to higher variability in the results. The studied isolates, while generating an acute infection, typically lead to 40-60% mortality within 24 h. Thereafter, mortality rates drop precipitously, leaving a group of surviving fish which rarely manifest clinical signs of *A. hydrophila*. Collection of tissues from challenged fish at early timepoints, therefore, of necessity included individuals which would have ultimately evaded acute infection and death. We utilized pooled samples for biological replicates to increase the likelihood of capturing expression signatures tied to pathogen attachment and entry. Further work is clearly needed to identify the basis of the observed pattern of intra-strain resistance and susceptibility. Candidate genes identified here may be valuable as markers for future identification of these groups prior to pathogen exposure.

We categorized differentially expressed genes into five broad categories based on GO analysis and manual literature and pathway analyses. These included antioxidant/cellular stress response, cytoskeletal arrangement, immune responses, junctional/adhesion, and neural/nervous system regulation (Table 4). Below we highlight key constituents of these categories and their potential

functions in the context of host responses to virulent *A. hydrophila*.

Antioxidant/Cellular Stress Response

Recent study of several *Aeromonas* species has highlighted that their infection pattern is characterized by stimulation of robust host production of reactive oxygen species (ROS) and nitrite oxide radical (NO), leading to loss of mitochondrial membrane potential and apoptosis [31]. The most potent virulence factor of *A. hydrophila* strains infecting mammalian species, cytotoxic enterotoxin Act, has been shown, upon binding, to stimulate monocyte/macrophage infiltration and to induce release of ROS [32, 33]. We observed dysregulation of a number of genes involved in mitochondrial regulation and antioxidant responses, largely at 12 h following infection (Table 4). This included strong downregulation (>50-fold) of several genes with roles as chaperones including 60kDa heat shock protein, mitochondrial and FK506 binding protein 4. By 12 h, a number of selenoproteins including SelO, SelT2, and SelX1b were upregulated suggesting a response to buildup of free radicals. Similarly, Mn-superoxide dismutase (SOD2), one of the key enzymes involved in destroying free superoxide radicals in the body [34], was upregulated 9.81-fold.

Cytoskeletal Arrangement

Bacterial toxins often seek to alter and disrupt the actin cytoskeleton of targeted cells in order to gain entry and/or manipulate cellular immunity [35, 36]. These disruptions themselves can often lead to cell death at sites of infection [37]. Actomyosin-driven contraction and dynamics

can also be important in the context of invasion as a central switch controlling both actin polymerization [38] and regulating permeability of apical junctions [39, 40]. In our results, we observed differential expression of several genes associated with manipulation of the actin cytoskeleton, including several filament-associated genes (gelsolin b, villin-1) with similar patterns of induction as in *Edwardsiella ictaluri* infection in catfish intestine [5]. Cdc42 and β4-integrin, both known to be perturbed by *A. hydrophila* effector *AexU* [41, 42], showed significant expression changes at 2 h after infection. Of particular interest was the observed 6.9-fold upregulation of β4-integrin (one of only 20 significantly upregulated genes at that timepoint). Abolghait and colleagues [41] demonstrated that β4-integrin mediates the cytotoxicity of *AexU* aiding in its internalization and progressive actin cytoskeletal disruptions.

Junctional/Adhesion

Pathogens also often seek to adhere to and/or disrupt cellular junctions to gain additional routes of access into the host [43]. We observed dysregulation of components of the apical junction complex (AJC), consisting of the tight junction, adherens junction, and desmosome. While most genes in this category were upregulated significantly at the 12 h timepoint, two showed large fold changes at the 2 h timepoint (Table 4). A claudin-like protein ZF-A89 was sharply downregulated at 2 h before recovering at later timepoints. Claudins are a diverse family of permeability-regulating genes in various epithelial and endothelial cell types [44]. Teleost fish claudins have expanded tremendously through duplication, resulting in teleost-specific family members such as ZF-A89. Although the functions and cell specificity of ZF-A89 and most other fish claudins are currently unknown, claudins in higher vertebrates are often manipulated or

disrupted by pathogens [45, 46]. The other junctional factor showing differential expression at 2 h post-infection was desmocollin 1a, a component of the desmosome. Several other components of desmosomes, intercellular adhesive junctions of epithelial cells, including desmoglein and plakoglobin were also perturbed at 12 h. Desmosomes are often targeted by *Staphylococcus aureus* in infectious skin diseases [47]. Further analyses are needed to identify the cellular locations and functional responses to bacterial infection of these junctional proteins in catfish.

Neural/Nervous System Regulation

A. hydrophila infections in fish have long been predicted to have impacts on the central nervous system via secretion of an extracellular acetylcholinesterase [48], but no molecular evidence of this disruption has ever been generated. A group of genes with putative functional classification as regulators of nervous system functions was strongly differentially expressed at both the 2 h and 12 h post-infection timepoints. Strikingly, expression of these genes was broadly repressed (Table 4). For example, contactin-1, a glycosylphosphatidylinositol (GPI)-anchored neuronal membrane protein that functions as a cell adhesion molecule, was downregulated -26.99-fold at 2 h and -93.55-fold at 12 h. While little is known of the function of these genes in teleost fish, we can speculate based on their roles in mammalian species that they are, in part, regulating a complex network transmitting status signals between the mucosal surface and the brain. In mammals, the cutaneous peripheral nervous system (PNS) is now understood to play a pivotal role in skin homeostasis and disease [49]. *A. hydrophila* infection appears to be disrupting these signaling interactions, though further work is needed to elucidate whether the observed expression patterns are the result of pathogen manipulation of the host or a

protective response to shunt cell signaling resources toward the inflammatory response.

Immune Response

A number of immune factors were differentially expressed in channel catfish skin in the early timepoints following *A. hydrophila* infection. The composition of the responding immune repertoire differed noticeably from other recent studies which have examined fish host gene responses to *A. hydrophila* through subtractive hybridization and RNA-seq approaches in catfish [24] and yellow croaker [50], respectively. These differences likely arise from variation in timing of post-infection sampling and in a focus on different tissues, head kidney and spleen, respectively. Of note, at least eight of the 20 upregulated genes at 2 h post-infection had clear roles in innate immunity, with a similar enrichment of immune factors in down-regulated genes at the same timepoint. Our recent examinations of mucosal immune responses to *E. ictaluri* and *Flavobacterium columnare* have suggested that these first responders are critical regulators of pathogen attachment and disease progression and are often the targets of pathogen-mediated manipulation [6, 21, 45]. We were particularly interested, therefore, in the small set of immune-related genes whose expression was significantly perturbed at the earliest point of measurement.

One such factor was Fc fragment of IgG binding protein (FCGBP), which was upregulated >18-fold at 2 h post challenge. FCGBP is a poorly-characterized mucin glycoprotein, known to associate with secreted gel-forming mucins in gastric epithelium [51]. Given the critical role of mucins in controlling the rate and nature of bacterial attachment on mucosal surfaces [1], changes in FCGBP may reflect important structural changes in the skin mucus of channel catfish following contact *with A. hydrophila* or its secreted effector proteins.

The chimera galectin, galectin-3, also responded rapidly post-challenge. Its expression was induced 13.45-fold at 2 h. While our knowledge of galectin-3 functions are limited in fish [52], it has been well-studied in mammalian species. Li et al. [53] reported that galectin-3, while protective of endotoxin shock, favored *Salmonella* survival. Similarly, research utilizing galectin-3 deficient mice, found that galectin-3 co-localizes with *Neisseria meningitides* and contributes to bacteraemia [54]. Studies dealing with bacterial pathogens from numerous genuses (*Helicobacter, Pseudomonas, Proteus*), have led to the consensus that galectin-3 may act as a cell surface docking site or a cross-linking molecule promoting adhesion [54-57]. Potentially of greatest relevance here is research reporting binding of *A. hydrophila* enterotoxin Act to galectin-3, contributing to host cell apoptosis [58]. Further work is warranted to examine whether channel catfish galectin-3 may play similar roles in supporting pathogen adhesion.

Other gene transcripts rapidly induced following challenge included beta-2-glycoprotein 1, recently identified as a novel component of the innate immune system responsible for neutralization and clearance of LPS [59]. In-vivo evidence is still lacking, however, whether this neutralization is beneficial in the context of infection, or whether, it ultimately favors bacterial survival. Expression of several chemokines and chemokine receptors [60] were induced following infection. In particular, CCL21 and CCR2 were among the genes responding at 2 h (Table 4), whereas CXCL12 and CCL-C11b were up-regulated by 8 h [61].

A suite of immune genes was also strongly down-regulated following *A. hydrophila* challenge. Interestingly, among these were several zona pellucida proteins (Table 4). These genes are important in immunocontraception, but little is known of broader immune roles [57]. Further work is needed to study the cellular localization of these glycoproteins in catfish skin and to examine the consequences of their potent downregulation. Also strongly downregulated relative

to control fish at both 2 h and 12 h, was the interleukin 2 receptor beta (IL2RB). Notably, IL2RB expression fell greater than 700-fold at 12 h. Such a reduction may be the result of a similar suppression of IL-2 production, but an IL-2 transcript has not been identified from catfish and was not, therefore, present on the microarray. Interleukin 2 is a lymphocyte-secreted cytokine which plays critical roles in stimulating proliferation of mucosal lymphocytes, natural killer cells, and macrophages [62, 63]. IL-2 receptors are present on the mucosal epithelium of several mammalian species [64, 65], and IL-2 deletion in mice leads to thymic and mucosal dysregulation [66]. Recent work has expanded the role of IL-2 in mucosal homeostasis [67]. We would predict, therefore, that potent downregulation of IL2RB may be a key immunosuppressive strategy of *A. hydrophila* to facilitate successful infection of the skin mucosal surface. Suppression of the IL-2R (and ligand) is known to occur through the action of prostaglandins and can be restored through addition of prostaglandin synthesis inhibitors [68, 69]. Notably, we observed the induction of several of several prostaglandin synthase genes, particularly prostaglandin E synthase, upregulated greater than 13.43-fold at 12 h (Table 4).

Several other important immune genes showed reduced expression following infection. Toll-like receptor 5a (TLR5a), known to recognize bacterial flagellin, was also significantly down-regulated beginning at 2 h post infection (Table 4). This was in contrast to other reports of upregulation following bacterial infection in catfish [14, 32, 70]. Potential antimicrobial peptide, histone H2AX [71, 72] expression was reduced greater than 25-fold at 2 h. Expression of a finTRIM family member declined significantly at 2 h and 12 h [73]. IL-1 beta and MFAP-4 expression was significantly downregulated at 8 h [10, 74]. Taken together, the immune response captured by the microarray was broadly indicative of a rapid and multifaceted pathogen-directed strategy aimed at immune-sculpting effector responses to improve chances of survival and

replication [75].

5. Conclusion

A transcriptomic profile of responses to *A. hydrophila* infection in channel catfish skin was obtained using a new 8 x 60K microarray. Expression of greater than 2000 genes was perturbed, including critical members of pathways regulating innate immunity and oxidative stress responses. These early signatures serve as a foundation for understanding mechanisms involved in the binding and invasion of virulent *A. hydrophila*. Accordingly, key candidate genes identified here (e.g. galectin-3, IL2RB, B4-integrin) will be utilized to compare and contrast catfish mucosal responses to bacterial isolates with differing virulence and in catfish populations with differing susceptibility to *A. hydrophila* infection.

References:

[1] Linden SK, Sutton P, Karlsson NG, Korolik V, McGuckin MA. Mucins in the mucosal barrier to infection. Mucosal Immunol 2008; 1:183-97.

[2] Rombout JH, Abelli L, Picchietti S, Scapigliati G, Kiron V. Teleost intestinal immunology. Fish Shellfish Immunol 2011; 31:616-26.

[3] Rajan B, Fernandes JM, Caipang CM, Kiron V, Rombout JH, Brinchmann MF. Proteome reference map of the skin mucus of Atlantic cod (*Gadus morhua*) revealing immune competent molecules. Fish Shellfish Immunol 2011; 31:224-31.

[4] Caipang CM, Lazado CC, Brinchmann MF, Rombout JH, Kiron V. Differential expression of immune and stress genes in the skin of Atlantic cod (*Gadus morhua*). Comp Biochem Physiol

Part D Genomics Proteomics 2011; 6:158-62.

[5] Li C, Zhang Y, Wang R, Lu J, Nandi S, Mohanty S, et al. RNA-seq analysis of mucosal immune responses reveals signatures of intestinal barrier disruption and pathogen entry following *Edwardsiella ictaluri* infection in channel catfish, *Ictalurus punctatus*. Fish Shellfish Immunol 2012; 32:816-27.

[6] Beck BH, Farmer BD, Straus DL, Li C, Peatman E. Putative roles for a rhamnose binding lectin in *Flavobacterium columnare* pathogenesis in channel catfish Ictalurus punctatus. Fish Shellfish Immunol 2012; 33:1008-15.

[7] Bengten E, Clem LW, Miller NW, Warr GW, Wilson M. Channel catfish immunoglobulins: repertoire and expression. Dev Comp Immunol 2006; 30:77-92.

[8] Sha Z, Abernathy JW, Wang S, Li P, Kucuktas H, Liu H, et al. NOD-like subfamily of the nucleotide-binding domain and leucine-rich repeat containing family receptors and their expression in channel catfish. Dev Comp Immunol 2009; 33:991-9.

[9] Zhang H, Peatman E, Liu H, Niu D, Feng T, Kucuktas H, et al. Characterization of a mannose-binding lectin from channel catfish (*Ictalurus punctatus*). Res Vet Sci 2012; 92:408-13.

[10] Niu D, Peatman E, Liu H, Lu J, Kucuktas H, Liu S, et al. Microfibrillar-associated protein 4 (MFAP4) genes in catfish play a novel role in innate immune responses. Dev Comp Immunol 2011; 35:568-79.

[11] Rajendran KV, Zhang J, Liu S, Kucuktas H, Wang X, Liu H, et al. Pathogen recognition receptors in channel catfish: I. Identification, phylogeny and expression of NOD-like receptors. Dev Comp Immunol 2012; 37:77-86.

[12] Rajendran KV, Zhang J, Liu S, Peatman E, Kucuktas H, Wang X, et al. Pathogen recognition receptors in channel catfish: II. Identification, phylogeny and expression of retinoic

acid-inducible gene I (RIG-I)-like receptors (RLRs). Dev Comp Immunol 2012; 37:381-9.

[13] Pridgeon JW, Klesius PH, Mu X, Carter D, Fleming K, Xu D, et al. Identification of unique DNA sequences present in highly virulent 2009 Alabama isolates of *Aeromonas hydrophila*. Vet Microbiol 2011; 152:117-25.

[14] Peatman E, Baoprasertkul P, Terhune J, Xu P, Nandi S, Kucuktas H, et al. Expression analysis of the acute phase response in channel catfish (*Ictalurus punctatus*) after infection with a Gram-negative bacterium. Dev Comp Immunol 2007; 31:1183-96.

[15] Peatman E, Terhune J, Baoprasertkul P, Xu P, Nandi S, Wang S, et al. Microarray analysis of gene expression in the blue catfish liver reveals early activation of the MHC class I pathway after infection with *Edwardsiella ictaluri*. Mol Immunol 2008; 45:553-66.

[16] Sun F, Peatman E, Li C, Liu S, Jiang Y, Zhou Z, et al. Transcriptomic signatures of attachment, NF-kappaB suppression and IFN stimulation in the catfish gill following columnaris bacterial infection. Dev Comp Immunol 2012; 38:169-80.

[17] Takano T, Sha Z, Peatman E, Terhune J, Liu H, Kucuktas H, et al. The two channel catfish intelectin genes exhibit highly differential patterns of tissue expression and regulation after infection with *Edwardsiella ictaluri*. Dev Comp Immunol 2008; 32:693-705.

[18] Wang S, Peatman E, Abernathy J, Waldbieser G, Lindquist E, Richardson P, et al. Assembly of 500,000 inter-specific catfish expressed sequence tags and large scale gene-associated marker development for whole genome association studies. Genome Biol 2010; 11:R8.

[19] Liu S, Zhou Z, Lu J, Sun F, Wang S, Liu H, et al. Generation of genome-scale gene-associated SNPs in catfish for the construction of a high-density SNP array. BMC Genomics 2011; 12:53.

[20] Smyth GK. Linear models and empirical bayes methods for assessing differential expression

in microarray experiments. Stat Appl Genet Mol Biol 2004; 3:Article3.

[21] Bauer S, Grossmann S, Vingron M, Robinson PN. Ontologizer 2.0--a multifunctional tool for GO term enrichment analysis and data exploration. Bioinformatics 2008; 24:1650-1.

[22] Grossmann S, Bauer S, Robinson PN, Vingron M. Improved detection of overrepresentation of Gene-Ontology annotations with parent child analysis. Bioinformatics 2007; 23:3024-31.

[23] Pfaffl MW, Horgan GW, Dempfle L. Relative expression software tool (REST) for group-wise comparison and statistical analysis of relative expression results in real-time PCR. Nucleic Acids Res 2002; 30:e36.

[24] Mu X, Pridgeon JW, Klesius PH. Transcriptional profiles of multiple genes in the anterior kidney of channel catfish vaccinated with an attenuated Aeromonas hydrophila. Fish Shellfish Immunol 2011; 31:1162-72.

[25] Cipriano RC, Bullock G, Pyle S. *Aeromonas Hydrophilaand* Motile Aeromonad Septicemias Of Fish. 1984.

[26] Ventura M, Grizzle JM. Evaluation of portals of entry of *Aeromonas hydrophila* in channel catfish. Aquaculture 1987; 65:205-14.

[27] Rodriguez I, Novoa B, Figueras A. Immune response of zebrafish (*Danio rerio*) against a newly isolated bacterial pathogen *Aeromonas hydrophila*. Fish Shellfish Immunol 2008; 25:239-49.

[28] Pridgeon JW, Klesius PH. Molecular identification and virulence of three *Aeromonas hydrophila* isolates cultured from infected channel catfish during a disease outbreak in west Alabama (USA) in 2009. Dis Aquat Organ 2011; 94:249-53.

[29] Snieszko S. The effects of environmental stress on outbreaks of infectious diseases of fishes. J Fish Biol 1974; 6:197-208.

[30] Chu W-H, Lu C-P. In vivo fish models for visualizing *Aeromonas hydrophila* invasion pathway using GFP as a biomarker. Aquaculture 2008; 277:152-55.

[31] Krzymińska S, Tańska A, Kaznowski A. Aeromonas spp. induce apoptosis of epithelial cells through an oxidant-dependent activation of the mitochondrial pathway. J Med Microbiol 2011; 60:889-98.

[32] Chopra AK, Xu X, Ribardo D, Gonzalez M, Kuhl K, Peterson JW, et al. The cytotoxic enterotoxin of *Aeromonas hydrophila* induces proinflammatory cytokine production and activates arachidonic acid metabolism in macrophages. Infect Immun 2000; 68:2808-18.

[33] Sha J, Kozlova EV, Chopra AK. Role of various enterotoxins in *Aeromonas hydrophila*-induced gastroenteritis: generation of enterotoxin gene-deficient mutants and evaluation of their enterotoxic activity. Infect Immun 2002; 70:1924-35.

[34] Miao L, St Clair DK. Regulation of superoxide dismutase genes: implications in disease. Free Radic Biol Med 2009; 47:344-56.

[35] Boquet P, Lemichez E. Bacterial virulence factors targeting Rho GTPases: parasitism or symbiosis? Trends Cell Biol 2003; 13:238-46.

[36] Aktories K, Barbieri JT. Bacterial cytotoxins: targeting eukaryotic switches. Nat Rev Microbiol 2005; 3:397-410.

[37] Suarez G, Khajanchi BK, Sierra JC, Erova TE, Sha J, Chopra AK. Actin cross-linking domain of *Aeromonas hydrophila* repeat in toxin A (RtxA) induces host cell rounding and apoptosis. Gene 2012; 506:369-76.

[38] Thune RL, Fernandez DH, Benoit JL, Kelly-Smith M, Rogge ML, Booth NJ, et al. Signature-tagged mutagenesis of *Edwardsiella ictaluri* identifies virulence-related genes, including a salmonella pathogenicity island 2 class of type III secretion systems. Appl Environ

Microbiol 2007; 73:7934-46.

[39] Ivanov AI, Bachar M, Babbin BA, Adelstein RS, Nusrat A, Parkos CA. A unique role for nonmuscle myosin heavy chain IIA in regulation of epithelial apical junctions. PLoS One 2007; 2:e658.

[40] Sousa S, Cabanes D, El-Amraoui A, Petit C, Lecuit M, Cossart P. Unconventional myosin VIIa and vezatin, two proteins crucial for Listeria entry into epithelial cells. J Cell Sci 2004; 117:2121-30.

[41] Abolghait SK, Iida T, Kodama T, Cantarelli VV, Akeda Y, Honda T. Recombinant AexU effector protein of Aeromonas veronii bv. sobria disrupts the actin cytoskeleton by downregulation of Rac1 and induces direct cytotoxicity to beta4-integrin expressing cell lines. Microb Pathog 2011; 51:454-65.

[42] Fehr D, Burr SE, Gibert M, d'Alayer J, Frey J, Popoff MR. Aeromonas exoenzyme T of Aeromonas salmonicida is a bifunctional protein that targets the host cytoskeleton. Journal of Biological Chemistry 2007; 282:28843-52.

[43] Guttman JA, Finlay BB. Tight junctions as targets of infectious agents. Biochimica et Biophysica Acta (BBA)-Biomembranes 2009; 1788:832-41.

[44] Angelow S, Ahlstrom R, Yu AS. Biology of claudins. Am J Physiol Renal Physiol 2008; 295:F867-76.

[45] Guttman JA, Samji FN, Li Y, Vogl AW, Finlay BB. Evidence that tight junctions are disrupted due to intimate bacterial contact and not inflammation during attaching and effacing pathogen infection in vivo. Infect Immun 2006; 74:6075-84.

[46] Farquhar MJ, Hu K, Harris HJ, Davis C, Brimacombe CL, Fletcher SJ, et al. Hepatitis C virus induces CD81 and claudin-1 endocytosis. J Virol 2012; 86:4305-16.

[47] Amagai M. Autoimmune and infectious skin diseases that target desmogleins. Proceedings of the Japan Academy. Series B, Physical and biological sciences 2010; 86:524.

[48] Nieto T, Santos Y, Rodriguez L, Ellis A. An extracellular acetylcholinesterase produced by *Aeromonas hydrophila* is a major lethal toxin for fish. Microb Pathog 1991; 11:101-10.

[49] Roosterman D, Goerge T, Schneider SW, Bunnett NW, Steinhoff M. Neuronal control of skin function: the skin as a neuroimmunoendocrine organ. Physiological Reviews 2006; 86:1309-79.

[50] Mu Y, Ding F, Cui P, Ao J, Hu S, Chen X. Transcriptome and expression profiling analysis revealed changes of multiple signaling pathways involved in immunity in the large yellow croaker during Aeromonas hydrophila infection. BMC Genomics 2010; 11:506.

[51] Johansson ME, Phillipson M, Petersson J, Velcich A, Holm L, Hansson GC. The inner of the two Muc2 mucin-dependent mucus layers in colon is devoid of bacteria. Proc Natl Acad Sci U S A 2008; 105:15064-69.

[52] Vasta GR, Ahmed H, Du S-J, Henrikson D. Galectins in teleost fish: Zebrafish (*Danio rerio*) as a model species to address their biological roles in development and innate immunity. Glycoconj J 2004; 21:503-21.

[53] Li Y, Komai-Koma M, Gilchrist DS, Hsu DK, Liu F-T, Springall T, et al. Galectin-3 is a negative regulator of lipopolysaccharide-mediated inflammation. J Immunol 2008; 181:2781-89.

[54] Quattroni P, Li Y, Lucchesi D, Lucas S, Hood DW, Herrmann M, et al. Galectin-3 binds Neisseria meningitidis and increases interaction with phagocytic cells. Cell Microbiol 2012; 14:1657-75.

[55] Altman E, Harrison BA, Latta RK, Lee KK, Kelly JF, Thibault P. Galectin-3-mediated adherence of Proteus mirabilis to Madin-Darby canine kidney cells. Biochem Cell Biol 2001;

79:783-8.

[56] Fowler M, Thomas RJ, Atherton J, Roberts IS, High NJ. Galectin-3 binds to Helicobacter pylori O-antigen: it is upregulated and rapidly secreted by gastric epithelial cells in response to H. pylori adhesion. Cell Microbiol 2006; 8:44-54.

[57] Gupta RS, Bhandari V. Phylogeny and molecular signatures for the phylum Thermotogae and its subgroups. Antonie Van Leeuwenhoek 2011; 100:1-34.

[58] Galindo CL, Gutierrez C, Jr., Chopra AK. Potential involvement of galectin-3 and SNAP23 in *Aeromonas hydrophila* cytotoxic enterotoxin-induced host cell apoptosis. Microb Pathog 2006; 40:56-68.

[59] Agar C, de Groot PG, Morgelin M, Monk SD, van Os G, Levels JH, et al. beta(2)-glycoprotein I: a novel component of innate immunity. Blood 2011; 117:6939-47.

[60] Peatman E, Liu Z. CC chemokines in zebrafish: evidence for extensive intrachromosomal gene duplications. Genomics 2006; 88:381-5.

[61] Baoprasertkul P, He C, Peatman E, Zhang S, Li P, Liu Z. Constitutive expression of three novel catfish CXC chemokines: homeostatic chemokines in teleost fish. Mol Immunol 2005; 42:1355-66.

[62] Secombes CJ, Wang T, Bird S. The interleukins of fish. Dev Comp Immunol 2011; 35:1336-45.

[63] Burchill MA, Yang J, Vang KB, Farrar MA. Interleukin-2 receptor signaling in regulatory T cell development and homeostasis. Immunol Lett 2007; 114:1-8.

[64] Ciacci C, Mahida YR, Dignass A, Koizumi M, Podolsky DK. Functional interleukin-2 receptors on intestinal epithelial cells. J Clin Invest 1993; 92:527-32.

[65] de Villiers WJ, Varilek GW, de Beer FC, Guo JT, Kindy MS. Increased serum amyloid a

levels reflect colitis severity and precede amyloid formation in IL-2 knockout mice. Cytokine 2000; 12:1337-47.

[66] Ehrhardt RO, Lúdvíksson BR. When immunization leads to autoimmunity: chronic inflammation as a result of thymic and mucosal dysregulation in IL-2 knock-out mice. Int Rev Immunol 1999; 18:591-612.

[67] Mishra J, Waters CM, Kumar N. Molecular mechanism of interleukin-2-induced mucosal homeostasis. Am J Physiol Cell Physiol 2012; 302:C735-47.

[68] Rappaport RS, Dodge GR. Prostaglandin E inhibits the production of human interleukin 2. J Exp Med 1982; 155:943-8.

[69] Sileghem M, Darji A, Remels L, Hamers R, De Baetselier P. Different mechanisms account for the suppression of interleukin 2 production and the suppression of interleukin 2 receptor expression in Trypanosoma brucei-infected mice. Eur J Immunol 1989; 19:119-24.

[70] Bilodeau AL, Waldbieser GC. Activation of TLR3 and TLR5 in channel catfish exposed to virulent Edwardsiella ictaluri. Dev Comp Immunol 2005; 29:713-21.

[71] Nam BH, Seo JK, Go HJ, Lee MJ, Kim YO, Kim DG, et al. Purification and characterization of an antimicrobial histone H1-like protein and its gene from the testes of olive flounder, Paralichthys olivaceus. Fish Shellfish Immunol 2012; 33:92-8.

[72] Robinette D, Wada S, Arroll T, Levy MG, Miller WL, Noga EJ. Antimicrobial activity in the skin of the channel catfish *Ictalurus punctatus*: characterization of broad-spectrum histone-like antimicrobial proteins. Cell Mol Life Sci 1998; 54:467-75.

[73] van der Aa LM, Jouneau L, Laplantine E, Bouchez O, Van Kemenade L, Boudinot P. FinTRIMs, fish virus-inducible proteins with E3 ubiquitin ligase activity. Dev Comp Immunol 2012; 36:433-41.

[74] Wang Y, Wang Q, Baoprasertkul P, Peatman E, Liu Z. Genomic organization, gene duplication, and expression analysis of interleukin-1β in channel catfish (*Ictalurus punctatus*). Mol Immunol 2006; 43:1653-64.

[75] Hertzog PJ, Mansell A, van Driel IR, Hartland EL. Sculpting the immune response to infection. Nat Immunol 2011; 12:579-82.

IV. BASAL POLARIZATION OF THE MUCOSAL COMPARTMENT IN *FLAVOBACTERIUM COLUMNARE* SUSCEPTIBLE AND RESISTANT CHANNEL CATFISH (*ICTALURUS PUNCTATUS*)

1. Introduction

Aquaculture is the fastest growing sector of agriculture, accounting for close to half of the world's total food fish supply. Wild harvests for numerous species have reached or exceeded maximum sustainable yields, and aquaculture is expected to fill the void. Meanwhile, growing populations have increased demand for high-quality dietary protein sources. Improvements to aquaculture practices are urgently needed to meet world seafood demands. One of the highest priority areas for improvement is the development of effective strategies for decreasing disease mortality levels in aquaculture production, including implementation of better complete diets, vaccines and genetic selection programs. Towards this end, a better understanding of the components of the fish immune system and their functions in the context of pathogen invasion is needed [1].

Mucosal surfaces in teleost fish (and their associated lymphoid tissue) form critical physical and immunological barriers between the organism and the external environment [2, 3]. While shared gross anatomy in the gut between terrestrial and aquatic vertebrates provides a starting context for functional studies in fish [4], the skin and gill mucosa are comparatively unexplored and poorly understood. These interfaces, in constant, direct contact with water, must integrate signals based on environmental conditions, social cues, nutritional status, and interactions with commensal and pathogenic microorganisms. Understanding the molecular actors which govern this complex interplay and maintain homeostasis is critical in the development of improved

rearing strategies, vaccines, and dietary formulations which provide for comprehensive mucosal health and protection. There are several short-term means by which such knowledge can be translated to real-world fish health solutions. Host mucosal receptors utilized by common bacterial pathogens can be identified and targeted for genetic selection or modulation through dietary or chemical supplements. Additionally, expression signatures indicative of high-health (resistant) fish can be utilized to evaluate the efficacy of different rearing systems, diets, and vaccines.

Columnaris disease, caused by the Gram-negative bacterium *Flavobacterium columnare*, is an opportunistic pathogen which impacts numerous freshwater cultured fish species worldwide [5]. Indeed, no wild or cultured freshwater fish, including ornamental fish in aquaria, are completely resistant to columnaris disease [5]. Members of the family Ictaluridae, particularly the economically important foodfish channel catfish (*Ictalurus punctatus*) are exceedingly susceptible to columnaris disease [6, 7]. In complete contrast to other bacterial pathogens of fish, experimental infection protocols with *F. columnare* are far more effective by contact exposure (i.e., immersion protocols) than by injection [8, 9]. This disparity in challenge routes is likely linked to the preferential external pathogenesis of columnaris, as evidenced by observations in both naturally and experimentally infected fish demonstrating that columnaris causes few to no internal lesions, yet induces marked pathologic changes in numerous ectopic tissues such as the skin and gill [10]. Accordingly, the predilection of columnaris disease to adhere to and initiate disease on external surfaces makes it an excellent model for the study of surface mucosal immunity. Previously, we characterized gill mucosal responses in pond-run catfish (*I. punctatus*) to virulent *F. columnare* infection [11]. We identified a putative host receptor of columnaris, a rhamnose-binding lectin whose expression was dramatically induced early after infection. A

more detailed subsequent study of rhamnose-binding lectin activity revealed that expression levels were correlated with columnaris susceptibility, and that saturation of the receptor with its putative ligands resulted in significantly decreased columnaris mortality [12]. To provide a larger context for this finding, here we have carried out RNA-seq analysis of basal and early post-challenge expression differences in the gill mucosa between individuals from families with differing columnaris susceptibility. Our findings provide novel insights connecting teleost mucosal immune status with the subsequent ability to withstand pathogen infection.

2. Materials and methods

2.1 Experimental animals and water quality parameters

The two families of channel catfish utilized in this study were previously revealed to have differing susceptibilities to columnaris disease [12, 13]. Channel catfish fingerlings (13.9 ± 0.44 g) from the two families were stocked into eight 20-L aquaria at a density of 20 fish/aquaria. Aquaria contained 10 L of aerated flow-through well water using the "Ultra Low-Flow System" described by Mitchell and Farmer [14]. The flow rate was set to 29 ± 1 ml/min and monitored daily; this rate allows for a natural progression of the disease after challenge in a flow-through environment [14]. Water temperatures averaged 26.5 ± 0.02 ℃ and dissolved oxygen averaged 5.81 ± 0.03 mg/L. Total Ammonia Nitrogen (TAN) concentrations were determined in each tank with a Hach DR/4000V spectrophotometer using the Nessler Method 8038 (Hach Company, Loveland, Colorado). An Accumet Basic AB15 pH meter (Fisher Scientific, Waltham, Massachusetts) was used to measure pH (7.5-8.2) during the study. Standard titration methods

(APHA 2005) were used to measure total alkalinity (213 mg/L) and total hardness (112 mg/L).

2.2 Experimental challenge

There were four tanks for each family, three of which were challenged with *F. columnare* and the remaining tank for each family served as a negative (unchallenged) control. Other replicates of challenged and control tanks were present during this study and were used to determine the differences in survival between the two families and to examine bacterial adhesion kinetics, which was published previously [12]. Tanks receiving a bacterial challenge were exposed to *F. columnare* isolate LV-359-01 (a genomovar II isolate as determined by using the methods of Arias et al.[7] which was previously demonstrated to produce mortality from columnaris disease in the described system [15]. The isolate was retrieved from a -80 ℃ freezer and streaked on Ordals' medium [16]; after 48 h the isolate was dislodged from the agar using a sterile cotton swab and inoculated into 5 ml of *F. columnare* Growth Medium (FCGM; [17]). This suspension was incubated at 28 ℃ for 24 h and was used to inoculate 1 L of FCGM. The inoculated 1 L broth was incubated for up to 24 h at 28 ℃ in an orbital shaker incubator set at 200 rpm; when the bacterial growth reached an absorbance of 0.70 at 550 nm (approximately $4.0E^{10}$ bacteria/mL) the flask was removed and placed on a stir plate at room temperature. For the challenge, 150 mL of bacterial suspension was added to the appropriate tanks. Animal care and experimental protocols were approved by the Stuttgart National Aquaculture Research Center Institutional Animal Care and Use Committee and conformed to Agricultural Research Service Policies and Procedures 130.4 and 635.1 [12].

2.3 Sample collection, RNA extraction, library construction and sequencing

Gill tissues from 4 fish per replicate tank were collected at 1 h, 2 h, and 8h after challenge. Equal amounts of tissue (approximately 50 mg) were collected from each fish within a pool. The fish were euthanized with tricaine methanesulfonate (MS 222) at 300 mg/L (buffered with sodium bicarbonate) before tissues were collected. Gill tissues in the 3 replicates were placed into 5 ml RNA later™ (Ambion, Austin, TX, USA) and stored at -80 ℃ until extractions could be completed at the end of the study. Samples were homogenized with mortar and pestle in the presence of liquid nitrogen.

Total RNA was extracted from tissues using the RNeasy Plus Universal Mini Kit (Qiagen) following manufacturer's instructions. RNA concentration and integrity of each sample was measured on an Agilent 2100 Bioanalyzer using a RNA Nano Bioanalysis chip. For each timepoint, equal amounts of RNA from the three replicates were pooled for RNA-seq library construction.

RNA-seq library preparation and sequencing was carried out by HudsonAlpha Genomic Services Lab (Huntsville, AL, USA). cDNA libraries were prepared with 2.14-3.25 ug of starting total RNA and using the Illumina TruSeq RNA Sample Preparation Kit (Illumina), as dictated by the TruSeq protocol. The libraries were amplified with 15 cycles of PCR and contained TruSeq indexes within the adaptors, specifically indexes 1-4. Finally, amplified library yields were 30 ul of 19.8-21.4 ng/ul with an average length of ~270 bp, indicating a concentration of 110-140 nM. After KAPA quantitation and dilution, the libraries were clustered 4 per lane and sequenced on an Illumina HiSeq 2000 instrument with 100 bp PE reads.

2.4 De novo assembly of sequencing reads

Before assembly, raw reads were trimmed by removing adaptor sequences and ambiguous nucleotides. Reads with quality scores less than 20 and length below 30 bp were all trimmed. The resulting high-quality sequences were used in the subsequent assembly [18]. The *de novo* assembly was performed by de Brujin graph assembler ABySS (version 1.3.2) [19]. Briefly, the clean reads were first hashed according to a predefined k-mer length, the 'k-mers'. After capturing overlaps of length k-1 between these k-mers, the short reads were assembled into contigs. The k-mer size was set from 50 to 96, assemblies from all k-mers were merged into one assembly by Trans-ABySS. In order to reduce redundancy, the assembly results from different assemblers were passed to CD-Hit version 4.5.4 [20] and CAP3 [21] for multiple alignments and consensus building after trimming contigs less than 200 bp. The threshold was set as identity equal to 1 in CD-Hit, the minimal overlap length and identity equal to 100 bp and 99% in CAP3.

2.5 Gene Annotation and Ontology

The assembly contigs were used as queries against the NCBI *zebrafish* protein database, the UniProtKB/SwissProt database and the non-redundant (nr) protein database using the BLASTX program. The cutoff E-value was set at 1e-5 and only the top gene id and name were initially assigned to each contig. Gene ontology (GO) annotation analysis was performed using the zebrafish BLAST results in Blast2GO version 2.6.4 [22], which is an automated tool for the assignment of gene ontology terms. The zebrafish BLAST result or the nr BLAST result (when a "hypothetical" result was returned in the zebrafish database), was imported to BLAST2GO. The

final annotation file was produced after gene-ID mapping, GO term assignment, annotation augmentation and generic GO-Slim process. The annotation result was categorized with respect to Biological Process, Molecular Function, and Cellular Component at level 2.

2.6 Identification of differentially expressed contigs

The high quality reads from each sample were mapped onto the TransABySS reference assembly using CLC Genomics Workbench software. During mapping, at least 95% of the bases were required to align to the reference and a maximum of two mismatches were allowed. The total mapped reads number for each transcript was determined and then normalized to detect RPKM (Reads Per Kilobase of exon model per Million mapped reads). The proportions-based test was used to identify the differently expressed genes between resistant and susceptible families at 0h, 1h, 2h and 8h with corrected p-value < 0.05 [23]. After scaling normalization of the RPKM values, fold changes were calculated. Analysis was performed using the RNA-seq module and the expression analysis module in CLC Genomics Workbench [24]. Transcripts with absolute fold change values of larger than 1.5 were included in analysis as differently expressed genes.

Contigs with previously identified gene matches were carried forward for further analysis. Functional groups and pathways encompassing the differently expressed genes were identified based on GO analysis, pathway analysis based on the Kyoto Encyclopedia of Genes and Genomes (KEGG) database, and manual literature review.

2.7 Gene Ontology and Enrichment Analysis

In order to identify overrepresented GO annotations in the differentially expressed gene set compared to the broader reference assembly, GO analysis and enrichment analysis of significantly expressed GO terms was performed using Ontologizer 2.0 using the Parent-Child-Intersection method with a Benjamini-Hochberg multiple testing correction [25, 26]. GO terms for each gene were obtained by utilizing zebrafish annotations for the unigene set. The difference of the frequency of assignment of gene ontology terms in the differentially expressed genes sets were compared to the overall catfish reference assembly. The threshold was set as FDR value < 0.1.

2.8 Experimental validation—QPCR

Thirteen significantly expressed genes with different expression patterns were selected for validation using real time QPCR with gene specific primers designed using Primer3 software. Primers were designed based on contig sequences. Total RNA was extracted using the RNeasy Plus kit (Qiagen) following manufacturer's instructions. First strand cDNA was synthesized by iScript™ cDNA Synthesis Kit (Bio-Rad) according to manufacturer's protocol. The iScript chemistry uses a blend of oligo-dT and random hexamer primers. All the cDNA products were diluted to 250 ng/μl and utilized for the quantitative real-time PCR reaction using the SsoFast™ EvaGreen® Supermix on a CFX96 real-time PCR Detection System (Bio-Rad Laboratories, Hercules, CA). The thermal cycling profile consisted of an initial denaturation at 95 ℃ (for 30 s), followed by 40 cycles of denaturation at 94 ℃ (5 s), and an appropriate annealing/extension temperature (58 ℃, 5 s). An additional temperature ramping step was utilized to produce melting curves of the reaction from 65 ℃ to 95 ℃. Results were expressed relative to the expression

levels of 18S rRNA in each sample using the Relative Expression Software Tool (REST) version 2009 [27]. The biological replicate fluorescence intensities of the control and treatment products for each gene, as measured by crossing-point (Ct) values, were compared and converted to fold differences by the relative quantification method. Expression differences between groups were assessed for statistical significance using a randomization test in the REST software. The mRNA expression levels of all samples were normalized to the levels of 18S ribosomal RNA gene in the same samples. Test amplifications were conducted to ensure that 18S and target genes were within an acceptable range. A no-template control was run on all plates. QPCR analysis was repeated in triplicate runs (technical replicates) to confirm expression patterns.

3. Results

3.1 F. columnare Challenge

As previously reported, the two catfish families exhibited different susceptibilities to columnaris disease [12]. No mortality was observed in the resistant family in the 7 day study period while 11 out of 60 (18.3%) fish died in the susceptible family. This rate of mortality was consistent with that previously published with the Ultra-Low-Flow system; a challenge system designed to reliably reproduce columnaris disease with the kinetics and severity of mortality approximating columnaris disease epizootics. The mortality observed in the susceptible family of fish occurred on days 2-5 post-challenge [12].

3.2 Sequencing of short expressed reads from catfish gill

Illumina-based RNA-sequencing (RNA-seq) was carried out on gill samples from the two catfish families. Reads from timepoint-specific samples were distinguished through the use of multiple identifier (MID) tags. A total of 350 million 100 bp high quality reads were generated on an Illumina HiSeq 2000 instrument in a single lane. Greater than 39 million reads were sequenced for each of the eight libraries. After removing ambiguous nucleotides, low-quality sequences (quality scores < 20) and short reads (length < 30 bp), the remaining high-quality reads were carried forward for assembly and analysis. Raw read data are archived at the NCBI Sequence Read Archive (SRA) under Accession **SRP017689**.

3.3 De novo assembly of catfish gill transcriptome with ABySS & Trans-ABySS

ABySS & Trans-ABySS were used to generate an optimized reference for mapping of high quality reads and accurate determination of differentially expressed genes after challenge, based on previously demonstrated superior assemblies when compared with Velvet and CLCbio [28]. Use of Trans-ABySS to merge ABySS multi-k-assembled contigs, resulted in approximately 1.1 million contigs with average length of 617.3 bp and N50 size of 1,418 bp. A total of 657,211 contigs with lengths greater than 200 bp were carried forward for additional analysis. Approximately 0.2 million contigs were removed during the length and redundancy filtration steps (CD-Hit and CAP-3), resulting in a final average contig size and contig number of 805.6 bp and 444,715, respectively (Table 1). This non-redundant, length-filtered assembly was used as the reference catfish gill transcriptome in the following steps of analysis including transcriptome annotation and gene expression profiling.

Table 1 Summary of *de novo* assembly results of Illumina sequence data from catfish gill using Trans-ABySS

	Trans-ABySS
Contigs(≥100bp)	1,117,006
Large contigs (≥1000bp)	197,119
Maximum length (bp)	26,890
Average length (bp)	617.3
N50 (bp)	1,418
Contigs after length filtering(≥200bp)	657,211
Percentage contigs kept after length filtering	58.84%
Average contig length after length filtering (bp)	950.7
Contigs (After CD-HIT-EST+ CAP3)	444,715
Average length (bp) (After CD-HIT-EST+ CAP3)	805.6
Reads mapped to final reference (%)	81.3%

3.4 Gene identification and annotation

BLAST-based gene identification was performed to annotate the channel catfish transcriptome and inform downstream differential expression analysis. After gene annotation, 140,210 of the Trans-ABySS contigs had a significant BLAST hit against 17,481 unique zebrafish genes (unigenes; Table 2). In order to further evaluate the quality of the assembled genes, 15,873 unigenes were identified based on hits to the zebrafish database with the more stringent criteria of a BLAST score ≥100 and E-value ≤ 1e-20 (quality matches). The same BLAST criteria were used in comparison of the Trans-ABySS reference contigs with the UniProt and nr databases. The largest number of matches was to the nr database with 148,313 contigs with putative gene matches to nr and 24,442 quality unigene matches (Table 2).

Table 2 Summary of gene identification and annotation of assembled catfish contigs based on BLAST homology searches against various protein databases (Zebrafish, UniProt, nr). Putative gene matches were at E-value ≤ 1e-5. Hypothetical gene matches denote those BLAST hits with uninformative annotation. Quality unigene hits denote more stringent parameters, including score≥100, E-value ≤ 1e-20

	Contigs with putative gene matches	Annotated contigs ≥500bp	Annotated contigs ≥1000bp	Unigene matches	Hypothetical gene matches	Quality Unigene matches
Zebrafish	140,210	95,705	60,930	17,481	1,104	15,873
UniProt	116,739	86,381	57,546	23,403	0	18,602
NR	148,313	101,596	64,279	33,303	2,473	24,442

3.5 Identification and analysis of differentially expressed genes—within group.

Differential expression in comparison to 0 h control samples was carried out for the resistant and susceptible fish groups, respectively (Table 3). Similar numbers of genes were differentially expressed at 1 h, 2 h, and 8 h, post-challenge in both groups, with the number of dysregulated genes rising with time. For example, at 1 h, 356 and 332 genes were differentially expressed in resistant and susceptible samples, respectively while these numbers rose to 1,198 and 1,352 genes in the same respective groups at 8 h. We also determined the number of genes that were significantly differentially expressed in the same direction in both groups at a given timepoint (magnitude differed). Greater numbers of upregulated genes were shared between groups than downregulated genes. By 8 h, a majority of upregulated (66.5%) and close to a majority of downregulated (45.2%) genes were shared between the two groups, indicating that many of the same response mechanisms and pathways were being initiated in both groups, albeit at different levels (Table 3).

Table 3 Statistics of differentially expressed genes at early timepoints following *F. columnare* challenge in resistant and susceptible fish relative to their 0 h control samples. *Shared* category indicates the number of genes significantly differentially expressed in the same direction in both groups at a given timepoint, while percentage is the number of shared genes/number of potentially shared genes. Values indicate contigs/genes passing cutoff values of fold change ≥1.5 ($p<0.05$).

	1h	**2h**	**8h**
Up-regulated			
Resistant	272	261	791
Susceptible	197	229	905
Shared (%)	78 (39.6%)	67 (29.3%)	526 (66.5%)
Down-regulated			
Resistant	84	209	407
Susceptible	135	228	447
Shared (%)	14 (16.7%)	40 (19.1%)	184 (45.2%)

3.6 Identification and analysis of differentially expressed genes—between groups

Additional levels of analysis were conducted on the comparisons of greatest interest, differences in gene expression profiles between resistant and susceptible fish at 0 h, and 1 h, 2 h, and 8 h post-*F. columnare* challenge. Designating the resistant family as the control group, a comparison of global transcription levels was made between resistant and susceptible families at each timepoint. A total of 8,584 of the 444,175 final reference contigs showed significant differential expression between groups for at least one timepoint following infection. The identified contigs represented 1,714 unigenes, including 1,581 unique genes with more stringent criteria of a BLAST score ≥100 and E-value ≤ 1e-20, and 133 unique genes with BLAST E-value from 1e-20 to 1e-5 (Table 4). The greatest degree of differential expression between groups was observed at 1 h (972 genes), followed by 0 h (795 genes). No clear trend toward overall higher expression levels in either the resistant or susceptible group was observed (Table 4).

Table 4 Statistics of differently expressed genes pre-challenge (0 h) and at 1, 2, and 8 h following *F. columnare* challenge. *Resistant<Susceptible* indicates numbers of genes with significantly higher expression (read numbers) in susceptible samples relative to resistant samples. These genes elsewhere are indicated with positive values. *Resistant>Susceptible* indicates numbers of genes with significantly lower expression (read numbers) in susceptible samples relative to resistant samples. These genes elsewhere are indicated with negative values. *Reads per contig* indicates average number of reads in differentially expressed contigs/genes being compared at a given timepoint. Values indicate contigs/genes passing cutoff values of fold change ≥1.5 ($p<0.05$)

Resistant VS Susceptible	0h	1h	2h	8h
Resistant<Susceptible (+)	388	382	385	319
Resistant>Susceptible (-)	407	590	362	276
Total	795	972	747	595
Reads per contig	125	245	140	166
Total unigenes		1,714		

3.7 Enrichment and Pathway Analysis

Differently expressed genes between the two groups were then used as inputs to perform gene ontology (GO) annotation by Blast2GO. A total of 3,033 GO terms including 795 (26.21%) cellular component terms, 816 (26.9%) molecular functions terms and 1,422 (42.88%) biological process terms were assigned to 1,478 unique gene matches. Analysis of level 2 GO term distribution showed that metabolic process (GO:0008152), cellular process (GO:0009987), binding (GO:0005488) and cell (GO:0005623) were the most common annotation terms in the three GO categories.

The differently expressed unique genes were then used as inputs to perform enrichment analysis using Ontologizer. Parent-child GO term enrichment analysis was performed for the 1,465 unigenes to detect significantly overrepresented GO terms. A total of 68 terms with p-value (FDR-corrected) < 0.1 were considered significantly overrepresented. Ten higher level GO terms were retained as informative for further pathway analysis. The GO terms include functions and processes including cellular nitrogen compound biosynthetic process, regulation of cell death,

regulation of cell adhesion and epithelial tube formation.

Based on enrichment analysis and manual annotation and literature searches, representative key genes were arranged into 4 broad functional categories believed to best reflect the polarization between resistant and susceptible fish particularly prior to challenge (0 hr). These included differences in putative mucosal immune factors and in mucin secretion and modification (Table 5; Figure 1 and 2) as well as cytoskeletal/junctional regulation and cell survival and proliferation. Putative functional roles of immune and mucin-related genes, judged to be the most critical in modulating differential disease resistance, are covered in-depth in the Discussion.

Table 5 Differentially expressed genes in the gill between catfish resistant and susceptible to *F. columnare* and with putative key functions in mucosal immunity. Timepoints of comparison are pre-challenge (0 h) and at 1, 2, and 8 h post-challenge. Positive values indicate higher expression in susceptible catfish, while negative values indicate higher expression in resistant catfish. Bold values indicate significant fold change ($p \leq 0.05$). When reads number equaled to 0 in resistant or susceptible group, the fold change is presented by normalized read number in resistant/normalized read number in susceptible.

Gene name	Contig ID	0h	1h	2h	8h
Immune Component					
Antimicrobial peptide NK-lysin-like	Contig30003	**8.11**	**1.35**	**3.25**	1.12
B7-H3 protein precursor	k90_1004142	-4.57	**28.64**	2.31	**-4.50**
Beta-2 microglobulin precursor	Contig27654	-1.17	1.31	**2.79**	**4.55**
Catalase	k68_2467845	-3.33	-5.85	**-6.19**	**-17.51**
CC chemokine SCYA120	k82_1576433	8.34	**10.45**	3.11	-2.71
C-C motif chemokine 19-like precursor	k71_2254471	**-3.51**	**-3.14**	**-1.88**	4.66
C-C motif chemokine 20-like	Contig23454	**3.13**	**1.70**	**2.20**	**2.23**
CD2 antigen cytoplasmic tail-binding protein 2	Contig8122	**5.15**	1.84	**3.23**	2.58
CD40 antigen precursor	Contig17086	3.06	**12.06**	**10.96**	**2.91**
CD74 molecule, MHC II invariant	k86_1288168	**4.43**	**4.24**	**4.62**	**4.95**
CD8 antigen, alpha polypeptide precursor	k60_3009101	**8.82**	-1.03	**3.81**	1.39
CD83	k81_1706265	**2.94**	1.53	**4.76**	3.91
Chemokine C-X-C motif receptor 4a	Contig3928	**3.69**	**1.75**	1.86	1.53
COMM domain-containing protein 6	k77_1936198	18.39	80.38	6.69	16.90
Complement C1q subcomponent subunit A precursor	Contig9882	-1.13	**2.25**	**1.62**	**4.07**
Complement factor I	k60_3040837	3.36	**5.64**	**16.97**	-1.64
Diacylglycerol kinase zeta	Contig22646	**-9.91**	**-35.17**	**-12.64**	**-7.40**
E3 ubiquitin/ISG15 ligase TRIM25 isoform 1	k52_3538500	**8.44**	**7.27**	**5.22**	8.31

Eosinophil peroxidase precursor	Contig28132	**2.88**	**2.72**	1.49	**1.89**
Fc receptor-like protein 5-like	Contig18486	-2.42	-9.62	1.42	**-45.37**
H-2 class I histocompatibility antigen, Q10 alpha	k72_2189144	**-10.70**	**-2.19**	**-2.43**	**-3.61**
Hephaestin-like	k60_3040383	-10.97	-39.81	-14.44	-12.33
HLA class II histocompatibility antigen, DP alpha 1	k73_2144285	**-31.28**	**-24.00**	**-13.34**	**-20.30**
IgGFc-binding protein-like	Contig27011	**3.49**	**6.92**	**4.58**	**6.72**
Immunoglobulin-binding protein 1	Contig20110	**-10.86**	**-6.94**	**-5.11**	**-12.62**
Integrin alpha-E-like (CD103)	Contig9090	**2.40**	1.34	**61.31**	**2.24**
Integrin alpha-M-like (CD11b)	Contig28672	**-1.71**	**-1.78**	**-2.11**	-1.63
Interferon, gamma 1-1 precursor	k62_2847986	**-5.47**	-2.18	2.50	1.88
Interferon-induced very large GTPase 1-like	Contig12397	**4.38**	**3.47**	2.42	-1.43
Interleukin 1 receptor accessory protein	Contig9637	**31.32**	**17.75**	**12.21**	**7.77**
Interleukin-10 receptor subunit beta precursor	k81_1681887	**2.97**	**2.92**	**3.11**	**4.14**
Interleukin-13 receptor subunit alpha-2 precursor	Contig475	**2.48**	**1.70**	**3.04**	2.06
Interleukin-17 receptor A	Contig15946	**1.69**	-1.04	1.21	1.25
Interleukin-22 receptor subunit alpha-2 precursor	k53_3522444	**-4.50**	1.00	**-2.80**	-1.32
Interleukin-8 variant 3	Contig89	**-2.54**	**-13.93**	**-5.16**	**-2.62**
Lectin, mannose-binding 2-like b precursor	Contig14979	-3.08	**-86.59**	-1.31	**-15.29**
Lipopolysaccharide-induced tumor necrosis factor-alpha	Contig24393	**-2.25**	**-2.27**	**-8.83**	**-3.33**
L-rhamnose-binding lectin CSL2	Contig1154	**3.17**	**-2.50**	-1.64	2.66
Lysozyme C	Contig6206	**-6.62**	**-7.48**	**-8.58**	**-2.71**
Macrophage mannose receptor 1-like	Contig12298	**3.94**	**3.45**	**6.39**	**3.62**
MHC I UDA precursor	Contig14838	**-7.64**	**4.60**	**-5.48**	**-2.12**
MHC I UXA2 precursor	Contig19729	**21.65**	**4.24**	-1.46	1.11
Matrix metalloproteinase 13a precursor	k96_511386	-2.77	-1.04	1.51	**5.34**
MHC class II beta chain	Contig15710	**8.59**	**-22.23**	**5.32**	**16.66**
Microfibril-associated glycoprotein 4-like	Contig17008	**6.12**	**16.05**	**20.74**	**12.55**
MALT lymphoma translocation gene 1	Contig5059	**-6.40**	**-4.94**	-1.09	-1.56
NACHT, LRR and PYD domains-containing protein 14	Contig27718	**2.91**	**3.03**	1.67	2.30
Natterin-like protein	k96_502354	**-4.23**	**-4.30**	**-2.94**	**-4.15**
Nitric oxide synthase 2b, inducible	Contig9783	**-5.20**	**-15.34**	**-4.21**	**-3.60**
Novel protein containing immunoglobulin domains	Contig29892	1.90	**13.90**	**3.63**	**21.07**
Protein LSM14 homolog A	k78_1881343	6.89	4.09	**24.59**	**93.27**
Protein NLRC3-like	k95_593007	**6.30**	-1.13	**-5.08**	2.15
Retinoic acid receptor alpha-B	Contig23851	**7.09**	1.63	2.20	2.82
Rhamnose binding lectin-like precursor	Contig2789	**10.08**	**11.05**	**16.72**	**14.83**
Serum amyloid P-component precursor	Contig1999	**3.40**	**1.48**	**1.93**	1.02
Similar to interferon-induced, hepatitis C-associated	k72_2228955	1.59	4.02	**9.41**	**13.43**
Stonustoxin subunit beta	Contig4216	**11.50**	**1.79**	**2.64**	1.50
Toll-like receptor 21 precursor	Contig3417	2.22	**1.98**	1.63	**4.35**
Toxin-1 precursor	Contig4333	**-11.91**	**-3.98**	-2.96	-1.91
Tumor necrosis factor ligand superfamily member 12	k67_2576854	1.99	**4.58**	**5.48**	3.80
Tumor necrosis factor receptor superfamily member 14	Contig14203	-1.23	**9.46**	-1.19	**102.40**
Immune Component (Reads number contain 0)					
CC chemokine SCYA105	Contig30409	**0/81**	**0/121**	**0/33**	**0/160**
Chemokine CCL-C25y precursor	k71_2311470	**22/0**	**-15.59**	**-9.52**	**-7.36**
Interleukin 17a/f2 precursor	k50_3550089	**12.43**	2.32	1.48	0/2

Interleukin 2 receptor, gamma b precursor	k55_3392983	**11.24**	**0.00**	**0/35**	**0/27**
Major histocompatibility complex class I UBA precursor	Contig19309	**379/0**	0/2	**244/0**	**67/0**
MHC I alpha chain, partial	k81_1660488	-1.75	**24/0**	**-25.08**	4/0
MHC II integral membrane protein alpha chain 3	k76_1957396	**0/199**	**0/319**	**0/295**	**0/51**
MHC non-classical class I heavy chain	k90_981934	**8/0**	**20/0**	**-25.82**	**10/0**
NACHT, LRR and PYD domains-containing protein 1	Contig27568	**42/0**	**-18.41**	**32/0**	**-25.89**
Signaling lymphocytic activation molecule-like	Contig19933	**46/0**	**20/0**	**69/0**	0/0
Similar to Poly [ADP-ribose] polymerase 14	Contig27481	**21.45**	**7.88**	**11.88**	**0/16**
Tumor necrosis factor alpha-induced protein 8-like protein 3	Contig18314	0/26	**14.07**	6.10	2.03
Tumor necrosis factor receptor superfamily member 14	k85_1384186	**0/79**	0/23	0/25	0/12
Vitelline membrane outer layer protein 1 homolog	k90_954683	0/589	**75.12**	**55.40**	**44.97**
Mucin Secretion and Modification					
Alpha-1,3-fucosyltransferase 9B	Contig23983	**-10.54**	-2.22	1.01	**-12.58**
Beta-1,3-galactosyltransferase 2-like	Contig2355	**5.16**	**9.23**	3.50	3.83
Mgat1a	Contig2190	**-12.40**	**-9.11**	**-5.18**	**-7.79**
Mucin-19-like, partial	Contig30403	**634.29**	**15.73**	**10.41**	**13.83**
Mucin-2	Contig28752	**30.39**	**7.10**	**1.95**	**2.51**
Mucin-2-like	Contig25990	**57.46**	**9.04**	**7.96**	**5.52**
Mucin-5AC	k96_156852	**2.92**	**1.56**	**-4.77**	1.14
Mucin-5AC-like	Contig28993	**157.30**	**2.04**	**3.43**	**6.29**
Mucolipin-3-like	Contig9791	2.16	**3.93**	**2.95**	1.47
Mucolipin-3-like	Contig30888	**4.05**	**3.33**	**3.16**	**2.62**
Ubiquitin carboxyl-terminal hydrolase 19	Contig18301	1.31	**9.92**	-2.09	5.58
Mucin Secretion and Modification (Reads number contain 0)					
Beta-1,4 N-acetylgalactosaminyltransferase 1-like	k60_2977720	5.45	3.16	**0/32**	1.47
CMP-N-acetylneuraminate-beta-galactosamide-alpha-2	Contig22040	**13.13**	**15.67**	1.25	**0/54**
Glycogenin 1a	k64_2782278	**9.70**	14.74	**9.84**	0/6
ST8SIA3	k52_715050	**-48.95**	13/0	-24.40	-15.78
Tissue specific transplantation antigen P35B	k85_1375453	**377.58**	**805.33**	0/0	1/0

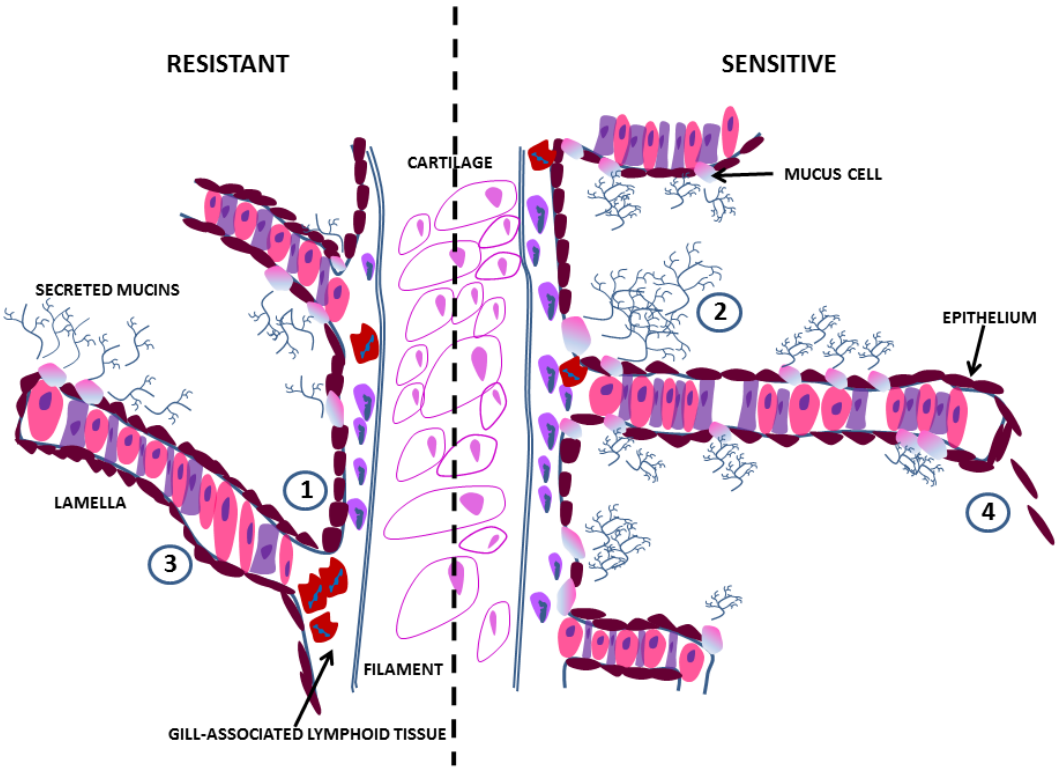

Fig. 1. Gill filament schematic (sagittal cross-section) depicting the four main signatures of polarization between resistant and sensitive catfish to *F. columnare* infection. These include differences in the 1) immune component, 2) mucin secretion and modification, 3) cytoskeletal/junctional regulation and 4) cell survival and proliferation

3.8 Validation of RNA-seq profiles by QPCR

In order to validate the differentially expressed genes identified by RNA-Seq, we selected 10 genes for QPCR confirmation, selecting from those with differing expression patterns and from genes of interest based on functional enrichment and pathway results. We also selected three genes among those with read counts of "0" in more than one sample in order to ascertain the reliability of this portion of the dataset. Samples from 0 h control, and 1 h, 2 h and 8 h following challenge (with three replicate sample pools per timepoint) were used for QPCR. Primers were designed based on contig sequences. Melting-curve analysis revealed a single product for all

tested genes. Fold changes from QPCR were compared with the RNA-seq expression analysis

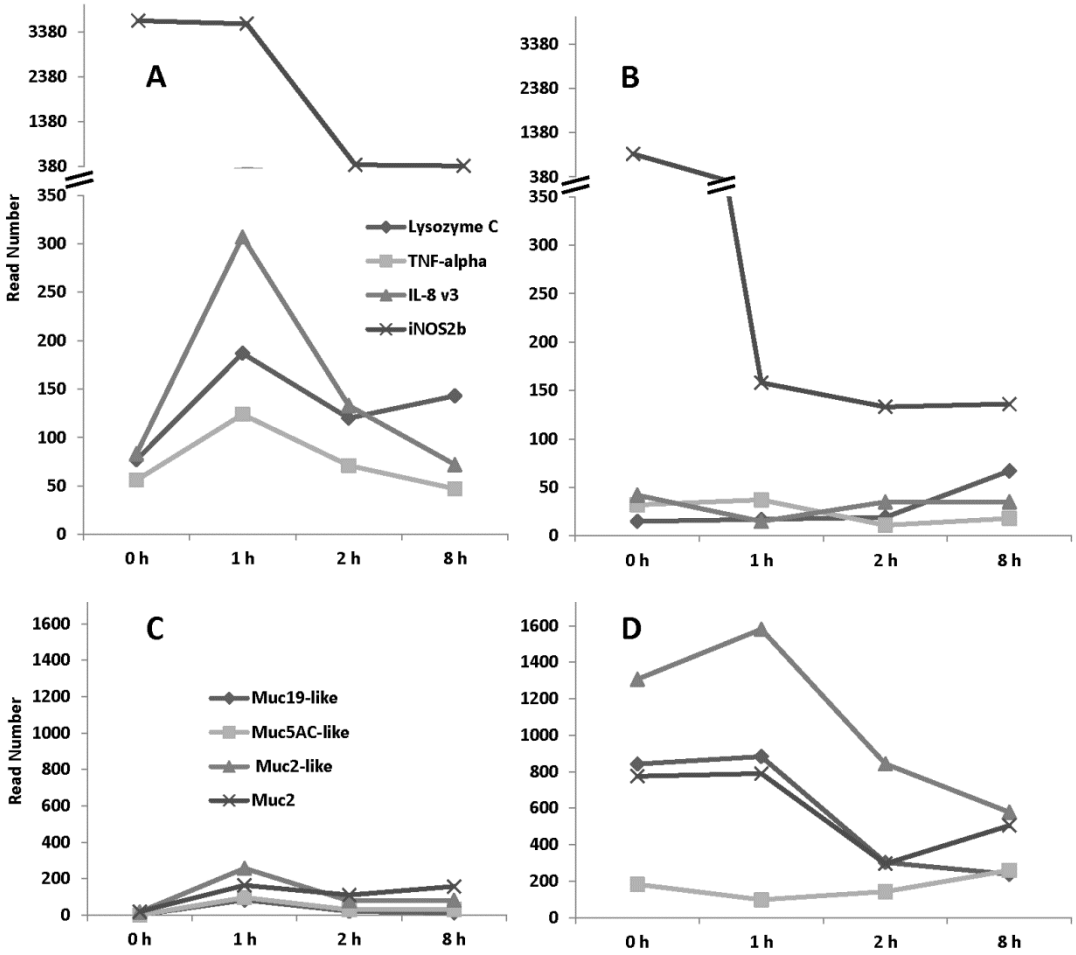

Fig.2. Representative signatures of polarization between resistant (left) and susceptible (right) catfish to *F. columnare*. **A** and **B**) Mucin (Muc) read numbers at 0 h, 1 h, 2 h, and 8 h post-infection in resistant and susceptible catfish, respectively. **C and D**) Key immune gene read numbers for lysozyme C, TNF-alpha, IL-8 v3, and iNOS2b in resistant and susceptible catfish, respectively.

results. As shown in Fig. 2, QPCR results from non-zero read genes were significantly correlated with the RNA-seq results at each timepoint (average correlation coefficient 0.87, p-value <0.001; Figure 2). Correlations were weaker among strongly dysregulated genes (>10-fold change), although no clear relationship between technology (RNA-seq or QPCR) and higher expression levels was observed. In the three "0" level genes tested, QPCR indicated that while this portion

of the RNA-seq results likely does indicate differentially expressed genes, fold-change levels cannot be accurately estimated from the assumption of no expression (0 reads captured) in a given sample. For example for the chemokine SCYA105, QPCR indicated 1,746-fold higher expression at 0 hr in susceptible fish than resistant fish, with 81 and 0 reads in the two groups, respectively. However, TNFRSF14, with 79 and 0 reads in susceptible and resistant fish, respectively, showed 11.76-fold higher expression in susceptible fish. The discrepancy between the two techniques on this subset of genes may be due to expression of alternatively spliced allelic forms or incorrect assignment of RNA-seq reads to paralogous genes. Given the lower reliability of "0" read genes, we separated key genes in this category into separate subheadings in Tables 5 and Supplementary Table 6. In general, however, the RNA-seq results were confirmed by the QPCR results, indicating the reliability and accuracy of the Trans-ABySS reference assembly and RNA-seq expression analysis.

4. Discussion

Knowledge of mucosal actors in the teleost gill and their impact on pathogen susceptibility has been limited. Recent studies have examined the gill transcriptome of several salmonid species in the context of stress [29, 30] and parasite infection [31, 32], but no studies have examined the basal status of fish mucosa in the context of disease resistance. Here, we have profiled global transcriptional differences in the gill both before and at early timepoints following *F. columnare* challenge in fish from resistant and susceptible families of channel catfish (*I. punctatus*). Our results indicate that a polarization in mucosal status prior to infection may impact early adherence, entry, and host inflammatory processes in a manner which ultimately determines disease outcome.

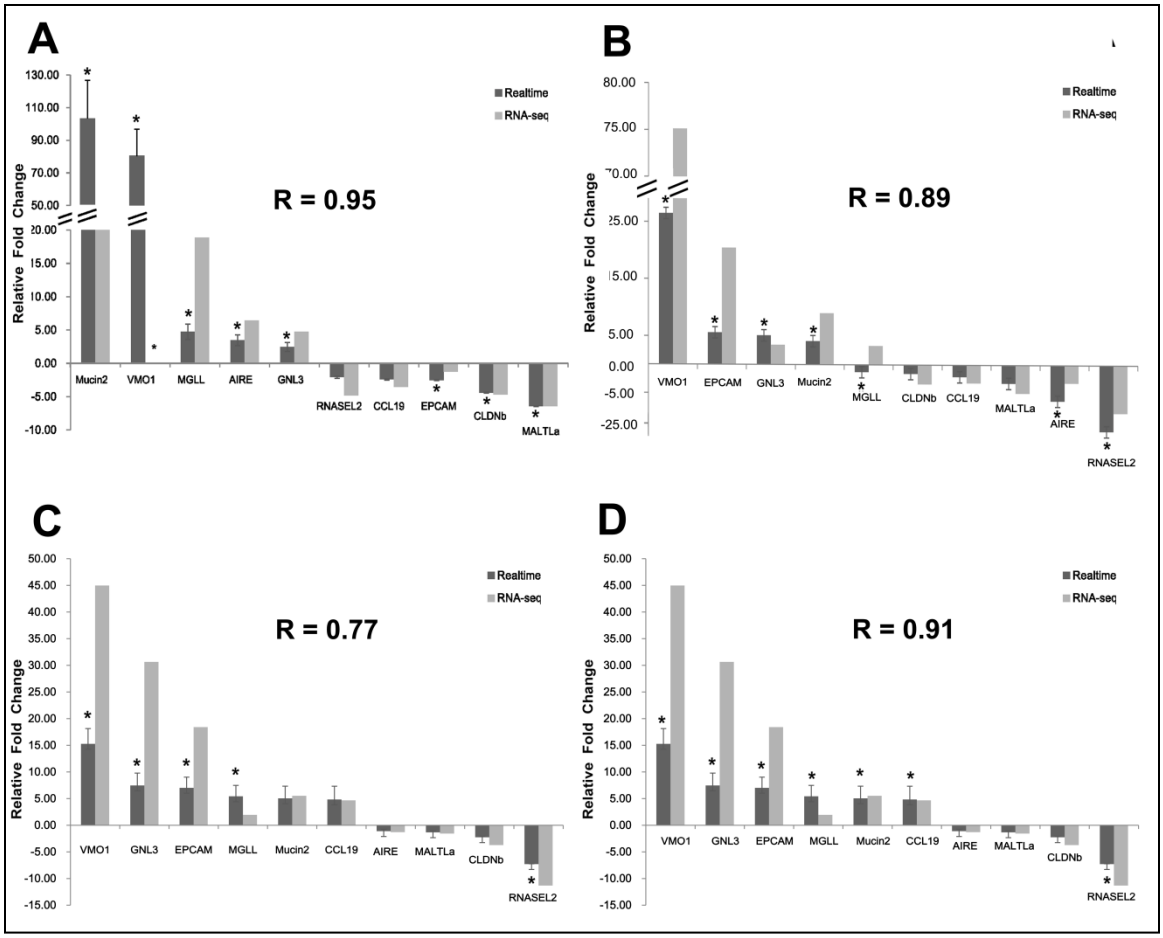

Fig. 2. Comparison of relative fold changes between RNA-seq and QPCR results in catfish gill Gene abbreviations are: Monoglyceride lipase, MGLL; Mucosa associated lymphoid tissue lymphoma translocation gene 1, MALTLa; C-C motif chemokine 19-like precursor, CCL19; Epithelial cell adhesion molecule precursor, EPCAM; Autoimmune regulator-like, AIRE; Ribonuclease like 2 precursor, RNASEL2; Guanine nucleotide-binding protein-like 3, GNL3; Claudin b, CLDNb; Vitelline membrane outer layer protein 1 homolog, VMO1 (*reads number equal to zero at 1h).

A clear correlation between *F. columnare* virulence and adherence to the gill epithelium has previously been demonstrated [33]. Additionally, surface mucus from both catfish and salmon has been shown to benefit *F. columnare* growth and promote chemotaxis [34, 35]. Recently, Olivares-Fuster et al. [36] observed cells of *F. columnare* aggregated within and surrounding mucus pores of the skin and capping tissue of the gill filament in channel catfish as soon as 30

minutes post-challenge. This mucosal host-pathogen association has previously been postulated to be lectin-mediated based on sugar-blocking studies in carp [37] and catfish [38]. Our recent work [12] identified a putative host lectin receptor in catfish gill, a rhamnose-binding lectin, with pre- and post-challenge expression levels inversely correlated with *F. columnare* resistance. We investigated here the larger context of differential RBL expression in resistant and susceptible catfish using RNA-seq profiling. Our greatest interest lay in capturing basal differences in expression prior to *F. columnare* challenge between resistant and susceptible fish, as these signatures could potentially serve as expression QTL and/or biomarkers for selection of catfish resistant to *F. columnare* without the necessity of repeated trial infections [39].

Comparison of expression levels of resistant and susceptible catfish by RPKM analysis of RNA-seq read numbers generated 1,714 unique genes differing in expression by 1.5-fold or greater at at least one timepoint. We categorized key genes within this set into four broad functional categories: immune-related, mucin secretion and modification, junction/cytoskeletal regulation, and cell survival and proliferation (Tables 5 and Figure 1). Below we highlight key aspects of two of these important pathways likely mediating the catfish response to columnaris infection.

Immune component

We first observed that our RNA-seq results validated our previous finding of higher gill expression of a rhamnose-binding lectin (RBL) in individual susceptible fish when compared with resistant individuals [12]. By RNA-seq, expression levels in our pooled samples were ~10-17-fold higher at all timepoints including 0 h (Table 5). Beyond RBL, several key innate defense genes differed in their expression levels between the two groups. Notably, inducible nitric oxide

synthase 2b (iNOS2b) was significantly higher in resistant fish gill at all timepoints. iNOS2b had the highest read counts of any differentially expressed gene captured in resistant samples (Figure 1), with 3,636 reads at 0 h compared with less than 1,000 in susceptible samples. Interestingly, iNOS2b levels were not induced in either group following *F. columnare* infection. Rather, they declined roughly 10-fold by 8 h from their basal levels (Figure 1). Inducible nitric oxide synthases (iNOS) generate nitric oxide (NO) from L-arginine. Often produced by macrophages, NO is a potent cytotoxic agent in immune defenses which can have beneficial antimicrobial activity, but which can also have far-reaching tissue-damaging effects [40, 41]. iNOS2b in zebrafish has been reported to be orthologous to mammalian NOS2 (iNOS), constitutively expressed in all studied tissues, and inducible by LPS and Poly I:C [42]. iNOS expression has been previously detected in the gills of bacterially-challenged rainbow trout [43, 44] but no constitutive expression was observed in this tissue. Our finding of high levels of constitutive iNOS expression in catfish gill matches often overlooked reports of continuous high-level iNOS expression in healthy human respiratory epithelium [45]. There, NO is believed to modulate mucociliary clearance and mediate cytotoxicity against a range of pathogens [40, 46]. Though further research is clearly needed, higher constitutive iNOS2b levels in resistant catfish may have far-ranging effects on mucosal health and explain, in part, other downstream differential expression.

Lysozyme C (chicken-type) also displayed consistently higher expression in resistant catfish gill than that observed in susceptible fish (Table 5). Plasma lysozyme levels have been studied for several decades in the context of fish immunity [47], but relatively little attention has been given to the level and roles of lysozyme in mucosal surfaces [48, 49]. In mammals, lysozymes are among the most abundant secreted mucosal enzymes from the epithelium as well as a major

component of granules of professional phagocytes. They help to kill bacterial pathogens through enzymatic and antimicrobial activity [50]. In previous studies in catfish challenged with *Edwardsiella ictaluri*, plasma lysozyme dynamics differed between resistant and susceptible fish, with a faster response [51] and elevated lysozyme levels [52] characterizing resistant catfish strains. Also supporting the potential importance of high mucosal levels of lysozyme for disease resistance is research from zebrafish. Yazawa et al. [53] established a transgenic zebrafish strain expressing a chicken lysozyme gene under the control of a keratin promoter which resulted in a 65% survival rate against *F. columnare* compared to 0% survival in wild-type fish. Future studies will characterize whether catfish mucosal lysozyme activity correlates with transcript levels observed in the current study.

Other important mediators of innate immunity, including an IL-8 variant [54] and TNF-alpha also were basally higher in resistant fish and showed a rapid induction upon infection relative to susceptible fish which failed to upregulate many proinflammatory cytokines immediately following challenge (Table 5, Figure 1). In contrast, several important immune antimicrobial peptides, cytokines, and mucosal cell population markers were basally higher in susceptible fish. These included the antimicrobial peptide NK-lysin [55], CD8, and CD103, a marker for mucosal dendritic cells believed to regulate tolerance in the mammalian gut [56] but uncharacterized to-date in fish. Also higher at time 0 in susceptible fish were IL-17A/F2 and IL-17RA, important mucosal cytokines recently described in fish for the first time [57]. A microfibril-associated glycoprotein 4 (MFAP4)-like molecule was more highly expressed at all timepoints in susceptible fish. We have previously observed marked differential expression of MFAP4 genes in several different bacterial challenges in catfish [11, 28, 58-61]. Previously, we characterized the ficolin-like nature of MFAP4 [62] and noted its use as macrophage-specific marker in zebrafish

[63]. While further cellular characterization is needed in catfish, MFAP4 genes have emerged as some of the most predictable markers of the early inflammatory response. In summary, further work is needed to determine if/how differences in prevalence of interbranchial lymphocyte populations [64] before and soon after infection contributed to the observed polarized immune signatures. These studies will be aided by growing resources of monoclonal antibodies directed at immune cell types in catfish [65, 66].

Mucin Secretion and Modification

Some of the most prominent differences in basal expression between resistant and susceptible catfish were found among mucin genes (Table 5; Figure 1). Mucin levels (MUC5AC, MUC5AC-like, MUC2-like, MUC19-like) were dramatically higher in the gill of susceptible fish at 0 h when compared to resistant fish. These differences (between groups) were reduced upon experimental infection with *F. columnare*, and only modest induction of mucin expression was observed within either group at 1 h post-infection (Figure 1). Mucins are large glycoproteins which can be divided into secreted (gel-forming and non-gel forming) and membrane-bound forms [67, 68]. In mammals, the secreted gel-forming mucins (MUC2, MUC5AC, MUC5B, MUC6, and MUC19) are the major constituent of mucus, forming a protective physiochemical matrix on mucosal surfaces. Additionally, mucins are extensively modified through addition of glycans (sugars) to various amino acid sites, offering protection from proteolytic enzymes. Increasingly, however, research into mammalian host-pathogen and host-commensal interactions is revealing that mucin production and glycosylation states can change dramatically during colonization and infection [69-73]. As particular host glycosylation states can be manipulated by

microbes, factors linked with glycolipid metabolism and modifications such as fucosyltransferase 1 (FUT1) are now understood to be critical in pathogen binding dynamics and host susceptibility [68, 74].

Our present understanding of the structure, abundance, and functions of fish mucins is very limited [75, 76] but a recent functional study in zebrafish revealed a role for retinoic acid (RA) in control of mucin expression and a mucosecretory phenotype in the gut [77]. This study indicated that, as in mammals, RA may be a critical factor in regulating mucus differentiation and mucin gene expression in fish. Research in human bronchial epithelial cells has shown that secreted gel-forming mucin expression is RA-dependent and that control is mediated through the RA receptor (RARα) [78, 79]. Furthermore, RA-deprived bronchial epithelial cells are reported to become squamous, fail to produce mucin, and instead secrete large amounts of lysozyme [80]. RA is additionally known to possess broad tolerogenic/anti-inflammatory properties including suppressing expression of TNF-alpha and iNOS [81]. Intriguingly, in our results (Table 5), RARα is over 7-fold higher in susceptible fish at 0 h (Table 5), with modest, non-significant differences between groups following infection.

5. Conclusions

Taken together, the immune and mucin profiles obtained by RNA-seq suggest a basal polarization in the gill mucosa with susceptible fish possessing a putative mucosecretory, tolerogenic phenotype which may predispose them to *F. columnare* infection. Furthermore, this polarization may be driven in part by RA-dependent mechanisms. Functional studies are currently underway to determine the impacts of Vitamin A and RA on mucin expression and

goblet cell abundance in fish gill and to explore how differing dietary regimens or commensal microbial populations may affect these factors.

References

[1] Marin-Esteban V, Turbica I, Dufour G, Semiramoth N, Gleizes A, Gorges R, et al. Afa/Dr diffusely adhering Escherichia coli strain C1845 induces neutrophil extracellular traps that kill bacteria and damage human enterocyte-like cells. Infect Immun 2012; 80:1891-9.

[2] Salinas I, Zhang YA, Sunyer JO. Mucosal immunoglobulins and B cells of teleost fish. Dev Comp Immunol 2011; 35:1346-65.

[3] Rombout JH, Abelli L, Picchietti S, Scapigliati G, Kiron V. Teleost intestinal immunology. Fish Shellfish Immunol 2011; 31:616-26.

[4] Perez T, Balcazar JL, Peix A, Valverde A, Velazquez E, de Blas I, et al. Lactococcus lactis subsp. tructae subsp. nov. isolated from the intestinal mucus of brown trout (*Salmo trutta*) and rainbow trout (*Oncorhynchus mykiss*). Int J Syst Evol Microbiol 2011; 61:1894-8.

[5] Plumb J, Hanson L. Health maintenance and principal microbial diseases of cultured fishes. 2011.

[6] National Animal Health Monitoring System (U.S.). Catfish 2010. Fort Collins, CO: United States Department of Agriculture, Animal and Plant Health Inspection Service, Veterinary Services, National Animal Health Monitoring System; 2010.

[7] Arias CR, Welker TL, Shoemaker CA, Abernathy JW, Klesius PH. Genetic fingerprinting of Flavobacterium columnare isolates from cultured fish. J Appl Microbiol 2004; 97:421-8.

[8] Decostere A, Haesebrouck F, Van Driessche E, Charlier G, Ducatelle R. Characterization of the adhesion of *Flavobacterium columnare* (*Flexibacter columnaris*) to gill tissue. J Fish Dis

1999; 22:465-74.

[9] Pacha R, Ordal E. Myxobacterial diseases of salmonids. Am Fish Soc Spec Publ 1970; 5:243-57.

[10] Wakabayashi H. Effect of environmental conditions on the infectivity of *Flexibacter columnaris* to fish. 1991.

[11] Sun F, Peatman E, Li C, Liu S, Jiang Y, Zhou Z, et al. Transcriptomic signatures of attachment, NF-kappaB suppression and IFN stimulation in the catfish gill following columnaris bacterial infection. Dev Comp Immunol 2012; 38:169-80.

[12] Beck BH, Farmer BD, Straus DL, Li C, Peatman E. Putative roles for a rhamnose binding lectin in *Flavobacterium columnare* pathogenesis in channel catfish Ictalurus punctatus. Fish Shellfish Immunol 2012; 33:1008-15.

[13] LaFrentz BR, Shoemaker CA, Booth NJ, Peterson BC, Ourth DD. Spleen Index and Mannose-Binding Lectin Levels in Four Channel Catfish Families Exhibiting Different Susceptibilities to *Flavobacterium columnare* and *Edwardsiella ictaluri*. J Aquat Anim Health 2012; 24:141-47.

[14] Mitchell A, Farmer B. Evaluation of an Ultra-Low-Flow Water Delivery System for Small Experimental Tanks. North American Journal of Aquaculture 2010; 72:195-200.

[15] Farmer BD, Mitchell AJ, Straus DL. The effect of high total ammonia concentration on the survival of channel catfish experimentally infected with *Flavobacterium columnare*. J Aquat Anim Health 2011; 23:162-8.

[16] Anacker RL, Ordal EJ. Studies on the myxobacterium Chondrococcus columnaris. I. Serological typing. J Bacteriol 1959; 78:25-32.

[17] Farmer B. Improved methods for the isolation and characterization of *Flavobacterium*

columnare: Faculty of the Louisiana State University and Agricultural and Mechanical College in partial fulfillment of the requirements for the degree of Master of Science in The Interdepartmental Program in Veterinary Medical Sciences through the Department of Pathobiological Sciences by Bradley Farmer BS, Northwestern State University; 2004.

[18] Miller JR, Koren S, Sutton G. Assembly algorithms for next-generation sequencing data. Genomics 2010; 95:315-27.

[19] Simpson JT, Wong K, Jackman SD, Schein JE, Jones SJ, Birol I. ABySS: a parallel assembler for short read sequence data. Genome Res 2009; 19:1117-23.

[20] Li W, Godzik A. Cd-hit: a fast program for clustering and comparing large sets of protein or nucleotide sequences. Bioinformatics 2006; 22:1658-9.

[21] Huang X, Madan A. CAP3: A DNA sequence assembly program. Genome Res 1999; 9:868-77.

[22] Gotz S, Garcia-Gomez JM, Terol J, Williams TD, Nagaraj SH, Nueda MJ, et al. High-throughput functional annotation and data mining with the Blast2GO suite. Nucleic Acids Res 2008; 36:3420-35.

[23] Kal AJ, van Zonneveld AJ, Benes V, van den Berg M, Koerkamp MG, Albermann K, et al. Dynamics of gene expression revealed by comparison of serial analysis of gene expression transcript profiles from yeast grown on two different carbon sources. Mol Biol Cell 1999; 10:1859-72.

[24] Robinson MD, Oshlack A. A scaling normalization method for differential expression analysis of RNA-seq data. Genome Biol 2010; 11:R25.

[25] Bauer S, Grossmann S, Vingron M, Robinson PN. Ontologizer 2.0--a multifunctional tool for GO term enrichment analysis and data exploration. Bioinformatics 2008; 24:1650-1.

[26] Grossmann S, Bauer S, Robinson PN, Vingron M. Improved detection of overrepresentation of Gene-Ontology annotations with parent child analysis. Bioinformatics 2007; 23:3024-31.

[27] Pfaffl MW, Horgan GW, Dempfle L. Relative expression software tool (REST) for group-wise comparison and statistical analysis of relative expression results in real-time PCR. Nucleic Acids Res 2002; 30:e36.

[28] Li C, Zhang Y, Wang R, Lu J, Nandi S, Mohanty S, et al. RNA-seq analysis of mucosal immune responses reveals signatures of intestinal barrier disruption and pathogen entry following *Edwardsiella ictaluri* infection in channel catfish, *Ictalurus punctatus*. Fish Shellfish Immunol 2012; 32:816-27.

[29] Jeffries KM, Hinch SG, Sierocinski T, Clark TD, Eliason EJ, Donaldson MR, et al. Consequences of high temperatures and premature mortality on the transcriptome and blood physiology of wild adult sockeye salmon (*Oncorhynchus nerka*). Ecol Evol 2012; 2:1747-64.

[30] Sánchez CC, Weber GM, Gao G, Cleveland BM, Yao J, Rexroad CE. Generation of a reference transcriptome for evaluating rainbow trout responses to various stressors. BMC Genomics 2011; 12:626.

[31] Morrison RN, Cooper GA, Koop BF, Rise ML, Bridle AR, Adams MB, et al. Transcriptome profiling the gills of amoebic gill disease (AGD)-affected Atlantic salmon (*Salmo salar L.*): a role for tumor suppressor p53 in AGD pathogenesis? Physiol Genomics 2006; 26:15-34.

[32] Wynne JW, O'Sullivan MG, Cook MT, Stone G, Nowak BF, Lovell DR, et al. Transcriptome analyses of amoebic gill disease-affected Atlantic salmon (*Salmo salar*) tissues reveal localized host gene suppression. Mar Biotechnol (NY) 2008; 10:388-403.

[33] Decostere A. *Flavobacterium columnare* infections in fish: the agent and its adhesion to the gill tissue. Verh K Acad Geneeskd Belg 2002; 64:421-30.

[34] Staroscik AM, Nelson DR. The influence of salmon surface mucus on the growth of *Flavobacterium columnare*. J Fish Dis 2008; 31:59-69.

[35] Klesius PH, Shoemaker CA, Evans JJ. *Flavobacterium columnare* chemotaxis to channel catfish mucus. FEMS Microbiol Lett 2008; 288:216-20.

[36] Olivares-Fuster O, Bullard SA, McElwain A, Llosa MJ, Arias CR. Adhesion dynamics of *Flavobacterium columnare* to channel catfish *Ictalurus punctatus* and zebrafish *Danio rerio* after immersion challenge. Dis Aquat Organ 2011; 96:221-7.

[37] Decostere A, Haesebrouck F, Charlier G, Ducatelle R. The association of Flavobacterium columnare strains of high and low virulence with gill tissue of black mollies (*Poecilia sphenops*). Vet Microbiol 1999; 67:287-98.

[38] Klesius PH, Pridgeon JW, Aksoy M. Chemotactic factors of *Flavobacterium columnare* to skin mucus of healthy channel catfish (*Ictalurus punctatus*). FEMS Microbiol Lett 2010; 310:145-51.

[39] Liu S, Zhou Z, Lu J, Sun F, Wang S, Liu H, et al. Generation of genome-scale gene-associated SNPs in catfish for the construction of a high-density SNP array. BMC Genomics 2011; 12:53.

[40] Bogdan C. Nitric oxide and the immune response. Nat Immunol 2001; 2:907-16.

[41] Aktan F. iNOS-mediated nitric oxide production and its regulation. Life Sci 2004; 75:639-53.

[42] Lepiller S, Franche N, Solary E, Chluba J, Laurens V. Comparative analysis of zebrafish nos2a and nos2b genes. Gene 2009; 445:58-65.

[43] Laing KJ, Hardie LJ, Aartsen W, Grabowski PS, Secombes CJ. Expression of an inducible nitric oxide synthase gene in rainbow trout *Oncorhynchus mykiss*. Dev Comp Immunol 1999; 23:71-85.

[44] Campos-Perez JJ, Ellis AE, Secombes CJ. Toxicity of nitric oxide and peroxynitrite to bacterial pathogens of fish. Dis Aquat Organ 2000; 43:109-15.

[45] Guo FH, De Raeve HR, Rice TW, Stuehr DJ, Thunnissen F, Erzurum SC. Continuous nitric oxide synthesis by inducible nitric oxide synthase in normal human airway epithelium in vivo. Proc Natl Acad Sci USA 1995; 92:7809-13.

[46] Jain B, Rubinstein I, Robbins RA, Leise KL, Sisson JH. Modulation of airway epithelial cell ciliary beat frequency by nitric oxide. Biochem Biophys Res Commun 1993; 191:83-8.

[47] Ellis A. Innate host defense mechanisms of fish against viruses and bacteria. Dev Comp Immunol 2001; 25:827-39.

[48] Bergsson G, Agerberth B, Jörnvall H, Gudmundsson GH. Isolation and identification of antimicrobial components from the epidermal mucus of Atlantic cod (*Gadus morhua*). Febs Journal 2005; 272:4960-69.

[49] Nigam AK, Kumari U, Mittal S, Mittal AK. Comparative analysis of innate immune parameters of the skin mucous secretions from certain freshwater teleosts, inhabiting different ecological niches. Fish Physiol Biochem 2012; 38:1245-56.

[50] Davis KM, Weiser JN. Modifications to the peptidoglycan backbone help bacteria to establish infection. Infect Immun 2011; 79:562-70.

[51] Bilodeau A, Small B, Wise D, Wolters W. Pathogen levels, lysozyme, and cortisol response in channel catfish with susceptibility differences to *Edwardsiella ictaluri*. J Aquat Animal Health. 2005; 17:138-46.

[52] Bilodeau-Bourgeois L, Bosworth BG, Peterson BC. Differences in mortality, growth, lysozyme, and Toll-like receptor gene expression among genetic groups of catfish exposed to virulent *Edwardsiella ictaluri*. Fish Shellfish Immunol 2008; 24:82-89.

[53] Yazawa R, Hirono I, Aoki T. Transgenic zebrafish expressing chicken lysozyme show resistance against bacterial diseases. Transgenic Res 2006; 15:385-91.

[54] Chen Y-C, Giovannucci E, Lazarus R, Kraft P, Ketkar S, Hunter DJ. Sequence variants of Toll-like receptor 4 and susceptibility to prostate cancer. Cancer Res 2005; 65:11771-78.

[55] Wang Q, Wang Y, Xu P, Liu Z. NK-lysin of channel catfish: gene triplication, sequence variation, and expression analysis. Mol Immunol 2006; 43:1676-86.

[56] Scott CL, Aumeunier AM, Mowat AM. Intestinal CD103+ dendritic cells: master regulators of tolerance? Trends Immunol 2011; 32:412-19.

[57] Monte MM, Wang T, Holland JW, Zou J, Secombes CJ. Cloning and characterization of rainbow trout interleukin-17A/F2 (IL-17A/F2) and IL-17 receptor A: expression during infection and bioactivity of recombinant IL-17A/F2. Infect Immun 2013; 81:340-53.

[58] Peatman E, Baoprasertkul P, Terhune J, Xu P, Nandi S, Kucuktas H, et al. Expression analysis of the acute phase response in channel catfish (*Ictalurus punctatus*) after infection with a Gram-negative bacterium. Dev Comp Immunol 2007; 31:1183-96.

[59] Peatman E, Terhune J, Baoprasertkul P, Xu P, Nandi S, Wang S, et al. Microarray analysis of gene expression in the blue catfish liver reveals early activation of the MHC class I pathway after infection with *Edwardsiella ictaluri*. Mol Immunol 2008; 45:553-66.

[60] Li C, Wang R, Su B, Luo Y, Terhune J, Beck B, et al. Evasion of mucosal defenses during Aeromonas hydrophila infection of channel catfish (*Ictalurus punctatus*) skin. Dev Comp Immunol 2012.

[61] Li C, Beck B, Su B, Terhune J, Peatman E. Early mucosal responses in blue catfish (*Ictalurus furcatus*) skin to *Aeromonas hydrophila* infection. Fish Shellfish Immunol 2013; 34:920-8.

[62] Niu D, Peatman E, Liu H, Lu J, Kucuktas H, Liu S, et al. Microfibrillar-associated protein 4 (MFAP4) genes in catfish play a novel role in innate immune responses. Dev Comp Immunol 2011; 35:568-79.

[63] Zakrzewska A, Cui C, Stockhammer OW, Benard EL, Spaink HP, Meijer AH. Macrophage-specific gene functions in Spi1-directed innate immunity. Blood 2010; 116:e1-11.

[64] Koppang EO, Fischer U, Moore L, Tranulis MA, Dijkstra JM, Kollner B, et al. Salmonid T cells assemble in the thymus, spleen and in novel interbranchial lymphoid tissue. J Anat 2010; 217:728-39.

[65] Edholm ES, Hudgens ED, Tompkins D, Sahoo M, Burkhalter B, Miller NW, et al. Characterization of anti-channel catfish IgL sigma monoclonal antibodies. Vet Immunol Immunopathol 2010; 135:325-8.

[66] Edholm ES, Bengten E, Wilson M. Insights into the function of IgD. Dev Comp Immunol 2011; 35:1309-16.

[67] Dharmani P, Srivastava V, Kissoon-Singh V, Chadee K. Role of Intestinal Mucins in Innate Host Defense Mechanisms against Pathogens. J Innate Immun 2009; 1:123-35.

[68] Moran AP, Gupta A, Joshi L. Sweet-talk: role of host glycosylation in bacterial pathogenesis of the gastrointestinal tract. Gut 2011; 60:1412-25.

[69] Navabi N, Johansson ME, Raghavan S, Lindén SK. Helicobacter pylori Infection Impairs the Mucin Production Rate and Turnover in the Murine Gastric Mucosa. Infect Immun 2013; 81:829-37.

[70] Colomb F, Krzewinski-Recchi MA, El Machhour F, Mensier E, Jaillard S, Steenackers A, et al. TNF regulates sialyl-Lewis(x) and 6-sulfo-sialyl-Lewis(x) expression in human lung through up-regulation of ST3GAL4 transcript isoform BX. Biochimie 2012; 94:2045-53.

[71] Mahdavi J, Sonden B, Hurtig M, Olfat FO, Forsberg L, Roche N, et al. Helicobacter pylori SabA adhesin in persistent infection and chronic inflammation. Science 2002; 297:573-8.

[72] Mack DR, Michail S, Wei S, McDougall L, Hollingsworth MA. Probiotics inhibit enteropathogenic *E. coliadherence* in vitro by inducing intestinal mucin gene expression. American Journal of Physiology-Gastrointestinal and Liver Physiology 1999; 276:G941-G50.

[73] Mack D, Ahrne S, Hyde L, Wei S, Hollingsworth M. Extracellular MUC3 mucin secretion follows adherence of Lactobacillus strains to intestinal epithelial cells in vitro. Gut 2003; 52:827-33.

[74] Bao WB, Ye L, Pan ZY, Zhu J, Du ZD, Zhu GQ, et al. Microarray analysis of differential gene expression in sensitive and resistant pig to Escherichia coli F18. Anim Genet 2012; 43:525-34.

[75] Micallef G, Bickerdike R, Reiff C, Fernandes JM, Bowman AS, Martin SA. Exploring the Transcriptome of Atlantic Salmon (*Salmo salar*) Skin, a Major Defense Organ. Marine Biotechnology 2012:1-11.

[76] Provan F, Jensen LB, Uleberg KE, Larssen E, Rajalahti T, Mullins J, et al. Proteomic analysis of epidermal mucus from sea lice-infected Atlantic salmon, *Salmo salar L*. J Fish Dis 2013; 36:311-21.

[77] Oehlers SH, Flores MV, Hall CJ, Crosier KE, Crosier PS. Retinoic acid suppresses intestinal mucus production and exacerbates experimental enterocolitis. Dis Model Mech 2012; 5:457-67.

[78] Koo JS, Yoon JH, Gray T, Norford D, Jetten AM, Nettesheim P. Restoration of the mucous phenotype by retinoic acid in retinoid-deficient human bronchial cell cultures: changes in mucin gene expression. Am J Respir Cell Mol Biol 1999; 20:43-52.

[79] Gray T, Koo JS, Nettesheim P. Regulation of mucous differentiation and mucin gene

expression in the tracheobronchial epithelium. Toxicology 2001; 160:35-46.

[80] Yoon J-H, Kim K-S, Kim HU, Linton JA, Lee J-G. Effects of TNF-a and IL-1 ß on Mucin, Lysozyme, IL-6 and IL-8 in passage-2 Normal Human Nasal Epithelial Cells. Acta oto-laryngologica 1999; 119:905-10.

[81] Dheen ST, Jun Y, Yan Z, Tay SS, Ang Ling E. Retinoic acid inhibits expression of TNF-α and iNOS in activated rat microglia. Glia 2004; 50:21-31.

V. SHORT-TERM FEED DEPRIVATION ALTERS IMMUNE STATUS OF SURFACE MUCOSA IN CHANNEL CATFISH (*ICTALURUS PUNCTATUS*)

1. Introduction

Alterations in feeding regimen are common practice in the modern aquaculture industry, predicated in part on research indicating that fasting is well tolerated by most fish species [1, 2]. Food deprivation strategies can be employed as part of a seasonal feeding pattern [3], in response to overproduction, or as a response to disease outbreak [4, 5]. When diseases prompt changes in feeding, producers must weigh potential savings on feed and the benefits of limiting fish-fish contact during feeding against reduced growth and heightened stress stemming from nutrient restriction. Traditionally missing in the equation has been any understanding on how short-term fasting may impact the immune status of farmed fish.

Most feed deprivation investigations to-date have focused on changes in intestinal cellular morphology and enzyme activity or on transcriptional changes in critical regulators of protein synthesis or glucose metabolism in tissues such as liver, muscle, and intestine [6-8]. Recent studies have documented changes in gene mediators of innate immunity following 4 week starvation studies in rainbow trout intestinal epithelia [9] and Atlantic salmon liver [10]. Comparatively little is known regarding the immune consequences of more common short-term fasting events. However, a small body of previous research indicates that short-term withdrawal of feed, while not visibly impacting growth parameters, can have striking effects, particularly at mucosal surfaces. Vieira et al. [11] reported broad impacts of a one week feed restriction regimen on skin healing and scale regeneration in sea bream utilizing an oligo microarray.

Krogdahl and Bakke-McKellep [7] observed rapid 20-50% decreases in intestinal tissue mass and enzyme activities after two days of fasting in Atlantic salmon. Perhaps of greatest relevance here is the recent report that a seven day feed deprivation caused significant changes in microbial density and community composition in the cutaneous mucus of Atlantic salmon [12].

The impact of feed deprivation on mortality rates of channel catfish (*Ictalurus punctatus*) exposed to the bacterial pathogens *Edwardsiella ictaluri* and *Flavobacterium columnare* has previously been established [4, 5]. *F. columnare*, a widespread opportunistic pathogen of freshwater fish, and a leading cause of mortality in the U.S. catfish industry [13], causes higher losses in fish that have been withheld from feed for as little as seven days [4]. Attachment and entry of *F. columnare* into catfish is via surface mucosa, skin and gill. Recently, we identified a rhamnose-binding lectin (RBL) whose expression is strongly induced in catfish gill by *F. columnare* infection [14]. A more detailed subsequent study of RBL activity revealed that expression levels in gill were correlated with columnaris susceptibility, and that saturation of the receptor with its putative ligands resulted in significantly decreased columnaris mortality. Furthermore, RBL expression increased greater than 100-fold in the gill tissue of catfish fingerlings fasted for seven days [15]. Given these results and the impact of feeding status on columnaris susceptibility, we wished to examine further the broader molecular effects of short-term fasting of channel catfish on surface mucosal health. Towards that end, here we utilized RNA-seq-based transcriptome profiling of skin and gill homogenates from fed and 7 d fasted channel catfish fingerlings to better understand immunonutritonal regulation in teleost fish.

2. Materials and Methods

2.1 Experimental animals and tissue collection

Juvenile channel catfish (42.2 ± 5.6 g) were stocked into four 600 L tanks with 30 fish per tank with forced air aeration and flow-through well water at 24.8 ± 0.02 ℃, pH 7.7, and dissolved oxygen of 7.4 ± 0.3 mg/L.

Channel catfish were subjected to two treatments with two replicate tanks per treatment. Fish in treatment group 1 were fed to satiation three times daily with a standard catfish ration (35% protein, 2.5% fat). In treatment 2, fish were withheld feed for 7 d. All fish were sacrificed on day 7, euthanized with tricaine methanesulfonate (MS 222) at 300 mg/L before tissues were collected.

Equivalent portions of the gill and skin were isolated from matching locations on each fish and stored in RNALater (Ambion® Brand Products, Life Technologies, Grand Island, New York) at -80 ˚C until RNA extraction. Three pools (five fish each) of tissue were generated from each condition. Equal amounts of tissue were collected from each fish within a pool. Samples were immediately placed in RNAlater and stored at -80 ℃ until extraction. Samples were homogenized with a mortar and pestle.

2.2 RNA extraction, library construction and sequencing

Extractions were performed according to the manufacturer's directions using an RNeasy Kit (Qiagen, Valencia, California). RNA concentration and integrity of each sample was measured on an Agilent 2100 Bioanalyzer. For each timepoint, equal amounts of RNA from skin and gill were pooled to generate three pooled replicates for RNA-seq library construction.

RNA-seq library preparation and sequencing was carried out by HudsonAlpha Genomic Services Lab (Huntsville, AL, USA) following the standard TruSeq protocols with 100 bp PE read chemistry on an Illumina HiSeq 2500 [14].

2.3 De novo assembly of sequencing reads

The *de novo* assembly of short reads was performed on channel catfish using both ABySS and Trinity [16, 17], versions 1.3.2 and the 2012-10-05 editions, respectively. Before assembly, raw reads were trimmed by removing adaptor sequences and ambiguous nucleotides. Reads with quality scores less than 20 and length below 30 bp were all trimmed. The resulting high-quality sequences were used in the subsequent assembly.

In ABySS, briefly, the clean reads were first hashed according to a predefined k-mer length, the 'k-mers'. After capturing overlaps of length k-1 between these k-mers, the short reads were assembled into contigs. The k-mer size was set from 50 to 96, assemblies from all k-mers were merged into one assembly by Trans-ABySS (version 1.4.4).

In Trinity, briefly, the raw reads were assembled into the unique sequences of transcripts in Inchworm via greedy K-mer extension (k-mer 25). After mapping of reads to Inchworm contigs, Chrysalis incorporated reads into deBruijn graphs and the Butterfly module processed the individual graphs to generate full-length transcripts.

In order to reduce redundancy, the assembly results from different assemblers were passed to CD-Hit version 4.5.4 [18] and CAP3 [19] for multiple alignments and consensus building. The threshold was set as identity equal to 1 in CD-Hit, the minimal overlap length and identity equal to 100 bp and 99% in CAP3.

2.4 Gene Annotation and Ontology

The selected assembly contigs were used as queries against the NCBI zebrafish protein database, the UniProtKB/SwissProt database and the non-redundant (nr) protein database using the BLASTX program. The cutoff E-value was set at 1e-5 and only the top gene id and name were initially assigned to each contig. Gene ontology (GO) annotation analysis was performed using the zebrafish BLAST results in Blast2GO version 2.6.3 [20]. The zebrafish BLAST result or the nr BLAST result was imported to BLAST2GO. The final annotation file was categorized with respect to Biological Process, Molecular Function, and Cellular Component at level 2.

2.5 Identification of differentially expressed contigs

The high quality reads from each sample were mapped onto the Trinity reference assembly using CLC Genomics Workbench software. During mapping, at least 95% of the bases were required to align to the reference and a maximum of two mismatches were allowed. The total mapped reads number for each transcript was determined and then normalized to detect RPKM (Reads Per Kilobase of exon model per Million mapped reads). The proportions-based test was used to identify the differently expressed genes between fed and fasted group with three replicates in each group with corrected p-value < 0.05 [21]. After scaling normalization of the RPKM values, fold changes were calculated. Analysis was performed using the RNA-seq module and the expression analysis module in CLC Genomics Workbench [22]. Transcripts with

absolute fold change values of larger than 1.5 were included in analysis as differently expressed genes.

Contigs with previously identified gene matches were carried forward for further analysis. Functional groups and pathways encompassing the differently expressed genes were identified based on GO analysis, pathway analysis based on the Kyoto Encyclopedia of Genes and Genomes (KEGG) database, and manual literature review.

2.6 Enrichment Analysis

Enrichment analysis of significantly expressed GO terms was performed using Ontologizer 2.0 using the Parent-Child-Intersection method with a Benjammini-Hochberg multiple testing correction [23, 24]. GO terms for each gene were obtained by utilizing zebrafish annotations for the unigene set. The threshold was set as FDR value < 0.1.

2.7 Experimental validation—QPCR

Ten significantly expressed genes with different expression patterns were selected for validation using real time QPCR with gene specific primers designed using Primer3 software. Total RNA was extracted using the RNeasy Plus kit (Qiagen) following manufacturer's instructions. All the cDNA products were diluted to 250 ng/µl and utilized for the quantitative real-time PCR reaction using the SsoFast™ EvaGreen® Supermix on a CFX96 real-time PCR Detection System (Bio-Rad Laboratories, Hercules, CA). The thermal cycling profile consisted of an initial denaturation at 95℃ (for 30 s), followed by 40 cycles of denaturation at 94℃ (5 s),

an appropriate annealing/extension temperature (58 ℃, 5 s). Results were expressed relative to the expression levels of 18S rRNA in each sample using the Relative Expression Software Tool (REST) version 2009 [25] as described in Sun et al. (2012).

3. Results

3.1 Sequencing of short expressed reads from catfish gill

A total of 209 million 100 bp high quality reads were generated for the fasted and fed samples. Greater than 26 million reads were generated for each of the six libraries. Raw read data are archived at the NCBI Sequence Read Archive (SRA) under Accession **SRP017689**.

3.2 De novo assembly of catfish gill and skin transcriptome

Given the importance of assembly of long, accurate contigs to capture catfish genes and to correctly identify differential expression, we compared two prominent options for *de novo* transcriptome assembly: Trans-ABySS and Trinity. We had previously developed an in-house bioinformatics pipeline around Trans-ABySS [14,26,27] and demonstrated its superior performance in comparison to use of CLC Genome Workbench or Velvet assemblers. However, we sought to determine whether use of Trinity [17] would improve assemblies further.

3.2.1 Trans-ABySS

Use of Trans-ABySS to merge ABySS multi-k-assembled contigs, resulted in approximately 301,500 contigs with average length of 1,036.1 bp and N50 size of 1,716 bp, with 24,345 contigs longer than 1,000 bp. After removing redundancy using CD-Hit and CAP-3, about 57.53% contigs were kept, resulting in a final assembly of 173,459 unique contigs with average length 887.3 bp (Table 1).

Table 1 Summary of *de novo* assembly results of Illumina sequence data from channel catfish gill and skin using Trans-ABySS and Trinity.

	Trans-ABySS	Trinity
Contigs	301,500	281,595
Large contigs (≥1000bp)	24,345	30,202
N50 (bp)	1,716	2,270
Average contig length	1,036.1	1046.9
Contigs (After CD-HIT-EST+ CAP3)	173,459	272,229
Percentage contigs kept after redundancy removal	57.6%	96.7%
Average length (bp) (After CD-HIT-EST+ CAP3)	887.3	996.5
Reads mapped in pairs (%)	66.3%	79.9%
Reads mapped to final reference (%)	80.8%	85.7%

3.2.2 Trinity

Trinity generated approximately 281,595 contigs in its initial contig assembly with average length of 1,046.9 bp and N50 size of 2,270 bp, with 30,202 contigs longer than 1,000 bp. After removing redundancy by CD-Hit and CAP-3, about 96.67% contigs were kept, resulting in a final 272,229 contigs with average length 996.5 (Table 1).

3.2.3 Gene identification and annotation

BLAST-based gene identification was performed to annotate the channel catfish gill/skin transcriptome and inform downstream differential expression analysis. After gene annotation, 60,892 contigs from the Trans-ABySS assembly had significant BLAST hits against 16,610 unigene (unique gene) matches from zebrafish, the closest available reference genome to catfish (Table 2). Using a more stringent criteria of a BLAST score ≥100 and E-value ≤ 1e-20 (quality matches) identified 14,679 zebrafish unigene matches. The same BLAST criteria were used to annotate the Trans-ABySS assembly based on matches against the UniProt and NCBI NR (non-redundant) databases.

Table 2 Summary of gene identification and annotation of assembled catfish contigs based on BLAST homology searches against various protein databases (Zebrafish, UniProt, nr). Putative gene matches were at E-value ≤ 1e-5. Hypothetical gene matches denote those BLAST hits with uninformative annotation. Quality unigene hits denote more stringent parameters, including score≥100, E-value ≤ 1e-20.

	Trans-ABySS			Trinity		
	Zebrafish	UniProt	NR	Zebrafish	UniProt	NR
Contigs with putative gene matches	60,892	50,766	64,788	82,365	68,797	83,972
Annotated contigs ≥500bp	41,313	37,468	44,019	71,782	61,658	73,849
Annotated contigs ≥1000bp	29,023	27,479	30,379	59,986	53,210	61,185
Unigene matches	16,610	19,341	25,416	17,892	19,970	26,549
Hypothetical gene matches	986	0	3,788	10,58	0	3,693
Quality Unigene matches	14,679	15,933	15,863	15,821	15,427	20,589

In contrast, 82,365 Trinity contigs had a significant BLAST hit against 17,892 unique zebrafish genes (Table 2). 15,821 unigenes were identified based on hits to the zebrafish database with the more stringent criteria of a BLAST score ≥100 and E-value ≤ 1e-20. As with the Trans-ABySS assembly, the same BLAST criteria were used in comparison of the Trinity reference contigs with the UniProt and nr databases. The largest number of matches was to the

NR database with 83,972 contigs with putative gene matches to nr and 20,589 quality unigene matches (Table 2).

3.2.4 Best assembly selection

In a comparison of the assemblies generated by Trans-ABySS and Trinity (Table 1), it was clear that although Trans-ABySS consistently generated a larger initial number of contigs, redundancy was much higher than that observed with Trinity. CD-HIT/CAP3 removed over 40% of Trans-ABySS contigs due to this redundancy, while almost all Trinity contigs were carried forward after this process. The final Trinity assembly contained almost 100,000 more contigs than Trans-ABySS due to Trinity's superior ability to distinguish splicing isoforms and gene paralogs. Trinity contigs also had larger N50 and average length, 2,270 bp and 996.5 bp, respectively, than Trans-ABySS. These metrics reflect Trinity's superior ability to map paired end reads into the same contig. Trinity mapped 79.9% of reads in pairs versus 66.3% in Trans-ABySS (Table 1). The superior de novo assembly produced by Trinity was also reflected in the number of quality unigene matches against zebrafish (15,821 vs. 14,679) and NR (20,589 vs. 15,863) databases. Given these results, we utilized the Trinity assembly for subsequent analysis of differential expression.

3.3 Identification and analysis of differentially expressed genes

A total of 1,545 genes (unique annotated contigs with significant BLAST identities) were differentially expressed greater than 1.5-fold, with 412 up-regulated genes and 1,133 down-

regulated genes (Table 3). Short read coverage within differentially expressed contigs is critical for accurate quantification of expression. We obtained good coverage of differentially expressed contigs, with an average of 784.6 reads/contig.

Table 3 Statistics of differently expressed genes between fasted and fed channel catfish. *Shared* category indicates the number of genes significantly differentially expressed in the same direction in both groups, while percentage is the number of shared genes/number of potentially shared genes. Values indicate contigs/genes passing cutoff values of fold change ≥1.5 ($p<0.05$). Average contig size refers to reads/contig.

Fed (Control)	Fasted Channel Catfish
Up-regulated	412
Down-regulated	1,133
Total	1,545
Reads per contig	784.6

3.4 Enrichment and Pathway Analysis

A total of 3,482 GO terms including 970 (27.86%) cellular component terms, 1,012 (29.06%) molecular functions terms and 1,491 (42.82%) biological process terms were assigned to 1,545 unique gene matches. The differently expressed unique genes were then used as inputs to perform enrichment analysis using Ontologizer. A total of 125 terms with p-value (FDR-corrected) < 0.05 were considered significantly overrepresented. Ten higher level GO terms were retained as informative for further pathway analysis. The GO terms included response to stress, regulation of cell death, and cell cycle regulation.

Based on enrichment analysis and manual annotation and literature searches, representative key genes were arranged into three broad categories, including immune response, energy

metabolism, and cell cycling (Table 4). Imputed putative functional roles of these genes are covered in the Discussion.

Table 4 Differentially expressed genes in the gill and skin between fasted and fed channel catfish in different functional classifications. Positive values indicate higher expression in fasted channel catfish, while negative values indicate higher expression in fed catfish. When reads number equaled to 0 in fed or fasted group, the fold change is presented by average normalized read number in fed/average normalized read number in fasted.

Gene Name	Contig_ID	Fold Change
Immune (Reads Number >0)		
Autoimmune regulator-like	comp99702_c0_seq1	-2.08
Beta-2-glycoprotein 1	comp100784_c1_seq4	9.82
cAMP-responsive element modulator	comp90058_c0_seq2	-6.47
CC chemokine SCYA113	comp82613_c0_seq1	-4.30
C-C motif chemokine 19-like precursor	comp81887_c0_seq1	-2.63
CD83	comp88858_c0_seq1	1.82
Chemokine CCL-C5a precursor	comp33700_c0_seq1	-3.30
Clusterin precursor	comp33405_c0_seq1	3.57
Complement C1q tumor necrosis factor-related protein 6	comp99810_c0_seq1	-3.04
Complement C4-B	comp99246_c0_seq3	4.40
C-X-C motif chemokine 10 precursor	comp90838_c0_seq1	-3.61
C-X-C motif chemokine 11-like	comp100129_c0_seq1	-3.46
Eosinophil peroxidase precursor	comp98419_c0_seq2	-2.14
Galectin-4-like isoform 1	comp93775_c0_seq1	-1.80
IgM chain C region precursor, secreted form - channel catfish	comp94145_c1_seq2	-1.69
IgGFc-binding protein-like	comp100810_c0_seq1	-2.62
Immunoresponsive gene 1, like	comp55693_c0_seq1	-53.66
Interferon-induced protein 44	Contig6350	3.46
Interferon-induced very large GTPase 1-like	comp102878_c0_seq1	1.73
Interleukin 17a/f1 precursor	comp102117_c4_seq2	-3.27
Interleukin-22 receptor subunit alpha-2 precursor	comp77551_c0_seq1	-2.13
Intestinal-type alkaline phosphatase precursor	comp60600_c0_seq1	90.69
Lymphokine-activated killer T-cell-originated protein kinase	comp89030_c0_seq1	-2.99
Lysozyme G	comp91870_c0_seq1	-2.78
Lysozyme G-like 1	comp91870_c0_seq2	-2.07
Lysozyme C	comp75157_c0_seq1	-6.35
Matrix metalloproteinase-19-like	comp100787_c0_seq1	-1.74
MHC class II antigen	Contig2104	2.13
MHC class II beta chain	comp101401_c0_seq1	1.91
Microfibril-associated glycoprotein 4-like	comp87348_c0_seq1	-5.74
Myxovirus (influenza virus) resistance G	Contig5990	-2.95
NACHT, LRR and PYD domains-containing protein 14-like	comp95945_c1_seq1	1.64
NADPH oxidase organizer 1a	comp100364_c0_seq1	-1.81
Nitric oxide synthase 2b, inducible	comp93125_c0_seq1	-17.22

Olfactomedin-like	comp100788_c0_seq4	-2.08
Peptidoglycan recognition protein 6	comp88793_c0_seq1	-9.13
Polymeric immunoglobulin receptor (pIgR)	comp93688_c0_seq2	-1.70
Protein canopy homolog 2 precursor	comp93948_c0_seq1	-3.35
SAM domain and HD domain-containing protein 1-like	comp98561_c0_seq8	6.64
Serum amyloid P-component precursor	comp91375_c0_seq2	1.69
Toxin-1 precursor	comp112912_c0_seq1	-6.89
Vitelline membrane outer layer protein 1 homolog	comp101161_c0_seq1	-3.55
Complement C1q 3-like	comp85071_c0_seq1	-3.41
Immune (Reads Number contain 0)		
Chitinase, acidic.1 precursor	comp84271_c0_seq1	0/84
Chitinase, acidic.3 precursor	comp72677_c0_seq1	0/51
Energy Metabolism		
6-phosphofructo-2-kinase/fructose-2,6-biphosphatase 4	comp97436_c0_seq2	2.77
Adipocyte enhancer-binding protein 1	comp97921_c0_seq1	3.26
Angiopoietin-related protein 4 precursor	comp95719_c0_seq1	3.16
Apolipoprotein Bb precursor	comp99989_c0_seq2	54.62
Apolipoprotein E precursor	comp53599_c0_seq1	3.80
Apolipoprotein L, 1	comp96519_c0_seq1	2.81
Carboxypeptidase A6-like	comp510161_c0_seq1	10.95
Carnitine O-acetyltransferase-like	comp97193_c0_seq1	2.35
Carnitine O-palmitoyltransferase 1, liver isoform	comp98534_c0_seq8	6.12
Corticosteroid 11-beta-dehydrogenase isozyme 2	comp84850_c0_seq1	5.72
Cytoplasmic phosphatidylinositol transfer protein 1	comp98091_c0_seq1	4.28
Diacylglycerol O-acyltransferase 2	Contig576	-5.78
Endothelial lipase precursor	comp118134_c0_seq1	-3.40
Fat storage-inducing transmembrane protein 2	comp85823_c0_seq1	-2.31
Fatty acid binding protein 1-B.1	comp143596_c0_seq1	11.26
Fatty acid-binding protein, brain	comp72920_c0_seq1	-3.57
Fatty acid-binding protein, intestinal	comp91705_c1_seq1	29.35
F-box only protein 32	comp83869_c0_seq1	9.07
Fructose-1,6-bisphosphatase 1b	comp99650_c0_seq4	3.96
Glutamine synthetase	comp90753_c0_seq1	-1.76
Glyceraldehyde 3-phosphate dehydrogenase 2	comp86158_c0_seq4	-2.03
Glycogen synthase 1	comp91600_c0_seq1	2.51
Growth hormone receptor b precursor	comp84382_c0_seq2	2.88
Hexokinase-2	comp93533_c0_seq1	-2.98
Krueppel-like factor 15	comp98940_c1_seq5	2.82
Lipoprotein lipase precursor	comp97781_c0_seq1	-2.15
Malate dehydrogenase	comp86729_c0_seq2	2.57
Mannose-1-phosphate guanyltransferase alpha-B	comp95181_c0_seq1	-5.29
Muscle RING finger 1	comp59139_c0_seq1	2.72
Probable fructose-2,6-bisphosphatase TIGAR A	comp91599_c0_seq3	-5.35
Relaxin-3 receptor 1-like	comp82094_c0_seq1	3.70
Solute carrier family 15 member 1	comp98443_c5_seq1	5.36
Solute carrier family 2, facilitated glucose transporter	comp91908_c0_seq2	-3.54
Squalene synthase	comp97820_c0_seq5	2.69

Star-related lipid transfer protein 4	comp102843_c2_seq1	-9.75
Stearoyl-coa desaturase 5	comp96892_c0_seq3	-8.22
Pyruvate dehydrogenase kinase, isozyme 4	comp101992_c0_seq2	5.99
Cell Cycling/Proliferation		
Anterior gradient protein 2 homolog precursor	comp74849_c0_seq1	-3.33
Antigen KI-67-like	comp93863_c1_seq1	-3.10
Borealin	comp98879_c0_seq1	-3.18
Cell division control protein 2 homolog	comp111617_c0_seq1	-3.88
Cell division cycle-associated protein 2	comp83275_c0_seq1	-3.08
Cell division cycle-associated protein 3	comp93142_c0_seq1	-3.18
Cell division cycle-associated protein 7	comp100916_c4_seq2	-2.89
Cyclin-A2	comp96163_c2_seq2	-3.71
Cyclin-dependent kinase inhibitor 1C-like	comp92450_c0_seq1	3.18
Cyclin-dependent kinase inhibitor 3	comp85776_c0_seq1	-2.89
DNA replication licensing factor MCM3	comp92554_c0_seq1	-3.36
DNA replication licensing factor MCM4	Contig155	-2.92
DNA replication licensing factor MCM5	comp85130_c0_seq1	-3.14
DNA replication licensing factor MCM6	comp88864_c0_seq1	-3.42
Eukaryotic translation initiation factor 2-alpha	Contig6286	-1.94
G1/S-specific cyclin-E2	comp82150_c0_seq2	-3.78
G2/mitotic-specific cyclin-B1	comp80016_c0_seq1	-3.63
G2/mitotic-specific cyclin-B3	comp102297_c0_seq2	-2.39
Mitotic checkpoint serine/threonine-protein kinase BUB1	comp94936_c0_seq1	-3.49
PCNA-associated factor-like	comp115121_c0_seq1	-2.52
Protein regulator of cytokinesis 1	comp92273_c0_seq4	-7.87
Structural maintenance of chromosomes 2	comp101484_c0_seq1	-3.01

3.5 Validation of RNA-seq profiles by QPCR

We selected 10 genes for QPCR confirmation, choosing from those with differing expression patterns and from genes of interest based on functional enrichment and pathway results. Samples from fasted and fed channel catfish (with three replicate sample pools per timepoint) were used for QPCR. Melting-curve analysis revealed a single product for all tested genes. Fold changes from QPCR were compared with the RNA-seq expression analysis results. As shown in Fig. 1, QPCR results were significantly correlated with the RNA-seq results (average correlation coefficient 0.91, p-value <0.001; Figure 1). With the exception of anterior gradient protein 2

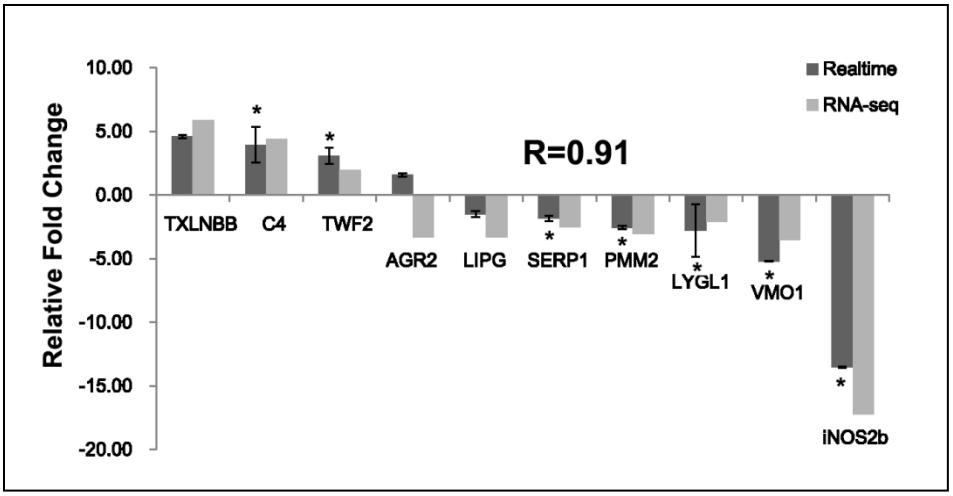

Fig. 1. Comparison of relative fold changes between RNA-seq and QPCR results in catfish**.** Gene abbreviations are: Lysozyme g-like 1, LYGL1; Taxilin beta b, TXLNBB; Twinfilin-2, TWF2; Endothelial lipase precursor, LIPG; Stress-associated endoplasmic reticulum protein 2, SERP1; Anterior gradient protein 2 homolog precursor, AGR2; Phosphomannomutase 2, PMM2; Complement c4, C4; Nitric oxide synthase 2b, inducible, iNOS2b; Vitelline membrane outer layer protein 1 homolog, VMO1.

(AGR2), all examined genes had the same direction of differential expression by both methods indicating the reliability and accuracy of the Trinity reference assembly and RNA-seq-based transcriptome expression analysis.

4. Discussion

While it is well understood that nutritional perturbations can modulate resistance to infectious diseases in agricultural animals [28], the molecular mechanisms by which dietary changes alter fish host immunity are largely unknown. The impact of these changes would be expected to differ depending on duration of feed withdrawal (fasting vs. starvation), species-specific evolutionary adaptation to natural levels of feed availability, season, and pathogen dynamics (prevalence, routes of infection, etc). Short (one week) periods of feed deprivation in channel

catfish can decrease mortality rates to a Gram-negative bacterial pathogen, *E. ictaluri* [5], but, conversely, appear to lead to higher mortality to *F. columnare* (4). Given that *F. columnare* gains entry through surface mucosa, we examined here transcriptomic changes in catfish gill and skin following a 7 d feed deprivation challenge. RNA-seq analysis revealed a total of 1,545 genes with expression perturbed by fasting. Fasting significantly altered expression of critical innate immune factors in a manner consistent with lower immune fitness as well as dysregulating key genes involved in energy metabolism and cell cycling/proliferation.

Studies of feed deprivation have traditionally focused on direct impacts on the digestive tract [29] or on systemic alterations in energy homeostasis [30]. Our understanding of the importance of mucosal surfaces as the front line in host immunity and the primary target for pathogen invasion continues to grow [31, 32]. However, the sensitivity of mucosal defensive barriers to nutritional changes is only now being explored in fish [12, 33]. Advances in next-generation sequencing now allow rapid, comprehensive analysis of the molecular underpinnings of these phenomena through RNA-seq approaches [34]. In order to gain a perspective on the molecular actors in the surface mucosa responding to fasting we pooled equal amounts of skin and gill from each fish contributing to the replicated tissue pools utilized for RNA-seq analysis. Clearly, by pooling heterogeneous cell populations stemming from the two tissues the potential exists for masking or confusing gene expression patterns from particular cellular subsets. However, we accepted this compromise in this initial study to more broadly capture novel genes and patterns in the surface mucosa. Future research will seek to ascertain which tissues and constituent cell types are contributing to key transcript profiles using laser capture micro-dissection and antibody-based cell sorting.

A total of 1,545 differentially expressed contigs could be annotated based on BLAST analysis. We attempted to classify key differentially expressed genes into broad functional categories based on GO annotation and manual imputation of putative function via literature search of studies in vertebrate model organisms (Table 4). Below we highlight several important pathways likely mediating the catfish mucosal response to short-term (7 d) fasting.

Immune Function

Recent work by our group examined how the gill transcriptome differed between *F. columnare* resistant and susceptible catfish both basally and at early timepoints following infection [27]. That dataset, combined with recent analysis of pathogen-mediated changes in the catfish skin and intestinal transcriptomes [26, 35, 36], provided a foundational reference of genes likely modulating immunity in mucosal tissues useful for comparison here. Initial analysis revealed enrichment of genes with immune functions among the mostly highly differentially expressed genes following fasting. Of the top 15 upregulated genes following fasting, 11 had immune functions according to a combination of GO annotation and manual literature searches. Similarly, 6 of the 15 most highly downregulated genes also had known immune functions. Among immune genes perturbed by fasting were acidic chitinase precursor genes which were not sequenced in fed fish (0 reads), but were present with between ~30-125 reads in the fasted replicates. Previously, we examined zero read data and concluded that although fold changes are difficult to predict, these data reflect true differential expression (27). Chitinases have received little attention in fish to-date and have not been reported in the skin or gill of any species. However, in mammals, chitinases have the ability to cleave inhaled or ingested chitins from

fungi, parasitic worms, crustaceans, and insects and are known to participate in the pathogenesis of allergic inflammation, particularly in the lung [37]. The acidic mammalian chitinase (AMCase) in particular has been found to be causative in lung inflammation and induced by IL-13 [38]. Also induced by fasting was an intestinal-type alkaline phosphatase (IAP; 90.69-fold, p=0.003). Known as a critical brush-border protein in mammals, its functions and expression patterns in fish have not been previously characterized. In mammals, IAP has the ability to detoxify lipopolysaccharide (LPS) and prevents infection across the gut mucosal barrier. Additionally, as here, IAP is reported to be sensitive to nutritional changes [39, 40]. However, IAP is silenced in the gut after 2 days of fasting, contrasting with the induced expression seen here in skin and gill samples. Clearly, additional study is required to delineate novel roles of IAP in modulating mucosal immune events in teleost fish.

Also induced following fasting were several genes whose expression had been perturbed in fish mucosa in previous studies in catfish. These included beta-2-glycoprotein 1, a novel mediator of innate immunity recently discovered to interact with LPS and activate macrophages [41]. We previously observed sharp upregulation of beta-2-glycoprotein 1 at 2 h after *Aeromonas hydrophila* infection of channel catfish skin [36]. Interestingly, beta-2-glycoprotein 1 was also reported to be upregulated following 7 d fasting in sea bream skin. Other examples such as SAM domain and HD domain-containing 1 (SAMHD1) and serum amyloid-P precursor (SAP) were induced here by fasting and upregulated in the gill following columnaris challenge [14].

A suite of immune genes were also strongly downregulated following fasting (Table 4). Immunoresponsive gene 1 (IRG1), for example, was downregulated over 53-fold after the 7 d fasting period. IRG1 is a LPS-inducible gene linked to susceptibility to Marek's Disease in chickens [42]. Additionally, we found basally lower levels of IRG1 in *F. columnare* susceptible

catfish gill when compared with resistant catfish (27). Also among downregulated immune genes following fasting was inducible nitric oxide synthase 2b (iNOS2b), previously established as the most likely orthologue of mammalian iNOS [43]. iNOS generates nitric oxide (NO) from L-arginine. NO is a potent cytotoxic agent in immune defenses which can have beneficial antimicrobial activity at mucosal surfaces including respiratory epithelium [44]. Previously, we reported high constitutive expression of iNOS2b in healthy catfish gill and higher iNOS2b levels in *F. columnare* resistant catfish than susceptible catfish (27). Here, following 7 d fasting, iNOS2b transcript levels plunged greater than 17-fold. Based on our previous studies, we would predict that these fasted levels of iNOS2b may open up channel catfish to heightened levels of pathogen colonization.

Another noteworthy alteration in immune status induced by food deprivation was the downregulation of peptidoglycan recognition protein 6 (PGRP6; -9.13-fold; p=4.28E-06). Peptidoglycan recognition proteins are poorly-studied pathogen recognition molecules which can bind and kill commensal and pathogenic bacteria, often upstream of the better characterized Toll pathway [45]. Host species from insects to mammals rely on a diverse array of PGRP molecules, some mucus-secreted, to shape and coordinate responses to a wide range of microorganisms. They appear particularly adapted to local responses at mucosal epithelial interfaces rather than more systemic immune responses [46]. For example, in Drosophila PGRP proteins mediate tolerance of gut epithelia toward endogenous microbiota [47]. PGRP6 is one of four PGRP genes in zebrafish. Suppression of PGRP6 by RNAi in zebrafish downregulated the Toll pathway and resulted in markedly increased susceptibility to *F. columnare* [48]. Taken together, these studies point to the potential importance of PGRP6 as a nutrition-sensitive mediator of mucosal health. Its presence at the mucosal surface in fish may be important for the establishment of tolerance to

commensal microbial populations through regulation of release of appropriate levels of antibacterial factors such as mucins and iNOS [46]. Future work should further characterize PGRP6 activity in catfish in the context of nutrition and disease.

In our previous study of patterns of gene expression linked to *F. columnare* resistance, levels of lysozyme C in catfish gill were markedly higher both pre-challenge and following infection in resistant fish (27). Here, fasting for 7 d decreased lysozyme C levels greater than 6-fold. In mammals, lysozymes are critical mucosal enzymes secreted from the epithelium as well as a major component of granules of professional phagocytes. They help to kill bacterial pathogens through enzymatic and antimicrobial activity [49]. Previous research in zebrafish, in which a transgenic zebrafish strain expressing a chicken lysozyme gene under the control of a keratin promoter resulted in a 65% survival rate against *F. columnare* compared to 0% survival in wild-type fish, also points to the importance of lysozyme in fish mucosal immunity [50]. Additional genes exhibiting co-regulation in both the context of feed deprivation and *F. columnare* immunity included autoimmune-regulator like, CCL19, CD83, IgFc-binding protein-like, IL-17A, MFAP4, polymeric immunoglobulin receptor (pIgR), and toxin-1 precursor (Table 4; [14]). The fasting-induced modulation of genes previously indicated to be critical in resistance to *F. columnare* may explain in part the heightened sensitivity to *F. columnare* observed in fasted fish [4]. Fasting appears to decrease levels of innate immune mediators including iNOS2b, Lysozyme C, and PGRP6 at the surface barriers where *F. columnare* gains entry.

Energy Metabolism

While our primary focus here was to examine direct impacts of short-term feed deprivation on immune regulation in catfish surface mucosa, we also examined broader physiological impacts on cellular health and function. Changes in metabolic or stress parameters may be important indicators of reallocation of energy reserves and/or changes in barrier permeability which may, in turn, impact host pathogen susceptibility [28, 51]. Among the most highly induced genes following fasting were several apolipoproteins. Apoliproteins are proteins which classically bind and transport lipids through the blood but are also recognized for roles in immunity and acute phase responses [52]. Greatest changes were seen in the apolipoprotein ApoBb (Table 4). ApoB serum levels in humans have been reported to rise following fasting [53]. ApoE and ApoL1 levels also rose in catfish skin/gill following fasting, contrasting with starvation-induced decreases of apolipoproteins in the liver of rainbow trout and salmon [10, 54].

Expression of several fatty-acid binding proteins (FABP) were perturbed by fasting (Table 4), indicating changes in lipid metabolism. Largest changes were observed in the intestinal FABP, FABP2, which was induced greater than 29-fold. FABPs are well studied as intracellular fatty acid transporters in vertebrates, with limited studies to-date in fish [55]. Better studied in fish are genes linked to proteolytic gene expression during muscle atrophy [56, 57]. The ubiquitin ligases F-box only protein 32 (Fbx32) and muscle RING finger 1 (MuRF1) were upregulated following fasting, 9.07-fold and 2.72-fold respectively.

The absorption of oligopeptides following protein digestion in vertebrates is facilitated by a member of the solute carrier 15 family, SLC15A1 or PepT1. In our results, the transporter was upregulated 5.36-fold in catfish following fasting. Given that most luminal products of protein digestion in fish are di- and tripeptides rather than individual free amino acids , PepT1 is thought to be the major transporter of ingested protein across the gut mucosa [58]. Considerable research

has been directed at understanding PepT1 function in a range of vertebrates including fish [59]. Studies in several teleost species have revealed that intestinal expression levels of PepT1 respond to fasting and refeeding, with expression levels rising in some species after short-term fasting, followed by a decline in long-term fasting/starvation. Refeeding stimulates upregulation of PepT1 above pre-fasted levels, indicating sensitive responsiveness to food availability and a potential role for the transporter in the phenomenon known as compensatory growth [60-63]. Aquaculture researchers are keenly interested in use of PepT1 as an indicator of protein uptake and as a direct predictor of animal growth [60, 64]. PepT1 may also serve as another bridge between nutritional and immune regulation, given its roles in binding bacterial peptides and stimulation of gut innate immune activation and inflammation [65]. However, all the aforementioned studies focus on PepT1 function in the intestine. While Terova et al. [63] reported second highest tissue expression of PepT1 in sea bass gills (behind some but not all intestinal segments), no previous reports of a PepT1 response to fasting in teleost surface mucosa exist. Given the importance of skin and gill epithelia for nutrient absorption in invertebrates and at least one ancient vertebrate, the hagfish [66, 67], one is tempted to speculate that catfish PepT1 fasting-induced expression in the skin/gill may reflect conserved mechanisms of nutrient sensing and/or uptake previously unknown in fish. Further research is needed to pinpoint cellular sources of PepT1 expression in surface mucosa and examine responses to longer-term fasting and refeeding.

Cell Cycling/Proliferation

A final notable category of genes perturbed in catfish skin/gill following short-term fasting were those involved in cell cycling and proliferation. Again here, while no previous study has examined how fasting may impact cell division in fish surface mucosa, our understanding of these processes in the mammalian gastrointestinal mucosa is fairly well refined [68]. There, fasting/starvation has been found to be one of the best models of a hypoproliferative response [69]. Subsequent studies have established a consistent pattern of feed deprivation reducing proliferation rates across multiple cell types, such that fasting and calorie restriction are now recommended as approaches to impede tumor growth [70]. We observed consistent downregulation of a large number of genes involved in cell cycling, proliferation, and differentiation (Table 4). These included Ki67 and PCNA-associated factors from catfish, cyclins, DNA replication licensing factors and checkpoint proteins (Table 4). The alteration of cell cycling indicated by these transcript changes may disrupt the integrity of catfish mucosal barriers with consequences for immune defenses at these surfaces [71].

5. Conclusion

RNA-seq-based transcriptome profiling in catfish revealed that short-term feed deprivation altered immune status in the surface mucosa. Changes in innate immune actors such as iNOS2b, Lysozyme C, and PGRP6 may impact the delicate recognition/ tolerance balance for commensal and pathogenic bacteria on the skin and gill. Furthermore, our analysis identified critical regulators of metabolism, cell cycling, and transport previously unstudied and/or unreported in these tissues whose expression was perturbed by fasting. The highlighted expression profiles

reveal potential mechanistic similarities between gut and surface mucosa and underscore the complex interrelationships between nutrition, mucosal integrity, and immunity in teleost fish.

References

[1] Larsson Å, Lewander K. Metabolic effects of starvation in the eel, *Anguilla anguilla L*. Comp Biochem Physiol A Comp Physiol 1973; 44:367-74.

[2] Navarro I, Gutiérrez J. Fasting and starvation. Biochemistry and molecular biology of fishes 1995; 4:393-434.

[3] Pottinger T, Rand-Weaver M, Sumpter J. Overwinter fasting and re-feeding in rainbow trout: plasma growth hormone and cortisol levels in relation to energy mobilisation. Comp Biochem Physiol A Comp Physiol 2003; 136:403-17.

[4] Shoemaker C, Klesius P, Lim C, Yildirim M. Feed deprivation of channel catfish, *Ictalurus punctatus* (Rafinesque), influences organosomatic indices, chemical composition and susceptibility to *Flavobacterium columnare*. J Fish Dis 2003; 26:553-61.

[5] Wise DJ, Greenway T, Li MH, Camus AC, Robinson EH. Effects of variable periods of food deprivation on the development of enteric septicemia in channel catfish. J Aquat Anim Health 2008; 20:39-44.

[6] Krogdahl Å, Nordrum S, Sorensen M, Brudeseth L, Rosjo C. Effects of diet composition on apparent nutrient absorption along the intestinal tract and of subsequent fasting on mucosal disaccharidase activities and plasma nutrient concentration in Atlantic salmon *Salmo salar L*. Aquacult Nutr 1999; 5:121-34.

[7] Krogdahl A, Bakke-McKellep AM. Fasting and refeeding cause rapid changes in intestinal tissue mass and digestive enzyme capacities of Atlantic salmon (*Salmo salar L.*). Comp Biochem Physiol A Mol Integr Physiol 2005; 141:450-60.

[8] Cleveland BM, Weber GM, Blemings KP, Silverstein JT. Insulin-like growth factor-I and genetic effects on indexes of protein degradation in response to feed deprivation in rainbow trout (*Oncorhynchus mykiss*). Am J Physiol Regul Integr Comp Physiol 2009; 297:R1332-42.

[9] Baumgarner BL, Bharadwaj AS, Inerowicz D, Goodman AS, Brown PB. Proteomic analysis of rainbow trout (*Oncorhynchus mykiss*) intestinal epithelia: physiological acclimation to short-term starvation. Comp Biochem Physiol Part D Genomics Proteomics 2013; 8:58-64.

[10] Martin SA, Douglas A, Houlihan DF, Secombes CJ. Starvation alters the liver transcriptome of the innate immune response in Atlantic salmon (*Salmo salar*). BMC Genomics 2010; 11:418.

[11] Vieira FA, Gregorio SF, Ferraresso S, Thorne MA, Costa R, Milan M, et al. Skin healing and scale regeneration in fed and unfed sea bream, Sparus auratus. BMC Genomics 2011; 12:490.

[12] Landeira-Dabarca A, Sieiro C, Alvarez M. Change in food ingestion induces rapid shifts in the diversity of microbiota associated with cutaneous mucus of Atlantic salmon *Salmo salar*. J Fish Biol 2013; 82:893-906.

[13] Arias CR, Cai W, Peatman E, Bullard SA. Catfish hybrid *Ictalurus punctatus* x *I. furcatus* exhibits higher resistance to columnaris disease than the parental species. Dis Aquat Organ 2012; 100:77-81.

[14] Sun F, Peatman E, Li C, Liu S, Jiang Y, Zhou Z, et al. Transcriptomic signatures of attachment, NF-kappaB suppression and IFN stimulation in the catfish gill following columnaris bacterial infection. Dev Comp Immunol 2012; 38:169-80.

[15] Beck BH, Farmer BD, Straus DL, Li C, Peatman E. Putative roles for a rhamnose binding lectin in *Flavobacterium columnare* pathogenesis in channel catfish Ictalurus punctatus. Fish Shellfish Immunol 2012; 33:1008-15.

[16] Simpson JT, Wong K, Jackman SD, Schein JE, Jones SJ, Birol I. ABySS: a parallel assembler for short read sequence data. Genome Res 2009; 19:1117-23.

[17] Grabherr MG, Haas BJ, Yassour M, Levin JZ, Thompson DA, Amit I, et al. Full-length transcriptome assembly from RNA-Seq data without a reference genome. Nat Biotechnol 2011; 29:644-52.

[18] Li W, Godzik A. Cd-hit: a fast program for clustering and comparing large sets of protein or nucleotide sequences. Bioinformatics 2006; 22:1658-9.

[19] Huang X, Madan A. CAP3: A DNA sequence assembly program. Genome Res 1999; 9:868-77.

[20] Gotz S, Garcia-Gomez JM, Terol J, Williams TD, Nagaraj SH, Nueda MJ, et al. High-throughput functional annotation and data mining with the Blast2GO suite. Nucleic Acids Res 2008; 36:3420-35.

[21] Baggerly KA, Deng L, Morris JS, Aldaz CM. Differential expression in SAGE: accounting for normal between-library variation. Bioinformatics 2003; 19:1477-83.

[22] Robinson MD, Oshlack A. A scaling normalization method for differential expression analysis of RNA-seq data. Genome Biol 2010; 11:R25.

[23] Bauer S, Grossmann S, Vingron M, Robinson PN. Ontologizer 2.0--a multifunctional tool for GO term enrichment analysis and data exploration. Bioinformatics 2008; 24:1650-1.

[24] Grossmann S, Bauer S, Robinson PN, Vingron M. Improved detection of overrepresentation of Gene-Ontology annotations with parent child analysis. Bioinformatics 2007; 23:3024-31.

[25] Pfaffl MW, Horgan GW, Dempfle L. Relative expression software tool (REST) for group-wise comparison and statistical analysis of relative expression results in real-time PCR. Nucleic Acids Res 2002; 30:e36.

[26] Li C, Zhang Y, Wang R, Lu J, Nandi S, Mohanty S, et al. RNA-seq analysis of mucosal immune responses reveals signatures of intestinal barrier disruption and pathogen entry following *Edwardsiella ictaluri* infection in channel catfish, *Ictalurus punctatus*. Fish Shellfish Immunol 2012; 32:816-27.

[27] Laukoetter MG, Nava P, Lee WY, Severson EA, Capaldo CT, Babbin BA, et al. JAM-A regulates permeability and inflammation in the intestine in vivo. J Exp Med 2007; 204:3067-76.

[28] Klasing K. Nutritional modulation of resistance to infectious diseases. Poultry Science 1998; 77:1119-25.

[29] Gisbert E, Fernández I, Alvarez-González C. Prolonged feed deprivation does not permanently compromise digestive function in migrating European glass eels *Anguilla anguilla*. J Fish Biol 2011; 78:580-92.

[30] Costas B, Aragão C, Ruiz-Jarabo I, Vargas-Chacoff L, Arjona FJ, Dinis MT, et al. Feed deprivation in Senegalese sole (*Solea senegalensis Kaup*, 1858) juveniles: effects on blood plasma metabolites and free amino acid levels. Fish Physiol Biochem 2011; 37:495-504.

[31] Ángeles Esteban M. An Overview of the Immunological Defenses in Fish Skin. ISRN Immunology 2012; 2012.

[32] Rombout JH, Abelli L, Picchietti S, Scapigliati G, Kiron V. Teleost intestinal immunology. Fish Shellfish Immunol 2011; 31:616-26.

[33] Florbela V, Silvia G, Serena F, Michael T, Rita C, Massimo M, et al. Skin healing and scale regeneration in fed and unfed sea bream, Sparus auratus. 2011.

[34] Liu G. Recent applications of DNA sequencing technologies in food, nutrition and agriculture. Recent Pat Food Nutr Agric 2011; 3:187.

[35] Li C, Beck B, Su B, Terhune J, Peatman E. Early mucosal responses in blue catfish (*Ictalurus furcatus*) skin to *Aeromonas hydrophila* infection. Fish Shellfish Immunol 2013; 34:920-8.

[36] Li C, Wang R, Su B, Luo Y, Terhune J, Beck B, et al. Evasion of mucosal defenses during *Aeromonas hydrophila* infection of channel catfish (*Ictalurus punctatus*) skin. Dev Comp Immunol 2013; 39:447-55.

[37] Goldman DL, Vicencio AG. The chitin connection. MBio 2012; 3.

[38] Zhu Z, Zheng T, Homer RJ, Kim YK, Chen NY, Cohn L, et al. Acidic mammalian chitinase in asthmatic Th2 inflammation and IL-13 pathway activation. Science 2004; 304:1678-82.

[39] Goldberg RF, Austen WG, Zhang X, Munene G, Mostafa G, Biswas S, et al. Intestinal alkaline phosphatase is a gut mucosal defense factor maintained by enteral nutrition. Proc Natl Acad Sci USA 2008; 105:3551-56.

[40] Lallès JP. Intestinal alkaline phosphatase: multiple biological roles in maintenance of intestinal homeostasis and modulation by diet. Nutr Rev 2010; 68:323-32.

[41] Ağar Ç, de Groot PG, Mörgelin M, Monk SD, van Os G, Levels JH, et al. β2-Glycoprotein I: a novel component of innate immunity. Blood 2011; 117:6939-47.

[42] Smith J, Sadeyen JR, Paton IR, Hocking PM, Salmon N, Fife M, et al. Systems analysis of immune responses in Marek's disease virus-infected chickens identifies a gene involved in susceptibility and highlights a possible novel pathogenicity mechanism. J Virol 2011; 85:11146-58.

[43] Lepiller S, Franche N, Solary E, Chluba J, Laurens V. Comparative analysis of zebrafish nos2a and nos2b genes. Gene 2009; 445:58-65.

[44] Bogdan C. Nitric oxide and the immune response. Nat Immunol 2001; 2:907-16.

[45] Kashyap DR, Wang M, Liu LH, Boons GJ, Gupta D, Dziarski R. Peptidoglycan recognition proteins kill bacteria by activating protein-sensing two-component systems. Nat Med 2011; 17:676-83.

[46] Royet J, Gupta D, Dziarski R. Peptidoglycan recognition proteins: modulators of the microbiome and inflammation. Nat Rev Immunol 2011; 11:837-51.

[47] Gendrin M, Welchman DP, Poidevin M, Hervé M, Lemaitre B. Long-range activation of systemic immunity through peptidoglycan diffusion in Drosophila. PLoS Pathog 2009; 5:e1000694.

[48] Chang M, Nie P. RNAi suppression of zebrafish peptidoglycan recognition protein 6 (zfPGRP6) mediated differentially expressed genes involved in Toll-like receptor signaling pathway and caused increased susceptibility to *Flavobacterium columnare*. Vet Immunol Immunopathol 2008; 124:295-301.

[49] Davis KM, Weiser JN. Modifications to the peptidoglycan backbone help bacteria to establish infection. Infect Immun 2011; 79:562-70.

[50] Yazawa R, Hirono I, Aoki T. Transgenic zebrafish expressing chicken lysozyme show resistance against bacterial diseases. Transgenic research 2006; 15:385-91.

[51] Polakof S, Panserat S, Soengas JL, Moon TW. Glucose metabolism in fish: a review. J Comp Physiol B 2012; 182:1015-45.

[52] Bolanos-Garcia VM, Miguel RN. On the structure and function of apolipoproteins: more than a family of lipid-binding proteins. Progress in biophysics and molecular biology 2003; 83:47-68.

[53] Savendahl L, Underwood LE. Fasting increases serum total cholesterol, LDL cholesterol and apolipoprotein B in healthy, nonobese humans. J Nutr 1999; 129:2005-8.

[54] Salem M, Silverstein J, Rexroad CE, 3rd, Yao J. Effect of starvation on global gene expression and proteolysis in rainbow trout (*Oncorhynchus mykiss*). BMC Genomics 2007; 8:328.

[55] Lai YY, Lubieniecki KP, Phillips RB, Chow W, Koop BF, Davidson WS. Genomic organization of Atlantic salmon (*Salmo salar*) fatty acid binding protein (fabp2) genes reveals independent loss of duplicate loci in teleosts. Mar Genomics 2009; 2:193-200.

[56] Wang J, Salem M, Qi N, Kenney PB, Rexroad CE, 3rd, Yao J. Molecular characterization of the MuRF genes in rainbow trout: Potential role in muscle degradation. Comp Biochem Physiol B Biochem Mol Biol 2011; 158:208-15.

[57] Tacchi L, Bickerdike R, Secombes CJ, Martin SA. Muscle-specific RING finger (MuRF) cDNAs in Atlantic salmon (*Salmo salar*) and their role as regulators of muscle protein degradation. Marine Biotechnology 2012; 14:35-45.

[58] Terova G, Cora S, Verri T, Rimoldi S, Bernardini G, Saroglia M. Impact of feed availability on PepT1 mRNA expression levels in sea bass (*Dicentrarchus labrax*). Aquaculture 2009; 294:288-99.

[59] Verri T, Kottra G, Romano A, Tiso N, Peric M, Maffia M, et al. Molecular and functional characterisation of the zebrafish (Danio rerio) PEPT1-type peptide transporter. FEBS Lett 2003; 549:115-22.

[60] Verri T, Terova G, Dabrowski K, Saroglia M. Peptide transport and animal growth: the fish paradigm. Biol Lett 2011; 7:597-600.

[61] Bucking C, Schulte PM. Environmental and nutritional regulation of expression and function of two peptide transporter (PepT1) isoforms in a euryhaline teleost. Comp Biochem Physiol A Mol Integr Physiol 2012; 161:379-87.

[62] Hakim Y, Harpaz S, Uni Z. Expression of brush border enzymes and transporters in the intestine of European sea bass (*Dicentrarchus labrax*) following food deprivation. Aquaculture 2009; 290:110-15.

[63] Terova G, Forchino A, Rimoldi S, Brambilla F, Antonini M, Saroglia M. Bio-Mos: an effective inducer of dicentracin gene expression in European sea bass (*Dicentrarchus labrax*). Comp Biochem Physiol B Biochem Mol Biol 2009; 153:372-7.

[64] Terova G, Robaina L, Izquierdo M, Cattaneo A, Molinari S, Bernardini G, et al. PepT1 mRNA expression levels in sea bream (*Sparus aurata*) fed different plant protein sources. SpringerPlus 2013; 2:1-14.

[65] Ingersoll SA, Ayyadurai S, Charania MA, Laroui H, Yan Y, Merlin D. The role and pathophysiological relevance of membrane transporter PepT1 in intestinal inflammation and inflammatory bowel disease. Am J Physiol Gastrointest Liver Physiol 2012; 302:G484-92.

[66] Meissner B, Boll M, Daniel H, Baumeister R. Deletion of the intestinal peptide transporter affects insulin and TOR signaling in Caenorhabditis elegans. J Biol Chem 2004; 279:36739-45.

[67] Glover CN, Bucking C, Wood CM. Adaptations to in situ feeding: novel nutrient acquisition pathways in an ancient vertebrate. Proc Biol Sci 2011; 278:3096-101.

[68] Wong WM, Wright NA. Cell proliferation in gastrointestinal mucosa. J Clin Pathol 1999; 52:321-33.

[69] Brown HO, Levine ML, Lipkin M. Inhibition of intestinal epithelial cell renewal and migration induced by starvation. American Journal of Physiology--Legacy Content 1963; 205:868-72.

[70] Lee C, Raffaghello L, Brandhorst S, Safdie FM, Bianchi G, Martin-Montalvo A, et al. Fasting cycles retard growth of tumors and sensitize a range of cancer cell types to chemotherapy. Sci Transl Med 2012; 4:124ra27.

[71] Knight DA, Rossi FM, Hackett TL. Mesenchymal stem cells for repair of the airway epithelium in asthma. Expert Rev Respir Med 2010; 4:747-58.

VI. OVERALL RESULTS AND FUTURE DIRECTIONS

In intestine, we utilized high-throughput RNA-seq to characterize the role of the intestinal epithelial barrier following *E. ictaluri* challenge. Comparison of digital gene expression between challenged and control samples revealed 1,633 differentially expressed genes at 3 h, 24 h, and 3 day following exposure. Gene pathway analysis of the differentially expressed gene set indicated the centrality of actin cytoskeletal polymerization/remodelling and junctional regulation in pathogen entry and subsequent inflammatory responses. The expression patterns of fifteen differentially expressed genes related to intestinal epithelial barrier dysfunction were validated by quantitative real time RT-PCR (average correlation coeff. 0.92, $p<0.001$).

In skin, we utilized a new 8 x 60K Agilent microarray for catfish to examine gene expression profiles at critical early timepoints following challenge—2 h, 8 h, and 12 h. Expression of a total of 2,168 unique genes was significantly perturbed during at least one timepoint. We observed dysregulation of genes involved in antioxidant, cytoskeletal, immune, junctional, and nervous system pathways. In particular, *A. hydrophila* infection rapidly altered a number of potentially critical lectins, chemokines, interleukins, and other mucosal factors in a manner predicted to enhance its ability to adhere to and invade the catfish host.

In gill, we used of RNA-seq to profile gill expression differences between channel catfish (*Ictalurus punctatus*) differing in their susceptibility to *F. columnare* both basally (before infection) and at three early timepoints post-infection (1 h, 2 h, and 8 h). In the large dataset, we focused our analysis on basal differential expression between resistant and susceptible catfish as these genes could potentially reveal genetic and/or environmental factors linked with differential rates of infection. A number of critical innate immune components including iNOS2b, lysozyme

C, IL-8, and TNF-alpha were constitutively higher in resistant catfish gill, while susceptible fish showed high expression levels of secreted mucin forms, a rhamnose-binding lectin previously linked to susceptibility, and mucosal immune factors such as CD103 and IL-17. Taken together, the immune and mucin profiles obtained by RNA-seq suggest a basal polarization in the gill mucosa, with susceptible fish possessing a putative mucosecretory, toleragenic phenotype which may predispose them to *F. columnare* infection.

In the gill ans skin, we examined changes in transcriptional regulation induced in these surface mucosal tissues due to short (7 day) fasting. RNA-seq expression analysis revealed a total of 1,545 genes perturbed by fasting. Fasting significantly altered expression of critical innate immune factors in a manner consistent with lower immune fitness as well as dysregulating key genes involved in energy metabolism and cell cycling/proliferation. Downregulation of innate immune actors such as iNOS2b, Lysozyme C, and peptidoglycan recognition protein 6 is predicted to impact the delicate recognition/tolerance balance for commensal and pathogenic bacteria on the skin and gill.

From the differentially expressed genes among different bacterial infection in the mucosal surfaces at the critical early timepoints, especially the shared key players, can help us to better understanding the complexity of the mucosal immunity in catfish, and facilite the future mucosal studies in teleost fish. The highlighted expression profiles give us the chance to design the predictive/diagnostic assays, manipulate the disease susceptibility, and provide more sophisticated means to understand/predict efficacy of topical therapeutants, feed additives, and feeding changes. These biomarkers can be used for indication of immune status and disease selection, serve as targets for vaccines/adjuvants/novel treatments development.

Taken together, our results highlight several putative immune pathways and individual

candidate genes deserving of further investigation in the context of development of therapeutic regimens and laying the foundation for selection of resistant catfish lines. It sets a foundation for future studies comparing mechanisms of pathogen entry and mucosal immunity across several important catfish pathogens. Understanding of molecular mechanisms of pathogen entry during infection will provide insight into strategies for selection of resistant catfish brood stocks against various diseases. Our findings can be used to compare and contrast catfish mucosal responses to bacterial isolates with differing virulence and in catfish populations with differing susceptibility to pathogens. Utilization of these findings will improve strategies for selection of disease-resistant catfish broodstock and evaluation of prevention and treatment options.